Identification of the Steering Dynamics of the Sea Swift

Källström, Claes G.

1978

Document Version:
Publisher's PDF, also known as Version of record

CODEN: LUTFD2/(TFRT-7155)/1-175/(1978)

IDENTIFICATION OF THE STEERING DYNAMICS OF THE SEA SWIFT

CLAES G. KÄLLSTRÖM

Department of Automatic Control
Lund Institute of Technology
October 1978

IDENTIFICATION OF THE STEERING DYNAMICS OF THE SEA SWIFT

Claes G. Källström

Dokumentutgivare
04T0 Lund Institute of Technology

Handläggare 26T0 Dept of Automatic Control
Claes G. Källström

Författare
08T0 Claes G. Källström

Dokumentnamn
04T4 Report

Utgivningsdatum
06T4 Oct 1978

Dokumentbeteckning
04T4 LUTFD2/(TFRT-7155)/1-175/ (1978)

Ärendebeteckning
06T6 STU 75 40 53
STU 77 57 66

10T4

Dokumenttitel och undertitel
18T0 Identification of the steering dynamics of the Sea Swift

Referat (sammandrag)
36T0 System identification techniques are applied to determine the steering dynamics of the tanker Sea Swift from 4 full-scale experiments. The output error method, the maximum likelihood method and the prediction error method are applied using the identification program LISPID. A few maximum likelihood identifications using the program IDPAC are also performed. Different linear and nonlinear models are investigated. The maximum likelihood method and the prediction error method are proved to be advantageous to the output error method, provided that an appropriate prediction interval is used. Good estimates of the hydrodynamic derivatives are obtained by using LISPID to data from the 4 experiments. Notice that two of the experiments were performed in closed loop.

Referat skrivet av
42T0 Author

Förslag till ytterligare nyckelord
44T0 ship, ship steering, ship dynamics

Klassifikationssystem och -klass(er)
50T0

Indextermer (ange källa)
52T0

Omfång
54T0 175 pages

Språk
58T0 English

Övriga bibliografiska uppgifter
56T2

Sekretessuppgifter
60T0

ISSN
60T4

ISBN
60T6

Dokumentet kan erhållas från
62T0 Department of Automatic Control
Lund Institute of Technology
P O Box 725, S-220 07 LUND 7, Sweden

Mottagarens uppgifter
62T4

Pris
66T0

SIS-DB 1

DOKUMENTDATABLAD enligt SIS 62 10 12

Blankett LU 11:25 1976–07

TABLE OF CONTENTS

1. INTRODUCTION

System identification techniques are applied to determine the steering dynamics of the Sea Swift from 4 full-scale experiments. Parameters of different linear and nonlinear models are estimated. The identification program LISPID (Källström, Essebo and Åström, 1976; Källström, 1978) is used to analyse the experiments. The output error method, the maximum likelihood method and the prediction error method are applied. A few maximum likelihood identifications using the program IDPAC (Wieslander, 1976) are also presented.

The Sea Swift is an oil tanker of 255 000 tdw built for the Salén Shipping Companies, Stockholm, by Kockums Shipyard, Malmö. The experiments were performed in full load condition. System identification techniques have previously been applied to data from experiments performed with the Sea Splendour and the Sea Scout, which are sister ships to the Sea Swift, in ballast condition (Åström and Källström, 1973, 1976; Åström, Källström, Norrbin and Byström, 1975; Källström, 1977a and 1977c; Norrbin, Byström, Åström and Källström, 1977; Byström and Källström, 1978). Some preliminary results of the Sea Swift experiments are presented in Norrbin, Byström, Åström and Källström (1977) and Gustavsson, Ljung and Söderström (1977).

2. EXPERIMENTS

The Sea Swift is a single-screw turbine tanker of 255 000 tdw with a half-spade rudder. The maximum power at 85 rpm is 32 000 shp and the trial speed at full draught is 15.7 knots. The length between perpendiculars L is 329.18 m, the breadth is 51.82 m, and the draught is 20.06 m when the ship is fully loaded. The displacement at full draught is 285 000 m^3.

The 4 experiments were performed in 1974 in the Mozambique Channel, which separates Madagascar from Africa. They are described in detail by Källström (1975). The tanker was fully loaded and it had a displacement ∇ of 284 300 m^3. The draught

at bow and stern was 20 m. The ship speed V was approximately 17 knots and the propeller rate of revolution was about 85.5 rpm. The wind speed was less than 4 m/s and the waves were small. The 4 experiments E1, E2, E3 and E4 lasted for 78, 59, 36 and 61 min. Experiemnts E1 and E4 were performed in open loop by approximately using a PRBS as rudder perturbations. Experiment E2 was carried out in closed loop, but extra rudder perturbations were added to secure the identifiability. The rudder command δ was determined from the P-controller

$$\delta = k(\psi_m - \psi_{ref}) + \delta_o \tag{2.1}$$

where ψ_m is the measured heading angle, ψ_{ref} is the requested heading angle and δ_o is the added perturbation signal, approximately chosen as a PRBS. The gain k was assigned the value 2 and ψ_{ref} the value 212 deg during experiment E2. Experiment E3 was also performed in closed loop, but no perturbations were added, i.e. $\delta_o = 0$ in (2.1). The requested heading angle ψ_{ref} was 212 deg. The identifiability was guaranteed by changing k from 0.5 to 3 after 31 min of the experiment. A very oscillating behaviour was unfortunately obtained with k = 3, therefore the experiment had to be terminated after a short time. Identification of processes in closed loop is discussed in Gustavsson, Ljung and Söderström (1977). A rudder limit of 10 deg was used during experiments E2 and E3. Rudder servo position, rudder angle, fore and aft sway velocities, yaw rate, heading angle, forward speed, propeller rate of revolution, and pitch angular velocity were measured during all experiments. The data were punched on paper tape. The onboard process computer made it possible to record the data with a precise, constant sampling rate. The sampling interval T_s was chosen to 10 s in all experiments. The input-output data used for the system identification are shown in Figs. 2.1 - 2.4. The rudder angles are positive towards port. The number of recorded samples of experiments E1, E2, E3 and E4 are 471, 354, 215 and 368.

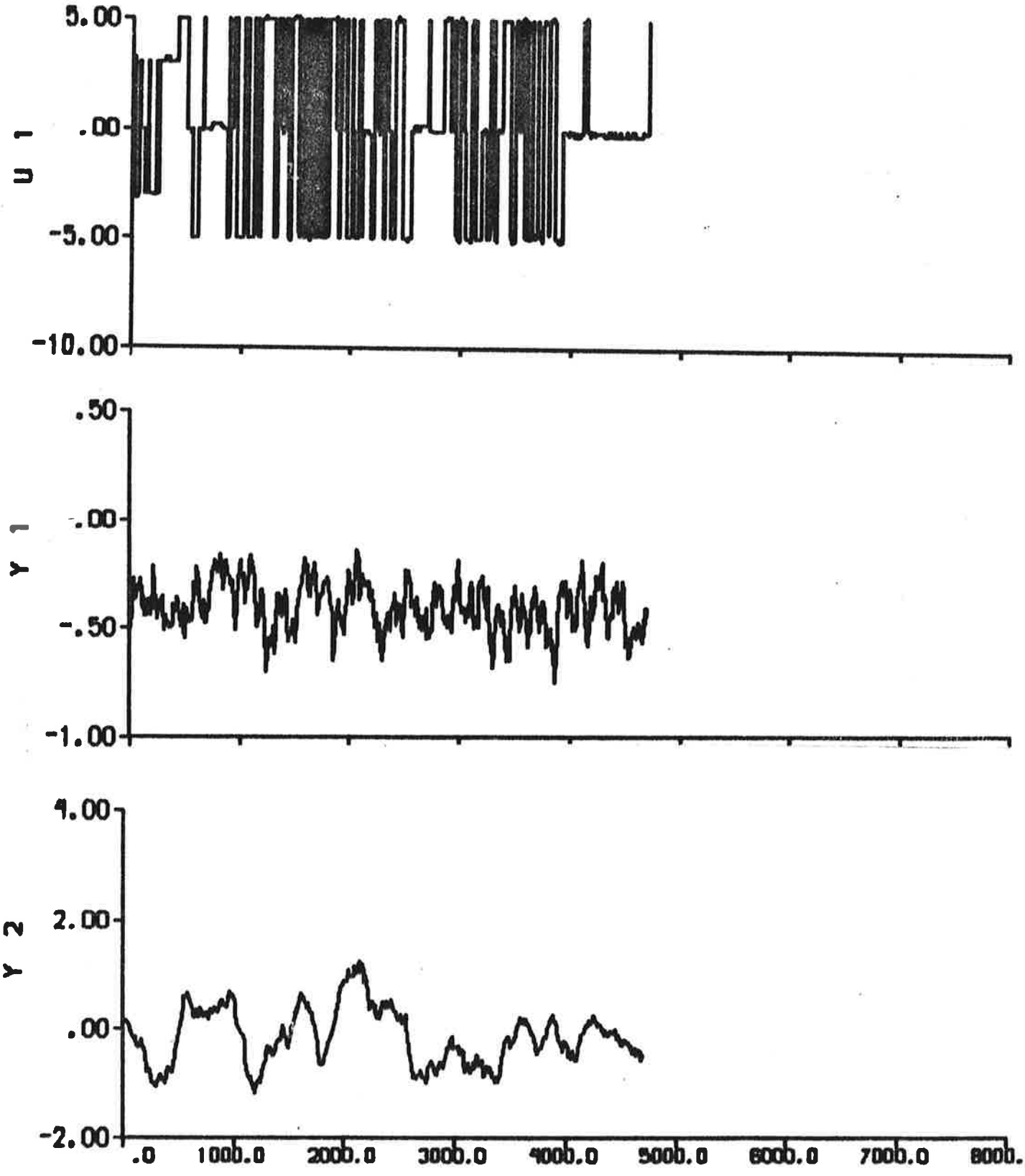

Fig. 2.1a - Input-output data obtained from experiment E1. The input is the rudder command U1 [deg] and the outputs are the fore sway velocity Y1 [knots], the aft sway velocity Y2 [knots], the yaw rate Y3 [deg/s], and the heading angle Y4 [deg].

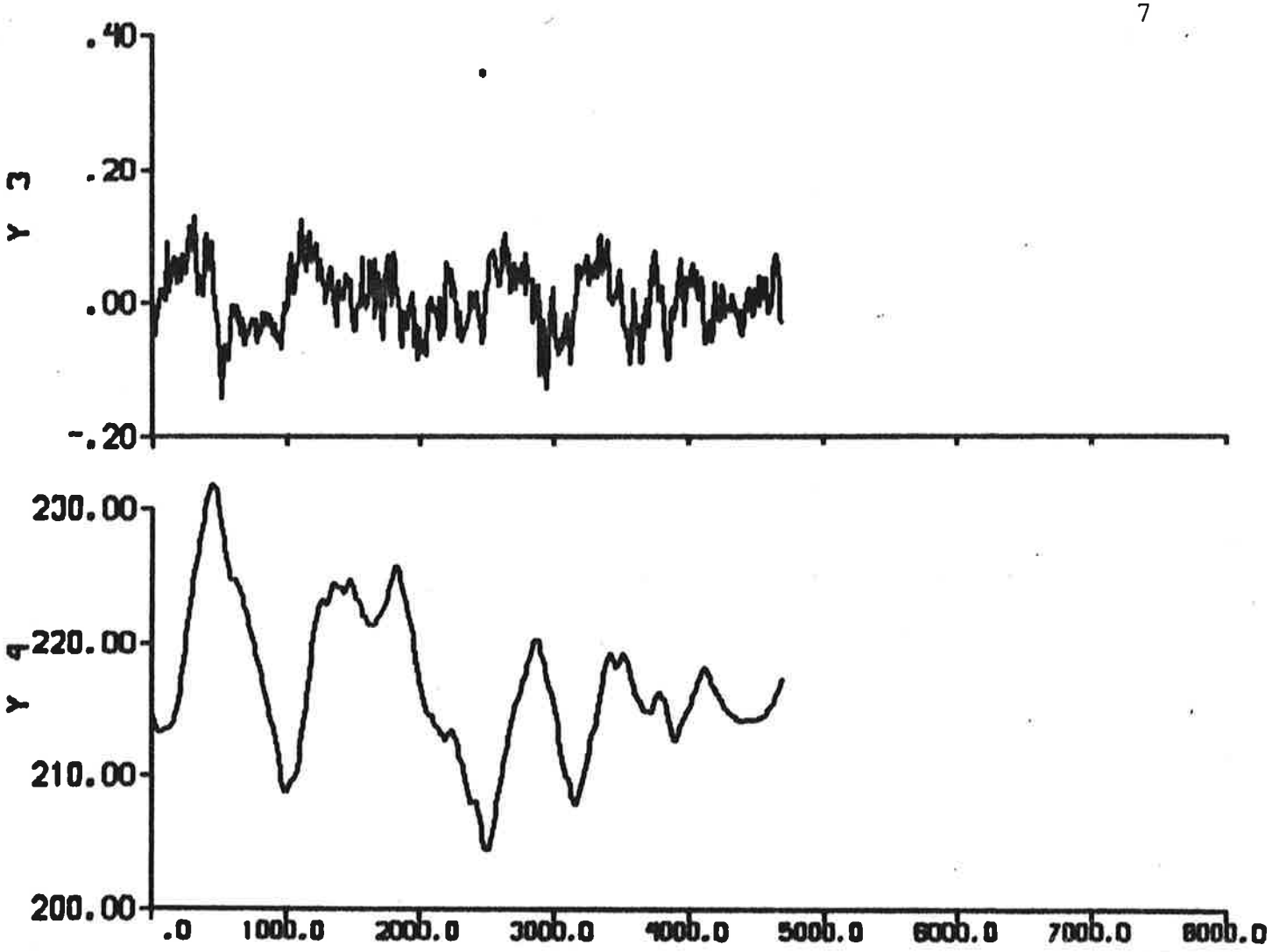
.40
.20
.00
-.20
Y 3
230.00
220.00
210.00
200.00
Y 4
.0
1000.0
2000.0
3000.0
4000.0
5000.0
6000.0
7000.0
8000.0
Time [s]

Fig. 2.1b

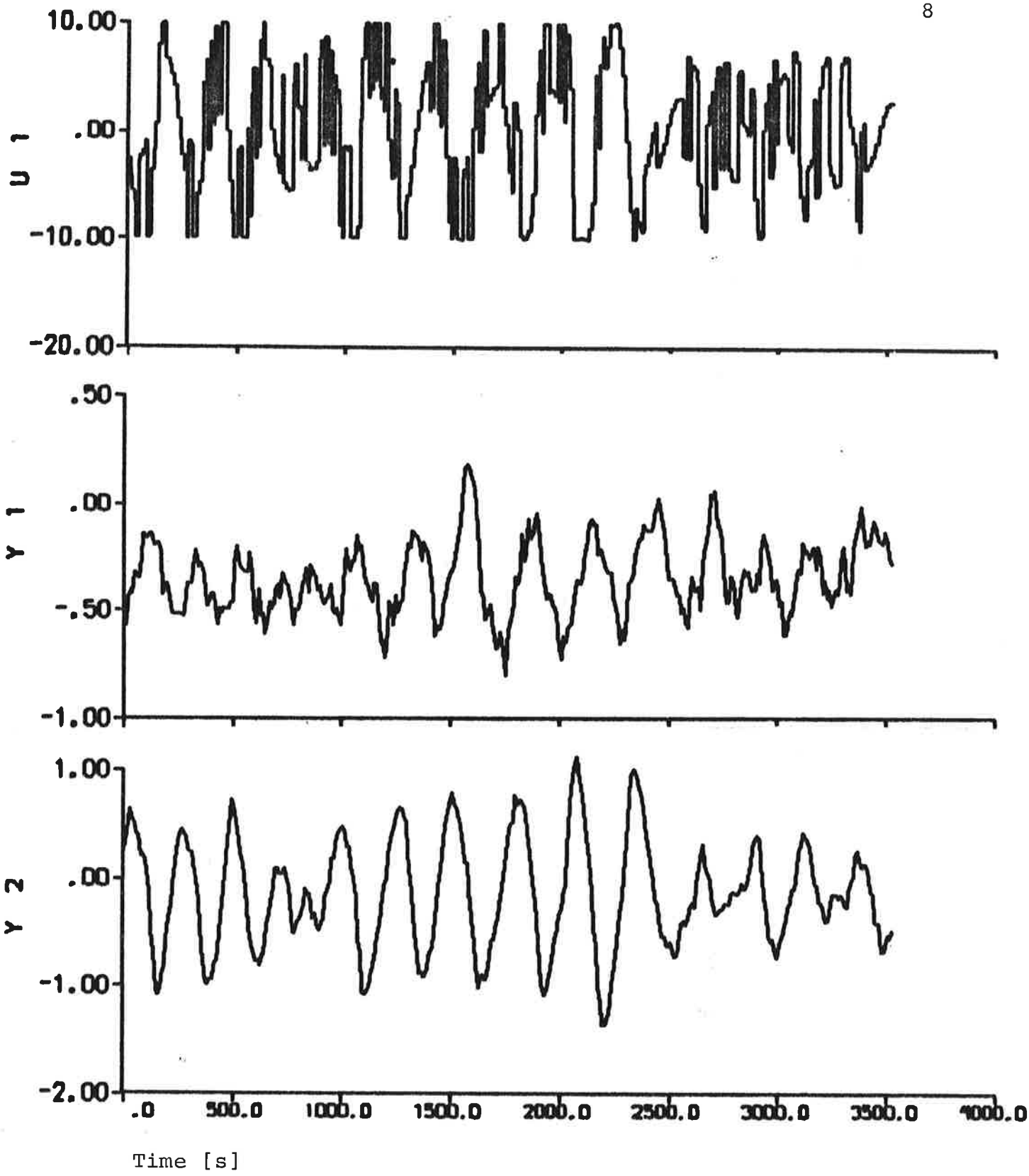

Fig. 2.2a - Input-output data obtained from experiment E2.

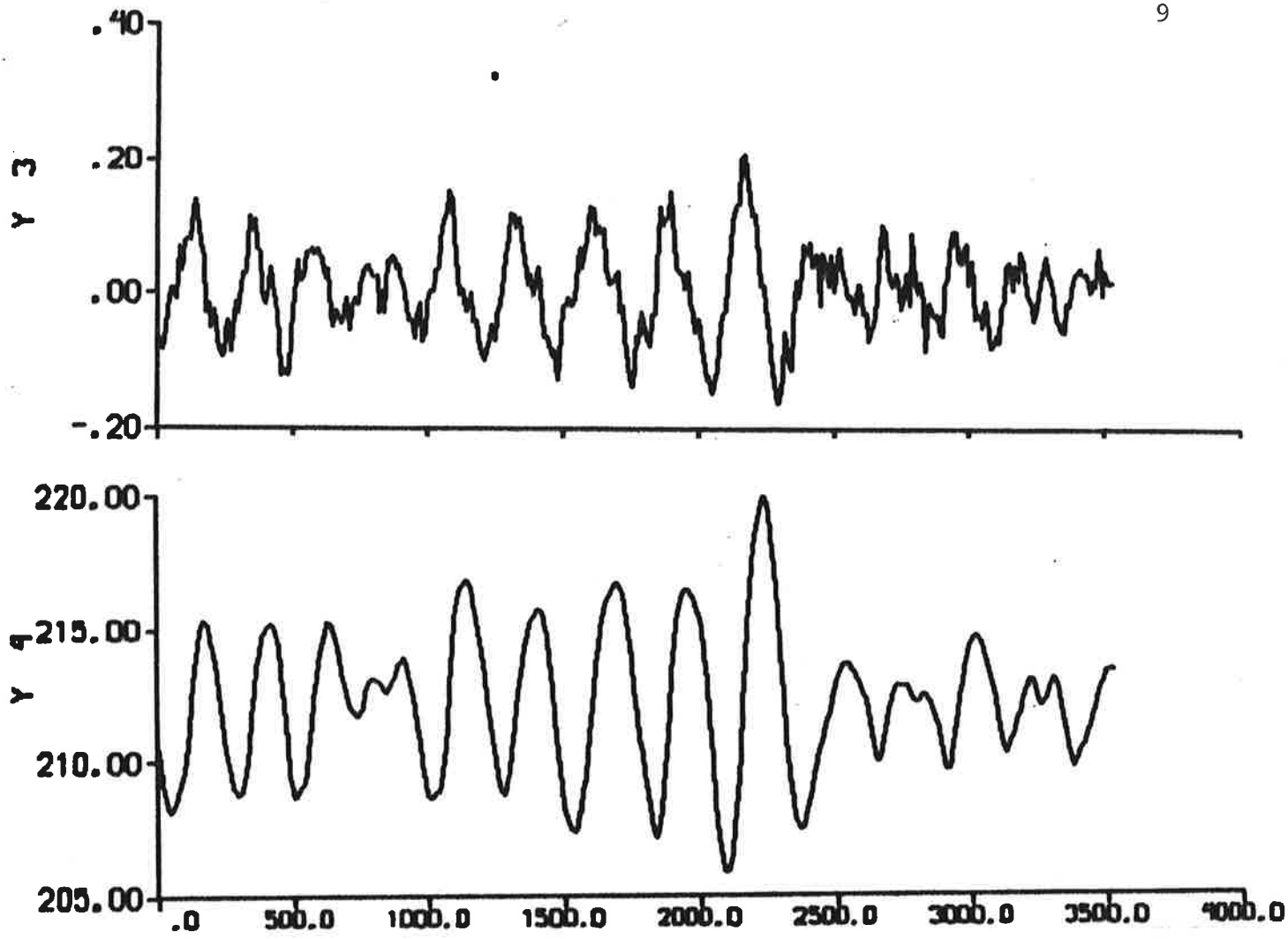
.40
.20
.00
-.20
Y 3
220.00
215.00
210.00
205.00
Y 4
.0
500.0
1000.0
1500.0
2000.0
2500.0
3000.0
3500.0
4000.0
Time [s]

Fig. 2.2b

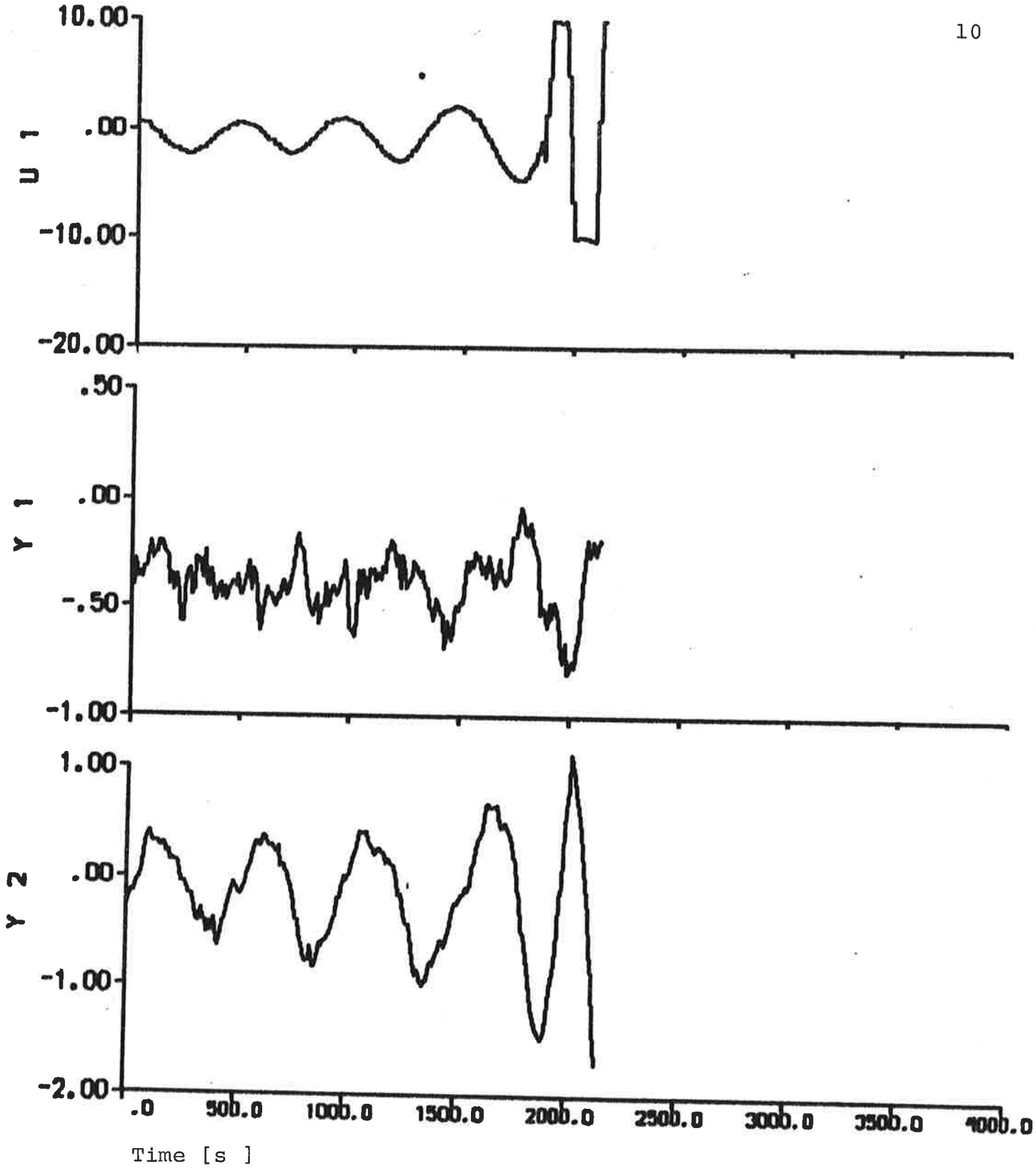

Fig. 2.3a - Input-output data obtained from experiment E3.

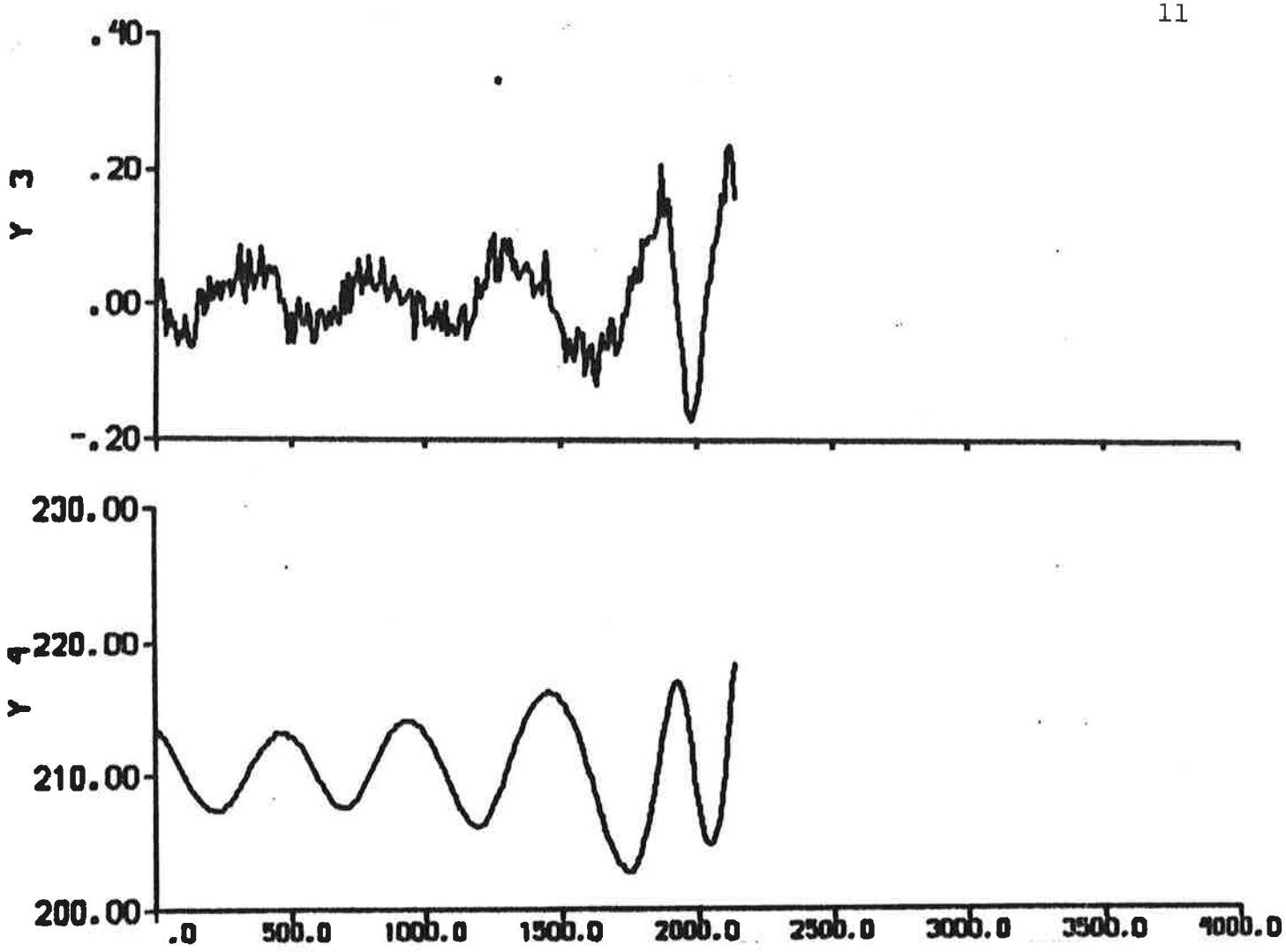
.40
.20
.00
-.20
Y 3
230.00
220.00
210.00
200.00
Y 4
.0
500.0
1000.0
1500.0
2000.0
2500.0
3000.0
3500.0
4000.0
Time [s]

Fig. 2.3b

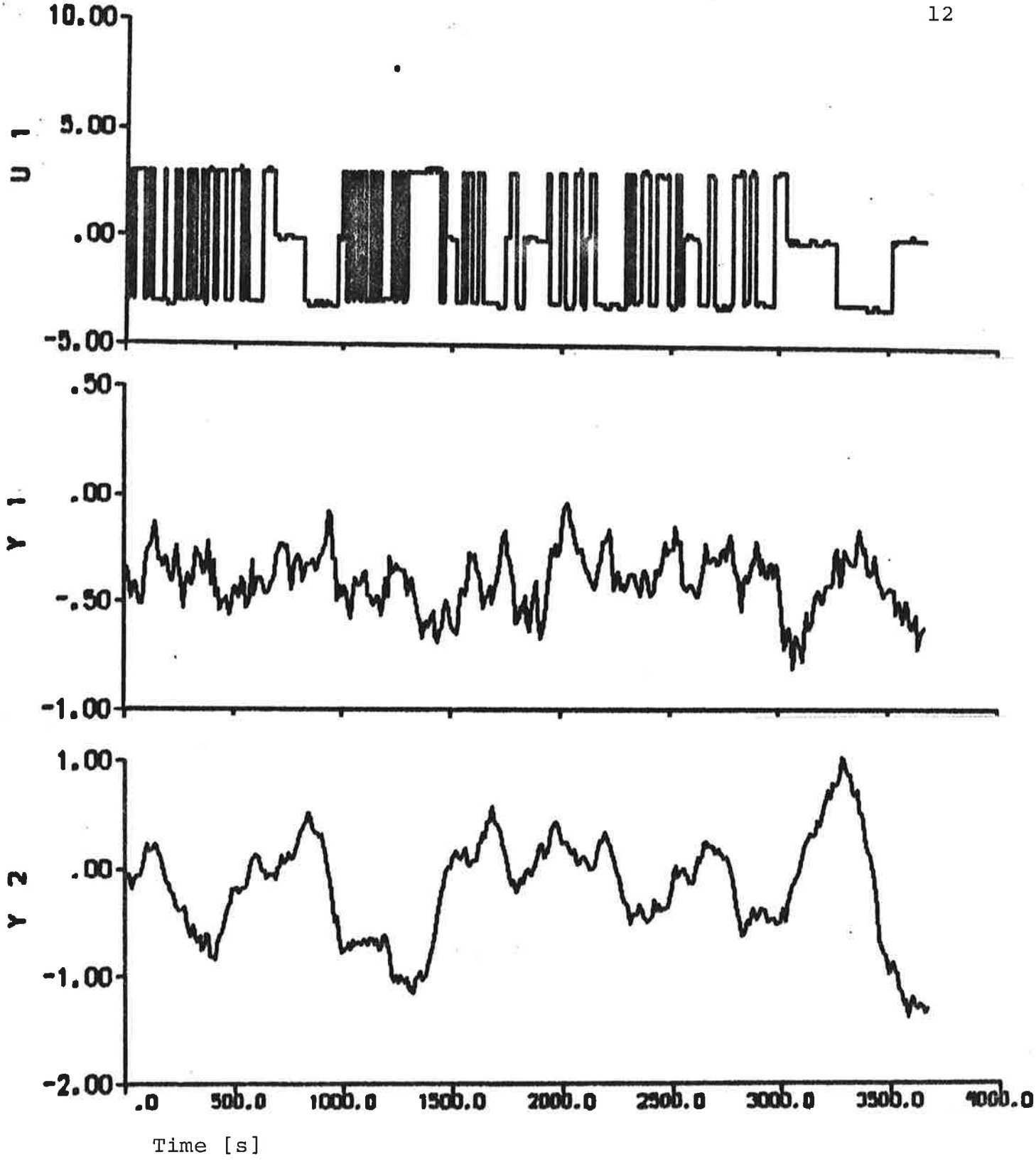

Fig. 2.4a - Input-output data obtained from experiment E4.

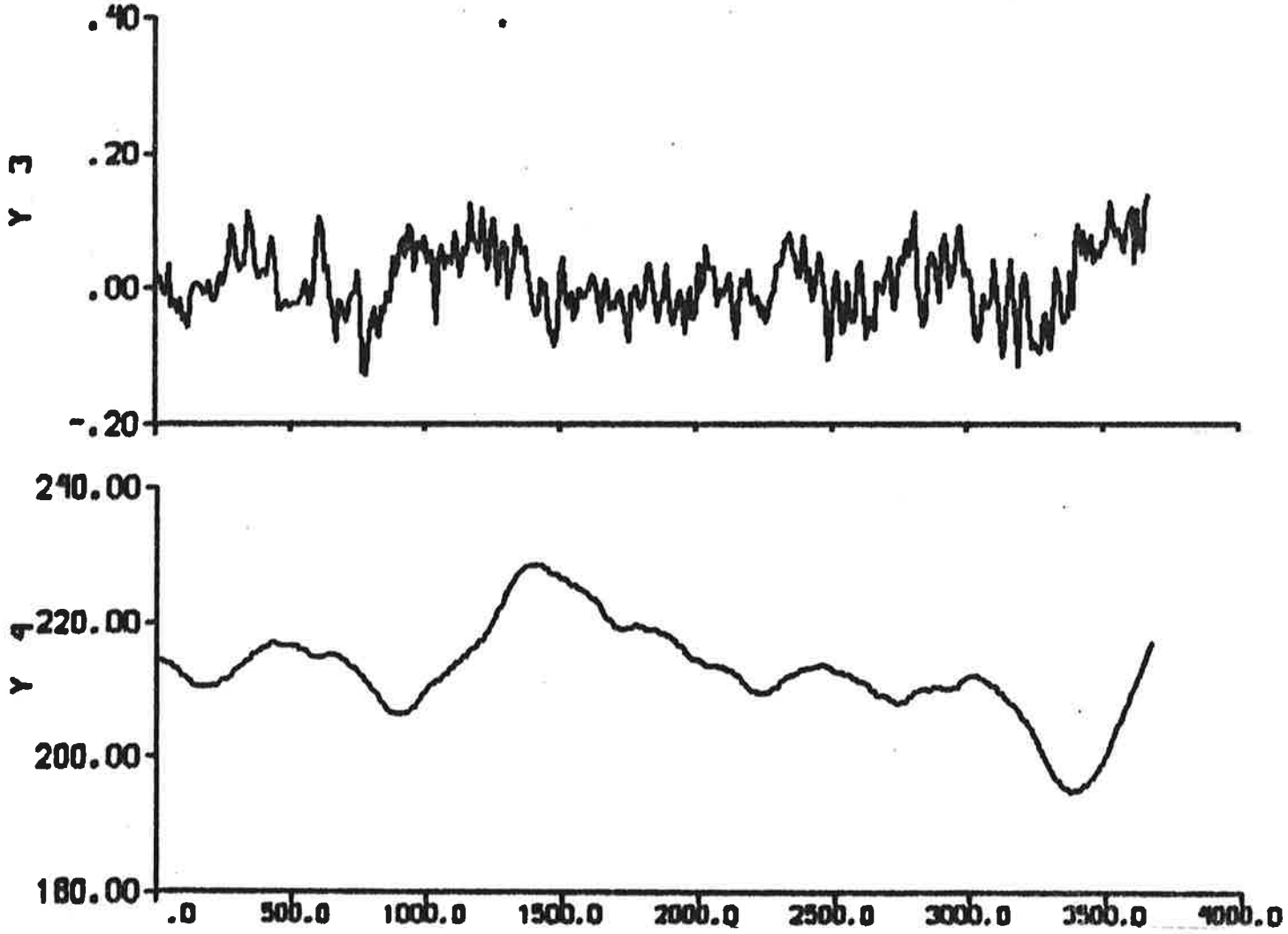
.40
.20
.00
-.20
Y 3
240.00
220.00
200.00
180.00
Y 4
.0
500.0
1000.0
1500.0
2000.0
2500.0
3000.0
3500.0
4000.0
Time [s]

Fig. 2.4b

The standard measurement equipment onboard the Sea Swift was used for the experiments. The sway velocities were measured by a doppler sonar equipment, type Ametek Straza, with a resolution of about 0.02 knots. The distance L_1 from midship to the fore doppler log was 155.68 m and the distance L_2 to the aft doppler log was 124.09 m. The yaw rates were measured by a rate gyro from AB ATEW, Flen, Sweden. The drift rate given by the manufacturer is 3 deg/h (0.0008 deg/s). However, the quality of the rate gyro signal varies with the sea conditions and the way the gyro is mounted, and an accuracy of about 0.005 deg/s seems to be realistic. The heading angles were measured by a Sperry gyro compass with an accuracy of about 0.1 deg. The heading signal was transformed by a synchro-digital converter with an accuracy of about 0.02 deg. Notice that the doppler sonar and the rate gyro may have biases. Figures 2.1 - 2.4 show that the bias of the fore sway velocity is approximately -0.4 knots.

3. SHIP STEERING DYNAMICS

The identification results described in Sections 4 and 5 are based on the following model of the ship steering dynamics (Åström, Norrbin, Källström and Byström, 1974; Åström, Källström, Norrbin and Byström, 1975):

$$\begin{bmatrix} \frac{L}{V^2}\theta_1 & \frac{L^2}{V^2}\theta_2 & 0 \\ \frac{L}{V^2}\theta_3 & \frac{L^2}{V^2}\theta_4 & 0 \\ 0 & 0 & 1 \end{bmatrix} \begin{bmatrix} dv \\ dr \\ d\psi \end{bmatrix} = \begin{bmatrix} \frac{1}{V}\theta_5 & \frac{L}{V}\theta_6 & \theta_9 \\ \frac{1}{V}\theta_7 & \frac{L}{V}\theta_8 & \theta_9\cdot\theta_{10} \\ 0 & 1 & 0 \end{bmatrix} \begin{bmatrix} v(t) \\ r(t) \\ \psi(t) \end{bmatrix} \cdot dt +$$

$$+ \begin{bmatrix} \alpha_1\cdot\theta_{11} & \theta_{13} \\ -\alpha_1\cdot\theta_{11}\theta_{12} & \theta_{14} \\ 0 & 0 \end{bmatrix} \begin{bmatrix} \delta(t-T_D) \\ U \end{bmatrix} \cdot dt + \theta_{35} \cdot \begin{bmatrix} f_Y(v,r) \\ f_N(v,r) \\ 0 \end{bmatrix} \cdot dt + dw \qquad (3.1)$$

$$\begin{bmatrix} v_1(t_k) \\ v_2(t_k) \\ r_m(t_k) \\ \psi_m(t_k) \end{bmatrix} = \begin{bmatrix} \alpha_2 & L_1\alpha_2 & 0 \\ \alpha_2 & -L_2\alpha_2 & 0 \\ 0 & 1/\alpha_1 & 0 \\ 0 & 0 & 1/\alpha_1 \end{bmatrix} \begin{bmatrix} v(t_k) \\ r(t_k) \\ \psi(t_k) \end{bmatrix} +$$

$$+ \begin{bmatrix} 0 & \theta_{15} \\ 0 & \theta_{16} \\ 0 & \theta_{17} \\ 0 & 0 \end{bmatrix} \begin{bmatrix} \delta(t_k - T_D) \\ U \end{bmatrix} + e(t_k) \qquad k = 0,1,\ldots,N-1$$

The Wiener process w has the incremental covariance $R_1 dt$, where

$$R_1 = \begin{bmatrix} |\theta_{18}| & \sqrt{|\theta_{18}||\theta_{19}|}\sin\theta_{20} & 0 \\ \sqrt{|\theta_{18}||\theta_{19}|}\sin\theta_{20} & |\theta_{19}| & 0 \\ 0 & 0 & 0 \end{bmatrix}$$

The measurement errors $\{e(t_k)\}$ are assumed to be independent and gaussian with zero mean and covariance R_2, where

$$R_2 = \begin{bmatrix} |\theta_{21}| & 0 & 0 & 0 \\ 0 & |\theta_{22}| & 0 & 0 \\ 0 & 0 & |\theta_{23}| & 0 \\ 0 & 0 & 0 & |\theta_{24}| \end{bmatrix}$$

The initial state is given by

$$\begin{bmatrix} v(t_0) \\ r(t_0) \\ \psi(t_0) \end{bmatrix} = \begin{bmatrix} \theta_{25}/\alpha_2 \\ \alpha_1\ \theta_{26} \\ \alpha_1\ \theta_{27} \end{bmatrix}$$

and the time delay T_D is computed as

$$T_D = T_s - T_s\ |\sin \theta_{34}|$$

where T_s is the sampling interval.

The following variables are introduced in (3.1):

Inputs

δ - rudder command [deg]
U - artificial unit step input [-]

States

v - sway velocity at midship [m/s]
r - yaw rate [rad/s]
ψ - heading angle [rad]

Outputs

v_1 - fore sway velocity [knots]
v_2 - aft sway velocity [knots]
r_m - yaw rate [deg/s]
ψ_m - heading angle [deg]

The model (3.1) is provided with the following fixed parameter values:

V - ship speed (8.75 m/s)
L - ship length (329.18 m)
L_1 - distance from midship to fore doppler log (155.68 m)
L_2 - distance from midship to aft doppler log (124.09 m)
α_1 - conversion factor from degrees to radians (0.01745)
α_2 - conversion factor from m/s to knots (1.944)
T_s - sampling interval (10 s)

The parameters θ_1 - θ_{35} can be estimated in LISPID. Notice, however, that it is possible to estimate only a subset of the 35 parameters and to give the other parameters arbitrary fixed values. The parameters θ_{28} - θ_{33} have been omitted in the model (3.1), because they have no meaning for the analysis performed in this report. It is concluded from (3.1) that θ_1 - θ_4 are normalized acceleration hydrodynamic derivatives, θ_5 - θ_8, θ_{11} and $-\theta_{11}\theta_{12}$ are normalized linear hydrodynamic derivatives, θ_9 and θ_{10} are wind parameters, θ_{13} and θ_{14} are force and moment biases, and θ_{15} - θ_{17} are measurement biases. The time delay T_D can be regarded as an approximation of the effective time constant of the steering engine (Källström, 1977c).

The only unknown parameter of the nonlinear contributions in the model (3.1) is the effective cross-flow drag coefficient $\theta_{35} = C$. The value is expected to be of the order of $0.4 < C < 1.4$. The commonly used linear model of the steering dynamics is obtained from (3.1) if $\theta_{35} = 0$. The nonlinear functions f_Y and f_N have been derived in Norrbin (1976) by considering the cross-flow drag. The nonlinear model (3.1) is in LISPID transformed into a linear model by introducing f_Y/m' and f_N/m' as additional inputs, where $m' = 2\nabla/L^3 = 0.01594$. The functions f_Y and f_N are dependent on the true sway velocity v and the true yaw rate r, which are unknown. The estimates $\hat{x}_1$ and $\hat{x}_2$ of v and r obtained through the filter

$$\begin{aligned} \hat{x}(t_{k+1}|t_k) &= A\,\hat{x}(t_k|t_k) + Bu(t_k) \\ \hat{x}(t_k|t_k) &= \hat{x}(t_k|t_{k-1}) + \bar{K}[y(t_k) - C\hat{x}(t_k|t_{k-1}) - Du(t_k)] \\ & \qquad k = 0,\ldots,N-1 \end{aligned} \tag{3.2}$$

are instead used when the additional inputs are generated. The input vector u, the state vector $\hat{x}$, and the output vector y are the same as in the model (3.1). The filter (3.2) is obtained from (3.1) by assuming $\theta_{35} = 0$ and by sampling. The stationary filter gain $\bar{K}$ is calculated by solving an appropriate, discrete

Riccati equation (Åström, 1970). Notice that $\bar{K} = 0$ if there is no process noise in (3.1), i.e. when $w = 0$. The problem of estimating unknown parameters in the nonlinear model (3.1) with $\theta_{35} \neq 0$ is thus transformed into the much easier problem of estimating parameters in a linear model.

The unknown parameters are in LISPID estimated with the prediction error method by minimizing the loss function

$$V = \frac{1}{N-p} \det \left[\sum_{k=p}^{N-1} \varepsilon_p(t_k) \varepsilon_p^T(t_k) \right] \tag{3.3}$$

where N is the number of samples. The p-step prediction errors ε_p are determined recursively from the innovations representation (see Källström, Essebo and Åström, 1976):

$$\begin{aligned}
&\varepsilon_p(t_k) = y(t_k) - C\,\hat{x}(t_k|t_{k-p}) - Du(t_k) \\
&\hat{x}(t_{i+1}|t_{k-p}) = A\,\hat{x}(t_i|t_{k-p}) + Bu(t_i), \quad i=k-p+1,\ldots,k-1 \\
&\hat{x}(t_{k-p+1}|t_{k-p}) = A\,\hat{x}(t_{k-p}|t_{k-p-1}) + Bu(t_{k-p}) + K\varepsilon_o(t_{k-p}) \\
&\varepsilon_o(t_{k-p}) = y(t_{k-p}) - C\,\hat{x}(t_{k-p}|t_{k-p-1}) - Du(t_{k-p}) \\
&\quad k = p,\ldots,N-1
\end{aligned} \tag{3.4}$$

Notice that $K = A\bar{K}$ and that the last two equations of (3.4) and (3.2) are equivalent if $\theta_{35} = 0$, i.e. if a linear model is used. The input vector u of (3.4) also contains the additional inputs when $\theta_{35} \neq 0$, i.e. when a nonlinear model is analysed.

The one-step prediction errors, i.e. the residuals, are minimized in the maximum likelihood method. This method is in LISPID obtained by assigning p=0 in (3.3) and (3.4), and by only using the last two equations of (3.4). The case p=1 has no meaning in LISPID. The output error method is easily obtained from the maximum likelihood method by assuming no process noise in (3.1), i.e. w=0. This implies that K=0 in (3.4). Different models obtained by the output error method and the maximum likelihood method can be compared by using Akaike's information criterion (Akaike, 1972):

$$AIC = -2 \log \hat{L} + 2\nu \qquad (3.5)$$

where $\hat{L}$ is the maximum of the likelihood function and ν is the number of estimated parameters. According to Akaike the quantity AIC should be minimum for the correct model structure. The following relation is obtained from (3.3) and (3.5):

$$AIC = (N-p)\log V + 2\nu + (1-n_y)(N-p)\log(N-p) + n_y(N-p)(1+\log 2\pi) \qquad (3.6)$$

where n_y is the number of outputs from the model.

The program LISPID allows for both uniform and varying sampling. The data from the Sea Swift experiments were, however, recorded with a constant sampling interval, so the nonuniform sampling facility will not be used.

It was concluded in Källström (1977a) that it is questionable if the wind parameters θ_9 and θ_{10} should be estimated, when the wind speed is less than 10 m/s. Since the wind speed was less than 4 m/s during the Sea Swift experiments it is decided to assume $\theta_9 = \theta_{10} = 0$.

The transfer function relating the heading ψ to the rudder angle δ (in radians), when the wind parameters θ_9 and θ_{10}, the time delay T_D, and the parameter θ_{35} are zero, is obtained from (3.1):

$$G_{\psi\delta}(s) = \frac{K(1+sT_3)}{s(1+sT_1)(1+sT_2)} = \frac{K_1\,(s+1/T_3)}{s(s+1/T_1)\,(s+1/T_2)} \qquad (3.7)$$

where $K_1 = \dfrac{KT_3}{T_1T_2}$. The corresponding transfer function relating

the sway velocity v to the rudder angle δ (in radians) is

$$G_{v\delta}(s) = \frac{K_v(1+sT_{3v})}{(1+sT_1)(1+sT_2)} = \frac{K_{1v}(s+1/T_{3v})}{(s+1/T_1)(s+1/T_2)} \qquad (3.8)$$

where $K_{1v} = \frac{K_v T_{3v}}{T_1 T_2}$. It is customary to normalize the gains and time constants of (3.7) and (3.8) by use of the 'prime' system:

$$\begin{aligned} K' &= K \cdot L/V & T_1' &= T_1 \cdot V/L \\ K_1' &= K_1 \cdot L^2/V^2 & T_2' &= T_2 \cdot V/L \\ K_v' &= K_v/V & T_3' &= T_3 \cdot V/L \\ K_{1v}' &= K_{1v} \cdot L/V^2 & T_{3v}' &= T_{3v} \cdot V/L \end{aligned} \qquad (3.9)$$

The identifiability aspects of the model (3.1) were discussed in Åström and Källström (1973, 1976). The linear hydrodynamic derivatives $\theta_5 - \theta_8$, θ_{11}, $-\theta_{11}\theta_{12}$, the wind parameters $\theta_9 - \theta_{10}$, the biases $\theta_{13} - \theta_{17}$, and the parameter θ_{35} can be determined if the acceleration hydrodynamic derivatives $\theta_1 - \theta_4$ are known and if the parameter values are such that the model (3.1) is completely observable and completely controllable. It is necessary that measurements of the sway velocity are available together with measurements of the yaw rate or the heading angle. All parameters $\theta_{18} - \theta_{24}$ of the covariance matrices R_1 and R_2 can not be determined when the prediction error method or the maximum likelihood method is applied, since it is possible to multiply R_1 and R_2 by an arbitrary coefficient and still obtain the same filter gain K (cf. (3.4)). Therefore, the parameter θ_{24} is always fixed in the sequel.

The hydrodynamic derivatives of the linear model (3.1) have been estimated by SSPA from model tests with a tanker similar to the Sea Swift. The estimates are shown in Table 3.1. The acceleration derivatives θ_1 - θ_4 are always fixed in the sequel to the values given in Table 3.1.

The transfer function relating the heading to the rudder angle is determined in Section 6. The only measurement signal used is the heading. The following state space model is then used in LISPID (Åström, Norrbin, Källström and Byström, 1974; Åström, Källström, Norrbin and Byström, 1975):

$$\begin{pmatrix} dx_1 \\ dr \\ d\psi \end{pmatrix} = \begin{pmatrix} 0 & 0 & -\frac{V^3}{L^3}\varphi_3 \\ 1 & -\frac{V}{L}\varphi_1 & -\frac{V^2}{L^2}\varphi_2 \\ 0 & 1 & 0 \end{pmatrix} \begin{pmatrix} x_1(t) \\ r(t) \\ \psi(t) \end{pmatrix} dt +$$

$$+ \begin{pmatrix} \alpha_1 \frac{V^3}{L^3}\varphi_5 & \varphi_6 \\ \alpha_1 \frac{V^2}{L^2}\varphi_4 & \varphi_7 \\ 0 & 0 \end{pmatrix} \begin{pmatrix} \delta(t-T_D) \\ U \end{pmatrix} dt + dw \qquad (3.10)$$

$$\psi_m(t_k) = [0 \quad 0 \quad 1/\alpha_1] \begin{pmatrix} x_1(t_k) \\ r(t_k) \\ \psi(t_k) \end{pmatrix} + e(t_k) \quad k = 0,1,\ldots, N-1$$

The Wiener process w has the incremental covariance R_1 dt, where

$$R_1 = \begin{pmatrix} |\varphi_9| & \sqrt{|\varphi_9|\,|\varphi_{10}|}\,\sin\varphi_{11} & 0 \\ \sqrt{|\varphi_9|\,|\varphi_{10}|}\,\sin\varphi_{11} & |\varphi_{10}| & 0 \\ 0 & 0 & 0 \end{pmatrix}$$

$m' - Y_{\dot{v}}'$	(θ_1)	0.02978
$m'x_G' - Y_{\dot{r}}'$	(θ_2)	0
$m'x_G' - N_{\dot{v}}'$	(θ_3)	0
$I_z' - N_{\dot{r}}'$	(θ_4)	0.00172
Y_v'	(θ_5)	-0.01422
$Y_r' - m'$	(θ_6)	-0.01152
N_v'	(θ_7)	-0.00738
$N_r' - m'x_G'$	(θ_8)	-0.00301
Y_δ'	(θ_{11})	0.00298
N_δ'	$(-\theta_{11}\theta_{12})$	-0.00140

Table 3.1 - Hydrodynamic derivatives estimated by SSPA. The estimates are adjusted values from model tests with a tanker similar to the Sea Swift. The hydrodynamic derivatives are normalized by use of the 'prime' system with mass unit $\rho L^3/2$. The corresponding values in the 'bis' system are obtained by dividing with m' = 0.01594. The origin of the co-ordinate system is assumed to be at midship.

The measurement errors $\{e(t_k)\}$ are assumed to be independent and gaussian with zero mean and covariance R_2, where $R_2 = |\varphi_{13}|$. The initial state is given by

$$\begin{pmatrix} x_1(t_0) \\ r(t_0) \\ \psi(t_0) \end{pmatrix} = \begin{pmatrix} \varphi_{15} \\ \alpha_1 \cdot \varphi_{16} \\ \alpha_1 \cdot \varphi_{17} \end{pmatrix}$$

and the time delay T_D is computed as

$$T_D = T_s - T_s \, |\sin \varphi_{24}|$$

where T_s is the sampling interval.

The notations are the same as in the model (3.1). The state x_1 $[1/s^2]$ is a linear combination of v, r and ψ. The parameters $\varphi_1 - \varphi_{24}$, or a subset of these parameters, can be estimated in LISPID. The parameters φ_8, φ_{12}, φ_{14}, $\varphi_{18} - \varphi_{23}$ have been omitted in the model (3.10), because they have no meaning for the analysis performed in this report. Notice that φ_3 is a wind parameter and that φ_6 and φ_7 are biases.

The transfer function relating the heading ψ to the rudder angle δ (in radians), when the time delay T_D is zero, is obtained from (3.10):

$$G_{\psi\delta}(s) = \frac{\frac{V^2}{L^2}\varphi_4 \, s + \frac{V^3}{L^3}\varphi_5}{s^3 + \frac{V}{L}\varphi_1 \, s^2 + \frac{V^2}{L^2}\varphi_2 \, s + \frac{V^3}{L^3}\varphi_3} \qquad (3.11)$$

If the wind parameter φ_3 is zero, (3.11) becomes (cf. (3.7)):

$$G_{\psi\delta}(s) = \frac{\frac{V^2}{L^2}\varphi_4 \, s + \frac{V^3}{L^3}\varphi_5}{s[s^2 + \frac{V}{L}\varphi_1 \, s + \frac{V^2}{L^2}\varphi_2]} = \tag{3.12}$$

$$= \frac{K(1+s\,T_3)}{s(1+sT_1)(1+sT_2)} = \frac{K_1(s+1/T_3)}{s(s+1/T_1)(s+1/T_2)}$$

Notice that Nomoto's model is obtained when $\varphi_2 = \varphi_5 = 0$:

$$G_{\psi\delta}(s) = \frac{\frac{V^2}{L^2}\varphi_4}{s(s+\frac{V}{L}\varphi_1)} = \frac{K}{s(1+sT)} = \frac{K_1}{s(s+1/T)} \tag{3.13}$$

where $K_1 = K/T$. The corresponding normalized parameters are defined by $K_1' = K_1 \cdot L^2/V^2$ and $T' = T \cdot V/L$ (cf. (3.9)).

The unknown parameters are in LISPID estimated by minimizing the loss function (3.3) and by using (3.4), where the recursion now is based on the model (3.10) instead of (3.1).

The identifiability aspects of the model (3.10) were discussed in Åström and Källström (1973, 1976). Tha parameters can be determined except in the case when there is a pole - zero cancellation. It is, however, necessary to fix one of the parameters of the covariance matrices R_1 and R_2, when the prediction error method or the maximum likelihood method is applied. Therefore, the parameter φ_{13} is always fixed in the sequel as well as the wind parameter φ_3.

The following transfer function parameters are obtained from SSPA:s model (Table 3.1):

$$\begin{aligned} \varphi_1 &= 2.23 \\ \varphi_2 &= -0.82 \\ \varphi_4 &= -0.82 \\ \varphi_5 &= -0.82 \end{aligned} \qquad (3.14)$$

The sampled version of the model (3.10) can be represented by the difference equation model

$$\psi_m(t) + a_1 \psi_m(t-1) + \ldots + a_n \psi_m(t-n) =$$

$$= b_1 \delta(t-1) + \ldots + b_n \delta(t-n) + \qquad (3.15)$$

$$+ \lambda[e(t) + c_1 e(t-1) + \ldots + c_n e(t-n)]$$

where a constant, unit sampling interval is assumed and where $\{e(t)\}$ is a sequence of random variables which accounts for the combined effect of process disturbances and measurement errors. The maximum likelihood estimation of the parameters of (3.15) can be simplified significantly as described in Åström and Bohlin (1965). The interactive program IDPAC (Wieslander, 1976) performs this. The program minimizes the loss function

$$V = \frac{1}{N} \sum_{0}^{N-1} \varepsilon^2(t) \qquad (3.16)$$

which is a special case of (3.3). Notice that (3.16) can be combined with (3.6).

If Nomoto's model (3.13) is combined with a time delay T_D describing the steering engine, then the following transfer function is obtained:

$$G_{\psi\delta}(s) = \frac{K}{s(1+sT)} e^{-sT_D} \qquad (3.17)$$

The discrete time model (cf. (3.15))

$$\psi_m(t) + a_1 \psi_m(t-1) + a_2 \psi_m(t-2) = \\ = b_1 \delta(t-1) + b_2 \delta(t-2) + b_3 \delta(t-3) \tag{3.18}$$

is obtained by sampling (3.17), where

$$a_1 = -(e^{-T_s/T} + 1)$$

$$a_2 = e^{-T_s/T}$$

$$b_1 = K[T\, e^{(T_D-T_s)/T} + T_s - T_D - T] \tag{3.19}$$

$$b_2 = -K[2T\, e^{(T_D-T_s)/T} + (T_s-T_D - T)\, e^{-T_s/T-T_D-T}]$$

$$b_3 = K[T\, e^{(T_D-T_s)/T} - (T_D + T)\, e^{-T_s/T}]$$

and where T_s is the sampling interval. Notice that $b_3 = 0$ when $T_D = 0$. If the parameters of the model (3.18) are known, then the parameters of (3.17) can be computed through

$$K = \frac{b_1+b_2+b_3}{T_s(1-a_2)}$$

$$T = -\frac{T_s}{\log a_2} \tag{3.20}$$

$$T_D = T_s \left[\frac{1}{\log a_2} + \frac{1}{1-a_2} + \frac{b_3-b_1}{b_1+b_2+b_3}\right]$$

provided that the model (3.18) has been obtained by sampling (3.17). One necessary conditon is $1 + a_1 + a_2 = 0$, i.e. (3.18) contains a pure integrator.

4. IDENTIFICATION OF LINEAR MODELS

Results of fitting the linear version of the model (3.1) to data from the 4 experiments are presented in this section. The following fixed parameter values are then used:

$$
\begin{aligned}
\theta_1 &= 0.02978 \\
\theta_2 &= 0 \\
\theta_3 &= 0 \\
\theta_4 &= 0.00172 \\
\theta_9 &= 0 \\
\theta_{10} &= 0 \\
\theta_{12} &= 0.471 \\
\theta_{24} &= 0.01 \text{ deg}^2 \\
\theta_{35} &= 0
\end{aligned}
\qquad (4.1)
$$

Notice that $\theta_{12} = -N_\delta'/Y_\delta'$ is fixed to the value obtained from SSPA:s model (Table 3.1). It was suggested in Källström (1977a and 1977b) to assign this relation a fixed value, since the relation is easy to determine from the hull geometry.

Estimated parameters from output error, ML and prediction error (p = 2, 3, 4) identifications are shown in Tables 4.1 - 4.4. The initial estimates are the values determined by SSPA (see Table 3.1). The results of output error, ML and prediction error (p = 4) identifications are shown in Figs 4.1 - 4.12. The continuous lines are the measurements and the dashed lines are the outputs of the deterministic models. The dashed lines in the diagrams of the correlation functions are the $\pm 2\sigma$-limits.

The models obtained from output error identifications to experiments E1 and E2 are strange. An improved model is determined from experiment E3. It is also concluded that a reasonable model is obtained when experiment E4 is analysed with the output error method. The estimated parameters are very close to the initial estimates in this case.

The models obtained by applying the ML method to data from the 4 experiments are strange in all cases. Notice, however, that Akaike´s information criterion AIC distinctly indicates that the process noise should be modelled.

The results are improved significantly when the prediction error method is applied. It is concluded that a prediction interval of 40 s, i.e. p = 4, is appropriate. Notice, however, that p = 2, 3 and 4 gave approximately the same results when experiment E1 was analysed. The parameter estimates obtained by applying the prediction error method with p = 4 to data from the 4 experiments do not differ much. An incorrect sign of the parameter $N_r' - m'x_G'$ was, however, obtained when experiment E4 was analysed. The following filter gains K (cf. (3.4)) are obtained from experiments E1, E2, E3 and E4 when p = 4:

$$K = \begin{pmatrix} 1.4 \cdot 10^{-1} & 2.3 \cdot 10^{-1} & -1.8 \cdot 10^{-1} & -7.6 \cdot 10^{-3} \\ -2.9 \cdot 10^{-5} & -8.2 \cdot 10^{-5} & 1.4 \cdot 10^{-3} & 2.2 \cdot 10^{-4} \\ 9.5 \cdot 10^{-5} & -8.3 \cdot 10^{-4} & 3.6 \cdot 10^{-2} & 1.0 \cdot 10^{-2} \end{pmatrix} \quad (4.2)$$

$$K = \begin{pmatrix} 1.4 \cdot 10^{-1} & 2.9 \cdot 10^{-1} & -4.7 \cdot 10^{-1} & 9.3 \cdot 10^{-3} \\ 5.1 \cdot 10^{-6} & -3.8 \cdot 10^{-4} & 4.5 \cdot 10^{-3} & 4.8 \cdot 10^{-4} \\ 2.3 \cdot 10^{-3} & -4.2 \cdot 10^{-3} & 9.6 \cdot 10^{-2} & 1.8 \cdot 10^{-2} \end{pmatrix} \quad (4.3)$$

$$K = \begin{pmatrix} 9.7 \cdot 10^{-6} & 4.0 \cdot 10^{-1} & 1.2 \cdot 10^{-1} & 2.2 \cdot 10^{-2} \\ 1.6 \cdot 10^{-7} & -3.9 \cdot 10^{-4} & 2.0 \cdot 10^{-3} & 3.7 \cdot 10^{-4} \\ 4.7 \cdot 10^{-6} & -3.1 \cdot 10^{-3} & 6.0 \cdot 10^{-2} & 1.7 \cdot 10^{-2} \end{pmatrix} \quad (4.4)$$

$$K = \begin{pmatrix} 1.6 \cdot 10^{-1} & 2.6 \cdot 10^{-1} & -1.4 \cdot 10^{-1} & -1.0 \cdot 10^{-2} \\ 6.0 \cdot 10^{-4} & -6.3 \cdot 10^{-4} & 3.1 \cdot 10^{-3} & 2.6 \cdot 10^{-4} \\ 1.1 \cdot 10^{-2} & -1.1 \cdot 10^{-2} & 5.5 \cdot 10^{-2} & 1.8 \cdot 10^{-2} \end{pmatrix} \quad (4.5)$$

Notice that it was necessary to fix the parameter θ_{23} of the covariance matrix R_2 and the parameters θ_{25} - θ_{27} of the initial state to obtain reasonable models when the prediction error method was applied.

The outputs of the deterministic models obtained by applying the ML and the prediction error methods differ in many cases significantly from the measurements. An improved consistency can, however, easily be achieved by readjusting the biases and the initial states.

The time delay T_D of Tables 4.1 - 4.4 can be regarded as an approximation of the effective time constant of the steering engine. The value is known to be of the order of 5 s.

It is difficult to decide which of the models obtained with $p = 4$ that is the best one. The 4 models are further investigated by fitting the biases, the initial state, and the time delay to data from the 4 experiments by use of the output error method. The hydrodynamic derivatives are then fixed. The results are summarized in Table 4.5 and the plots are shown in Figs. 4.13 - 4.28. The performances of the 4 models do not differ much, but it is concluded that the model obtained from experiment E4 (model D) is slightly better than the other models.

	Initial estimates	Output error	M L	Prediction error p = 2	p = 3	p = 4
Figure		4.1	4.2	-	-	4.3
ν		14	20	16	16	16
V		3450.1	0.3	2.4	5.8	11.5
AIC		517	-3866	-	-	-
Y_v'	-0.01422	-0.01519	-0.01557	-0.03199	-0.02905	-0.02754
$Y_r' - m'$	-0.01152	-0.01155	-0.00953	-0.01831	-0.01675	-0.01586
N_v'	-0.00738	0.00052	0.00002	-0.00044	-0.00042	-0.00042
$N_r' - m'x_G'$	-0.00301	0.00028	0.00002	-0.00012	-0.00012	-0.00011
Y_δ'	0.00298	0.00030	0.00054	0.00143	0.00141	0.00141
N_δ'	-0.00140	-0.00014	-0.00026	-0.00067	-0.00067	-0.00067
$\theta_{13} \cdot 10^5$		0.9	-0.1	5.8	5.4	4.8
$\theta_{14} \cdot 10^6$		0.5	2.2	5.7	5.7	5.6
θ_{15} [knots]		-0.41	-0.41	-0.44	-0.44	-0.44
θ_{16} [knots]		-0.13	-0.14	-0.17	-0.17	-0.17
θ_{17} [deg/s]		0.006	0.006	0.006	0.006	0.006
$R_1(1,1)$ [s]		-	$3.1 \cdot 10^{-2}$	$1.5 \cdot 10^{-4}$	$1.8 \cdot 10^{-4}$	$1.5 \cdot 10^{-4}$
$R_1(1,2)$ [s]		-	$-1.1 \cdot 10^{-2}$	$1.0 \cdot 10^{-7}$	$1.4 \cdot 10^{-7}$	$9.8 \cdot 10^{-8}$
$R_1(2,2)$ [s]		-	$1.2 \cdot 10^{-2}$	$7.1 \cdot 10^{-11}$	$1.1 \cdot 10^{-10}$	$6.4 \cdot 10^{-11}$
$R_2(1,1)$ [knots]^2		-	$5.3 \cdot 10^{-5}$	$6.0 \cdot 10^{-2}$	$5.6 \cdot 10^{-2}$	$5.5 \cdot 10^{-2}$
$R_2(2,2)$ [knots]^2		-	$1.3 \cdot 10^{-4}$	$3.4 \cdot 10^{-2}$	$3.5 \cdot 10^{-2}$	$3.5 \cdot 10^{-2}$
$R_2(3,3)$ [deg/s]^2		-	$1.2 \cdot 10^{-5}$	10^{-4} *	10^{-4} *	10^{-4} *
θ_{25} [knots]		0.01	0.13	0*	0*	0*
θ_{26} [deg/s]		0.028	-0.033	0*	0*	0*
θ_{27} [deg]		213.77	214.30	214.41*	214.41*	214.41*
T_D [s]		9.8	7.9	5.8	6.3	6.4
K'	0.99	-1.15	34.75	5.24	5.46	5.18
K_1'	-0.82	-	-0.15	-0.39	-0.39	-0.39
K_v'	-0.60	0.89	-21.23	-2.96	-3.10	-2.93
K_{1v}'	0.10	-	0.02	0.05	0.05	0.05
T_1'	-3.09	complex	-230.99	-14.67	-15.54	-14.79
T_2'	0.39	poles	1.94	0.83	0.90	0.95
T_3'	1.00	2.11	1.92	0.90	0.99	1.05
T_{3v}'	0.20	0.33	0.38	0.20	0.21	0.23

* = fixed value

Table 4.1 - Estimated parameters from identifications to data from experiment E1.

	Initial estimates	Output error	M L	Prediction error		
				p = 2	p = 3	p = 4
Figure		4.4	4.5	-	-	4.6
ν		14	20	16	16	16
V		281.4	0.2	1.9	6.4	12.5
AIC		-187	-2734	-	-	-
Y_v'	-0.01422	-0.05864	-0.01628	-0.01987	-0.01986	-0.01988
$Y_r'-m'$	-0.01152	0.01489	-0.01685	-0.01638	-0.01543	-0.01507
N_v'	-0.00738	-0.00982	-0.00081	-0.00080	-0.00080	-0.00079
$N_r'-m'x_G'$	-0.00301	0.00195	-0.00006	-0.00032	-0.00030	-0.00029
Y_δ'	0.00298	0.00020	0.00018	0.00063	0.00126	0.00147
N_δ'	-0.00140	-0.00009	-0.00009	-0.00030	-0.00059	-0.00069
$\theta_{13}\cdot 10^5$		-9.5	-16.7	765.7	767.2	768.4
$\theta_{14}\cdot 10^6$		-15.9	-9.4	310.2	310.8	306.8
θ_{15} [knots]		-0.32	-0.16	-6.90	-6.91	-6.91
θ_{16} [knots]		-0.12	0.03	-6.69	-6.69	-6.68
θ_{17} [deg/s]		0.005	0.005	0.005	0.005	0.005
$R_1(1,1)$ [s]		-	$3.8\cdot 10^{-2}$	$6.0\cdot 10^{-2}$	$6.1\cdot 10^{-2}$	$8.8\cdot 10^{-3}$
$R_1(1,2)$ [s]		-	$-2.7\cdot 10^{-2}$	$-9.2\cdot 10^{-4}$	$-8.9\cdot 10^{-4}$	$-1.0\cdot 10^{-4}$
$R_1(2,2)$ [s]		-	$2.5\cdot 10^{-2}$	$1.4\cdot 10^{-5}$	$1.3\cdot 10^{-5}$	$1.2\cdot 10^{-6}$
$R_2(1,1)$ [knots]^2		-	$1.3\cdot 10^{-4}$	$8.4\cdot 10^{-3}$	$1.4\cdot 10^{-2}$	$2.0\cdot 10^{-2}$
$R_2(2,2)$ [knots]^2		-	$3.4\cdot 10^{-4}$	$5.8\cdot 10^{-3}$	$9.9\cdot 10^{-3}$	$1.1\cdot 10^{-2}$
$R_2(3,3)$ [deg/s]^2		-	$2.5\cdot 10^{-5}$	10^{-4*}	10^{-4*}	10^{-4*}
θ_{25} [knots]		-0.18	-0.03	0*	0*	0*
θ_{26} [deg/s]		-0.051	-0.071	0*	0*	0*
θ_{27} [deg]		211.84	209.95	2.09.86*	209.86*	2 09.86*
T_D [s]		10.0	0.9	9.4	9.1	9.7
K'	0.99	-0.23	0.12	0.95	1.99	2.43
K_1'	-0.82	-	-0.05	-0.17	-0.34	-0.40
K_v'	-0.60	-0.06	-0.12	-0.75	-1.48	-1.77
K_{1v}'	0.10	-	0.01	0.02	0.04	0.05
T_1'	-3.09	complex	-3.49	-7.44	-7.76	-8.04
T_2'	0.39	poles	1.15	1.01	1.03	1.04
T_3'	1.00	0.37	1.65	1.38	1.38	1.38
T_{3v}'	0.20	-0.19	0.22	0.21	0.23	0.23

* = fixed value

Table 4.2 - Estimated parameters from identifications to data from experiment E2.

	Initial estimates	Output error	M L	Prediction error		
				p = 2	p = 3	p = 4
Figure		4.7	4.8	-	-	4.9
ν		14	20	17	16	16
V		24.8	0.03	0.3	0.3	0.6
AIC		-301	-1726	-	-	-
Y_v'	-0.01422	-0.02468	-0.01265	-0.02064	-0.02901	-0.02451
$Y_r'-m'$	-0.01152	-0.01552	-0.01042	-0.01417	-0.01899	-0.01656
N_v'	-0.00738	-0.00043	0.00094	-0.00387	-0.00035	-0.00044
$N_r'-m'x_G'$	-0.00301	-0.00007	0.00062	-0.00176	-0.00013	-0.00016
Y_δ'	0.00298	0.00146	0.00013	0.00077	0.00168	0.00184
N_δ'	-0.00140	-0.00069	-0.00006	-0.00036	-0.00079	-0.00087
$\theta_{13}\cdot 10^5$		4.9	-12.6	31.1	33.1	29.6
$\theta_{14}\cdot 10^6$		-6.7	9.7	55.8	-4.5	-4.4
θ_{15} [knots]		-0.43	-0.24	-0.65	-0.57	-0.58
θ_{16} [knots]		-0.19	0.02	-0.38	-0.30	-0.30
θ_{17} [deg/s]		0.012	0.009	0.008	0.008	0.008
$R_1(1,1)$ [s]		-	$8.0\cdot 10^{-1}$	$2.0\cdot 10^{-2}$	$3.0\cdot 10^{-3}$	$2.8\cdot 10^{-3}$
$R_1(1,2)$ [s]		-	$-1.4\cdot 10^{-1}$	$-1.8\cdot 10^{-3}$	$-4.8\cdot 10^{-5}$	$-3.8\cdot 10^{-5}$
$R_1(2,2)$ [s]		-	$2.5\cdot 10^{-2}$	$1.7\cdot 10^{-4}$	$7.7\cdot 10^{-7}$	$5.1\cdot 10^{-7}$
$R_2(1,1)$ $[\text{knots}]^2$		-	$2.9\cdot 10^{-4}$	$6.7\cdot 10^{-4}$	8.8	12.0
$R_2(2,2)$ $[\text{knots}]^2$		-	$3.5\cdot 10^{-4}$	$3.2\cdot 10^{-4}$	$2.9\cdot 10^{-4}$	$5.3\cdot 10^{-6}$
$R_2(3,3)$ $[\text{deg/s}]^2$		-	$3.5\cdot 10^{-5}$	$4.2\cdot 10^{-6}$	10^{-4}*	10^{-4}*
θ_{25} [knots]		0.21	-0.19	0*	0*	0*
θ_{26} [deg/s]		-0.013	0.007	0*	0*	0*
θ_{27} [deg]		216.77	213.40	213.35*	213.35*	213.35*
T_D [s]		10.0	10.0	10.0	9.6	8.8
K'	0.99	3.58	-0.33	0.57	8.02	6.74
K_1'	-0.82	-0.40	-	-0.21	-0.46	-0.50
K_v'	-0.60	-2.19	0.28	-0.35	-5.19	-4.48
K_{1v}'	0.10	0.05	-	0.03	0.06	0.06
T_1'	-3.09	-10.06	complex	-5.30	-19.22	-15.34
T_2'	0.39	1.03	poles	0.52	0.91	1.02
T_3'	1.00	1.16	2.80	1.03	1.00	1.17
T_{3v}'	0.20	0.23	0.40	0.20	0.19	0.22

* = fixed value

Table 4.3 - Estimated parameters from identifications to data from experiment E3.

	Initial estimates	Output error	M L	Prediction error		
				p = 2	p = 3	p = 4
Figure		4.10	4.11	-	-	4.12
ν		14	20	16	16	16
V		293.2	0.06	0.9	1.8	3.9
AIC		-223	-3328	-	-	-
Y_v'		-0.01422	-0.01578	-0.01928	-0.02380	-0.02253	-0.02244
$Y_r'-m'$		-0.01152	-0.01106	-0.01376	-0.01686	-0.01573	-0.01556
N_v'		-0.00738	-0.00679	0.00045	-0.00002	-0.00004	-0.00003
$N_r'-m'x_G'$		-0.00301	-0.00377	0.00032	0.00015	0.00013	0.00009
Y_δ'		0.00298	0.00333	0.00047	0.00038	0.00080	0.00088
N_δ'		-0.00140	-0.00157	-0.00022	-0.00018	-0.00037	-0.00041
$\theta_{13}\cdot 10^5$			4.8	-27.4	1.4	-14.7	-14.4
$\theta_{14}\cdot 10^6$			-1.3	5.4	-0.5	-2.5	-2.7
θ_{15}	[knots]		-0.43	-0.17	-0.42	-0.30	-0.30
θ_{16}	[knots]		-0.19	0.06	-0.19	-0.07	-0.07
θ_{17}	[deg/s]		0.005	0.009	0.009	0.009	0.009
$R_1(1,1)$	[s]		-	$7.2\cdot 10^{-3}$	$6.6\cdot 10^{-1}$	3.7	4.6
$R_1(1,2)$	[s]		-	$-7.1\cdot 10^{-4}$	$-7.7\cdot 10^{-4}$	$-9.8\cdot 10^{-3}$	$-9.1\cdot 10^{-3}$
$R_1(2,2)$	[s]		-	$7.1\cdot 10^{-5}$	$9.1\cdot 10^{-7}$	$2.6\cdot 10^{-5}$	$1.8\cdot 10^{-5}$
$R_2(1,1)$	$[\text{knots}]^2$		-	$4.6\cdot 10^{-5}$	$1.1\cdot 10^{-1}$	$1.9\cdot 10^{-3}$	$2.3\cdot 10^{-3}$
$R_2(2,2)$	$[\text{knots}]^2$		-	$1.8\cdot 10^{-4}$	$6.0\cdot 10^{-2}$	$1.8\cdot 10^{-3}$	$2.0\cdot 10^{-3}$
$R_2(3,3)$	$[\text{deg/s}]^2$		-	$2.3\cdot 10^{-5}$	10^{-4}*	10^{-4}*	10^{-4}*
θ_{25}	[knots]		-0.09	-0.14	0*	0*	0*
θ_{26}	[deg/s]		0.008	-0.009	0*	0*	0*
θ_{27}	[deg]		205.54	214.38	214.41*	214.41*	214.41*
T_D	[s]		7.3	4.0	3.5	10.0	10.0
K'		0.99	3.03	34.21	1.08	2.31	3.71
K_1'		-0.82	-0.92	-0.13	-0.11	-0.22	-0.24
K_v'		-0.60	-1.92	-24.39	-0.75	-1.58	-2.53
K_{1v}'		0.10	0.11	0.02	0.01	0.03	0.03
T_1'		-3.09	-9.28	-200.74	-10.34	-10.77	-15.66
T_2'		0.39	0.35	2.15	1.24	1.29	1.31
T_3'		1.00	0.99	1.62	1.25	1.32	1.32
T_{3v}'		0.20	0.19	0.28	0.22	0.24	0.24

* = fixed value

Table 4.4 - Estimated parameters from identifications to data from experiment E4.

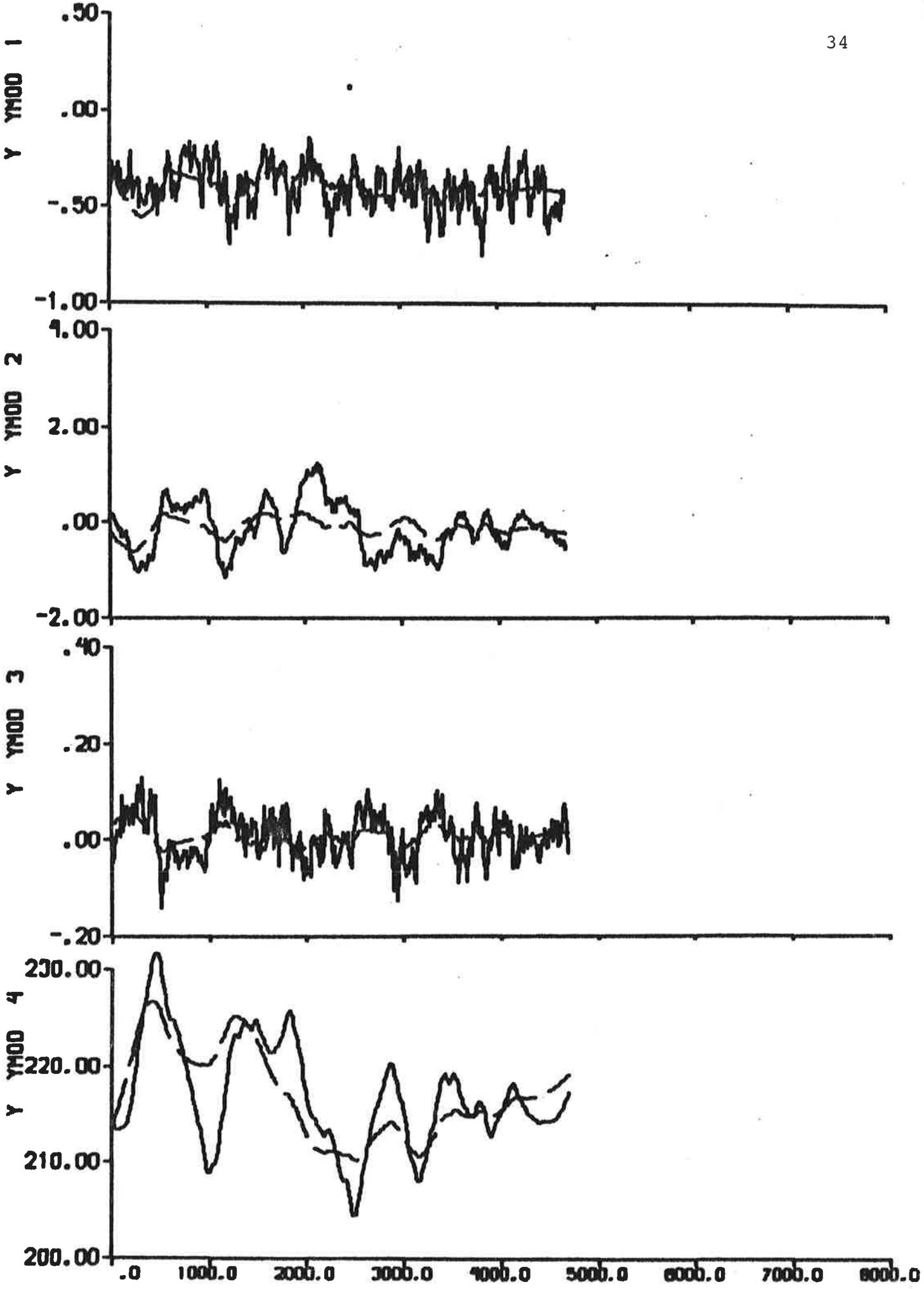

Fig. 4.1a - Result of output error identification to data from experiment E1.

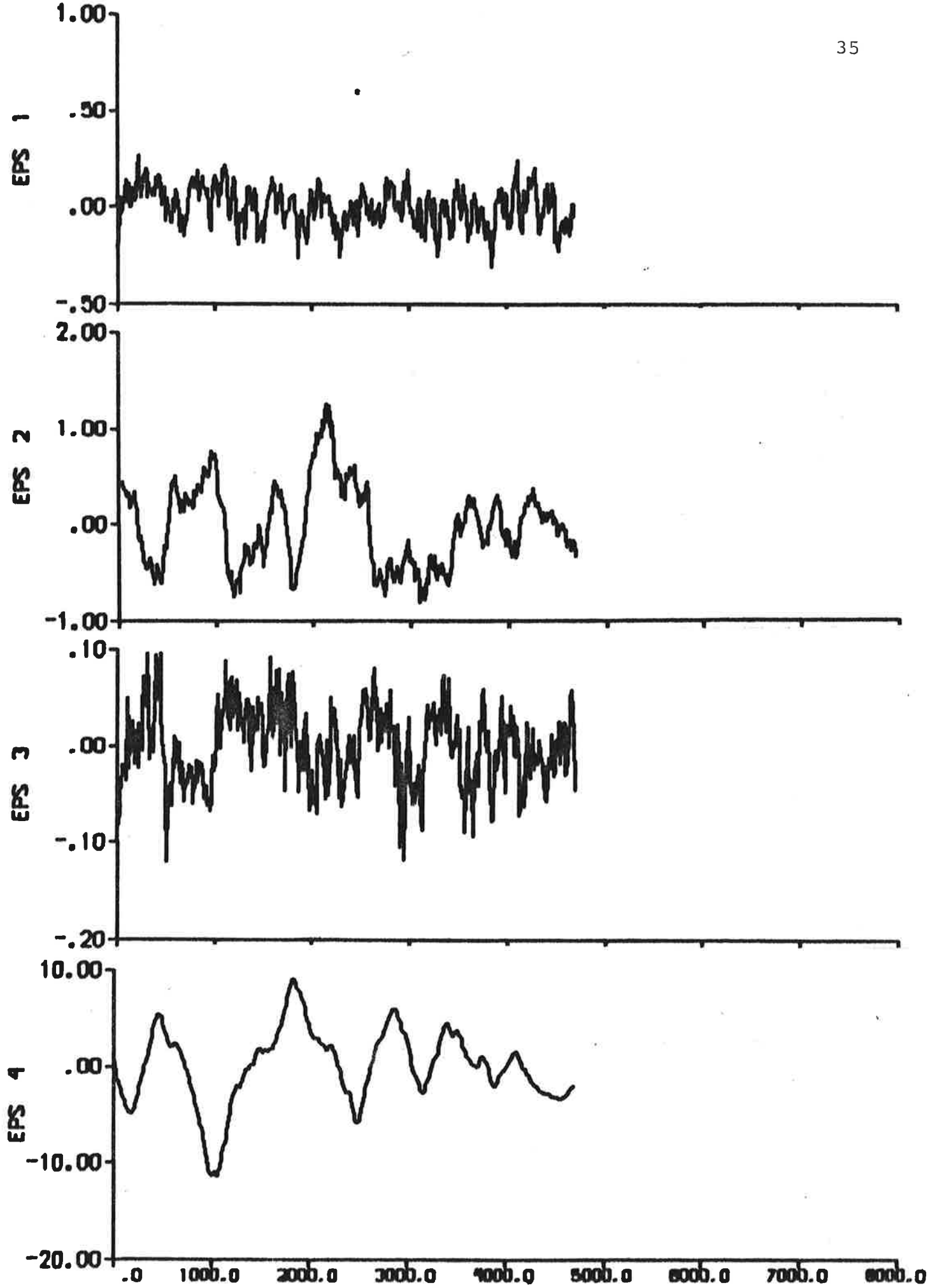

Fig. 4.1b - Prediction errors.

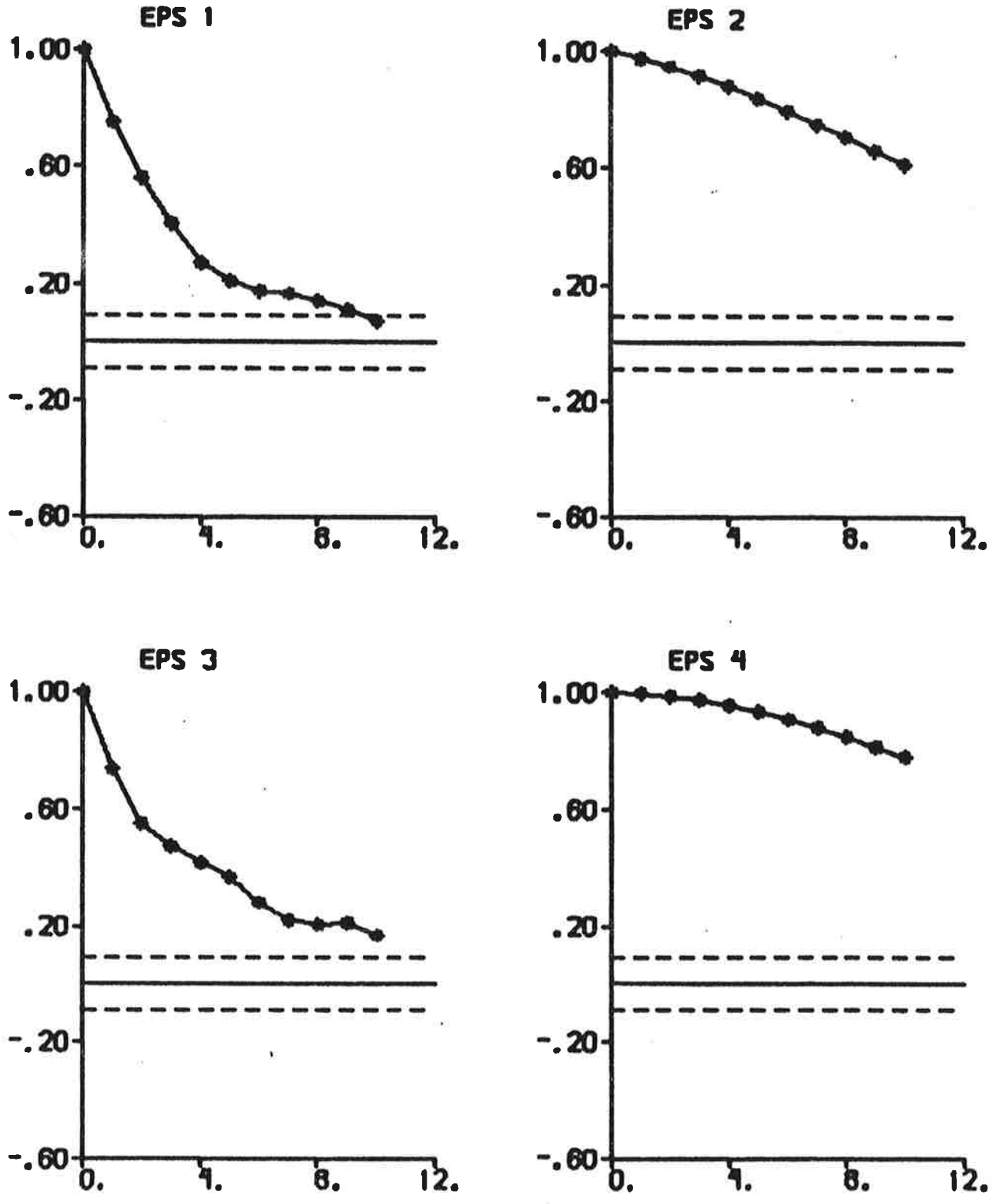

Fig. 4.1c - Autocorrelation functions of prediction errors.

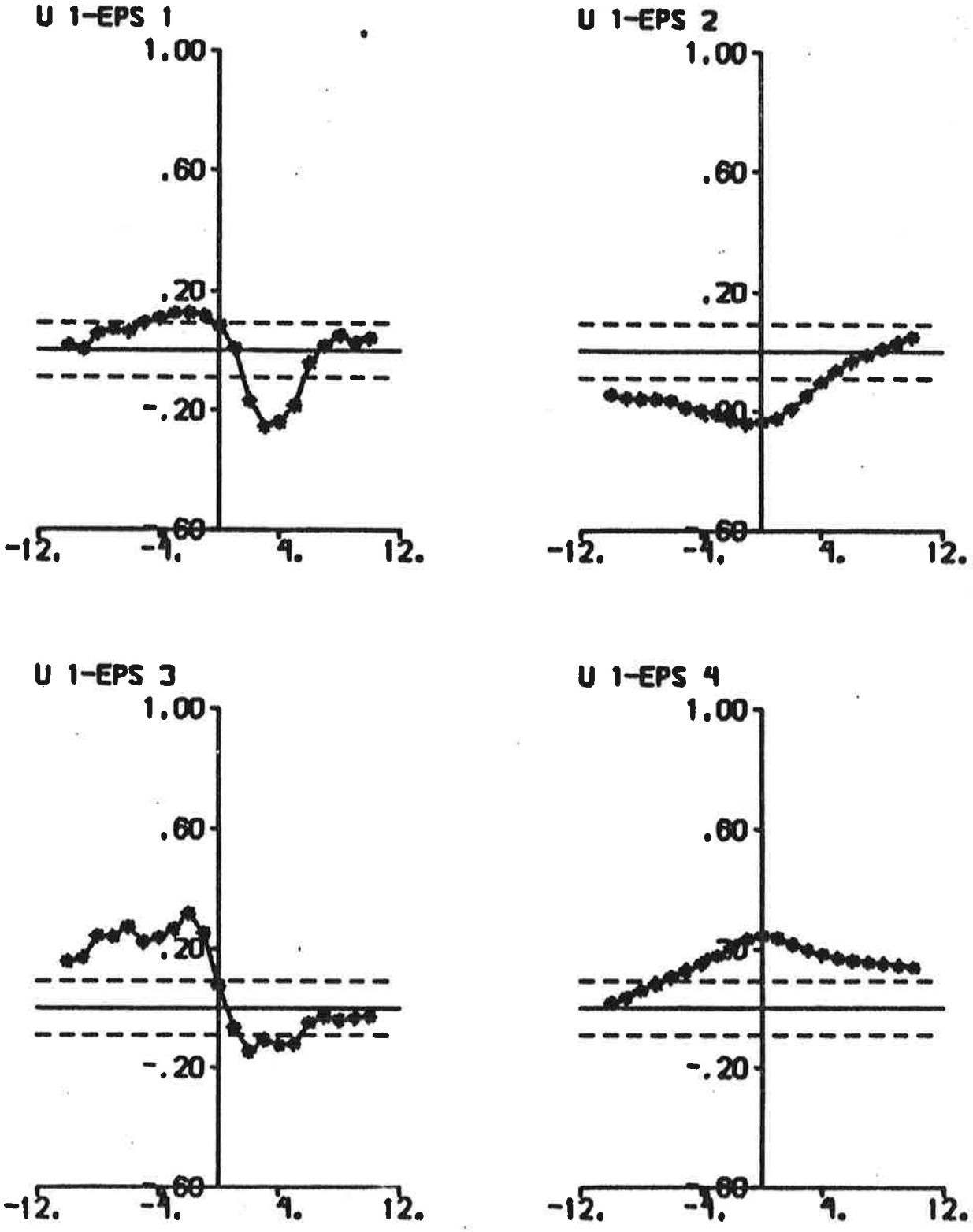

Fig. 4.1d - Cross correlation functions between rudder input and prediction errors.

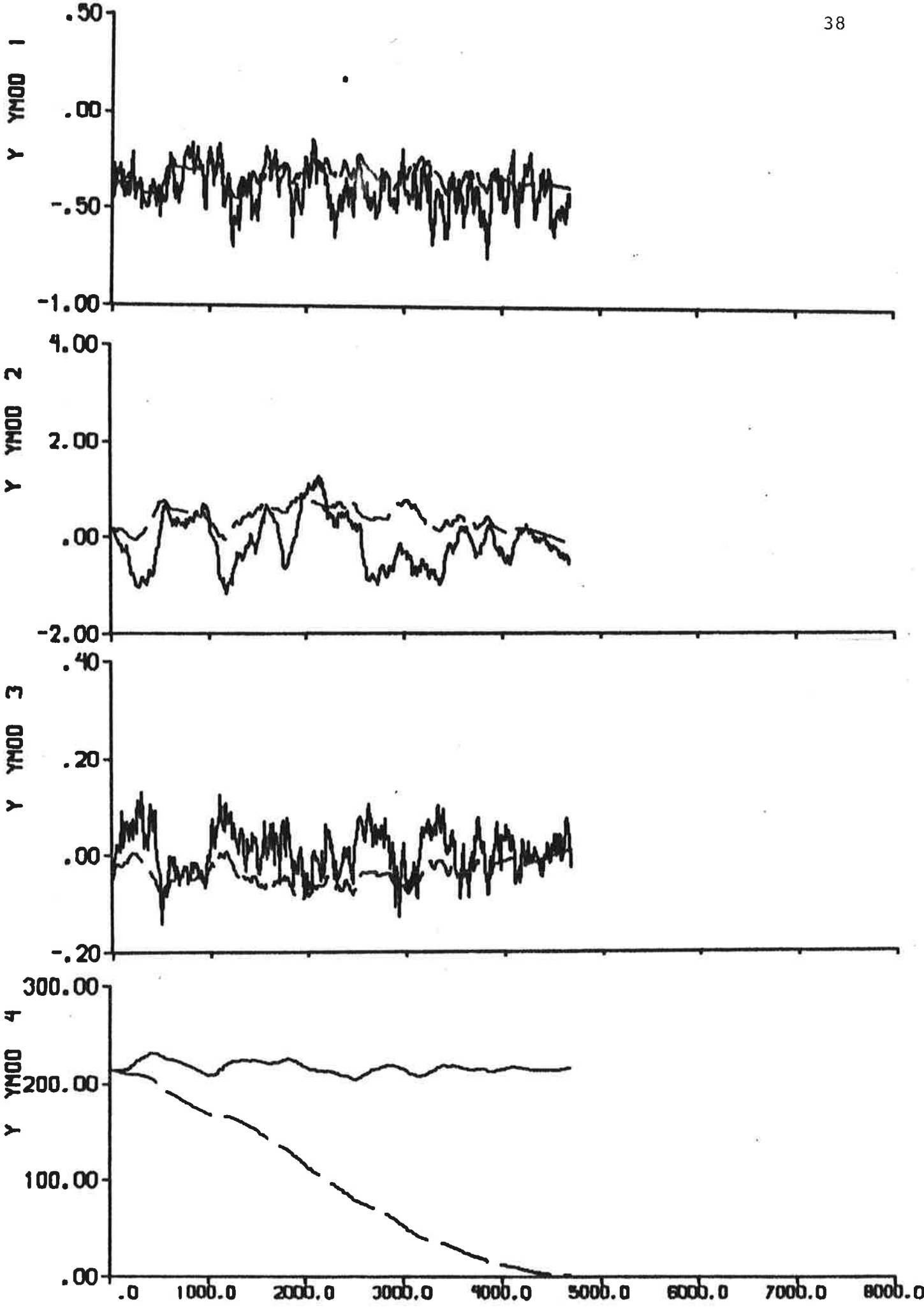

Fig. 4.2a - Result of ML identification to data from experiment E1.

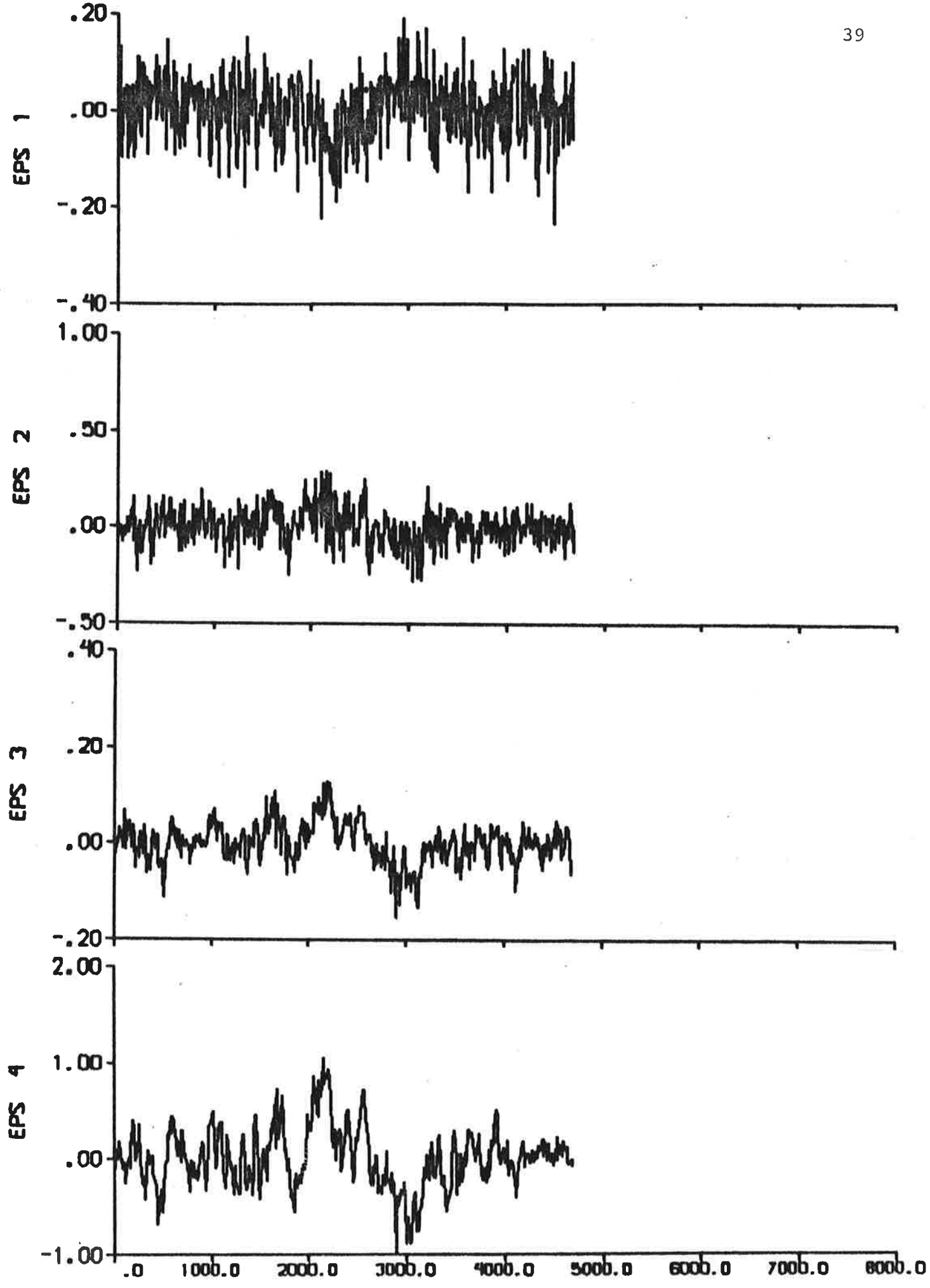

Fig. 4.2b - Prediction errors.

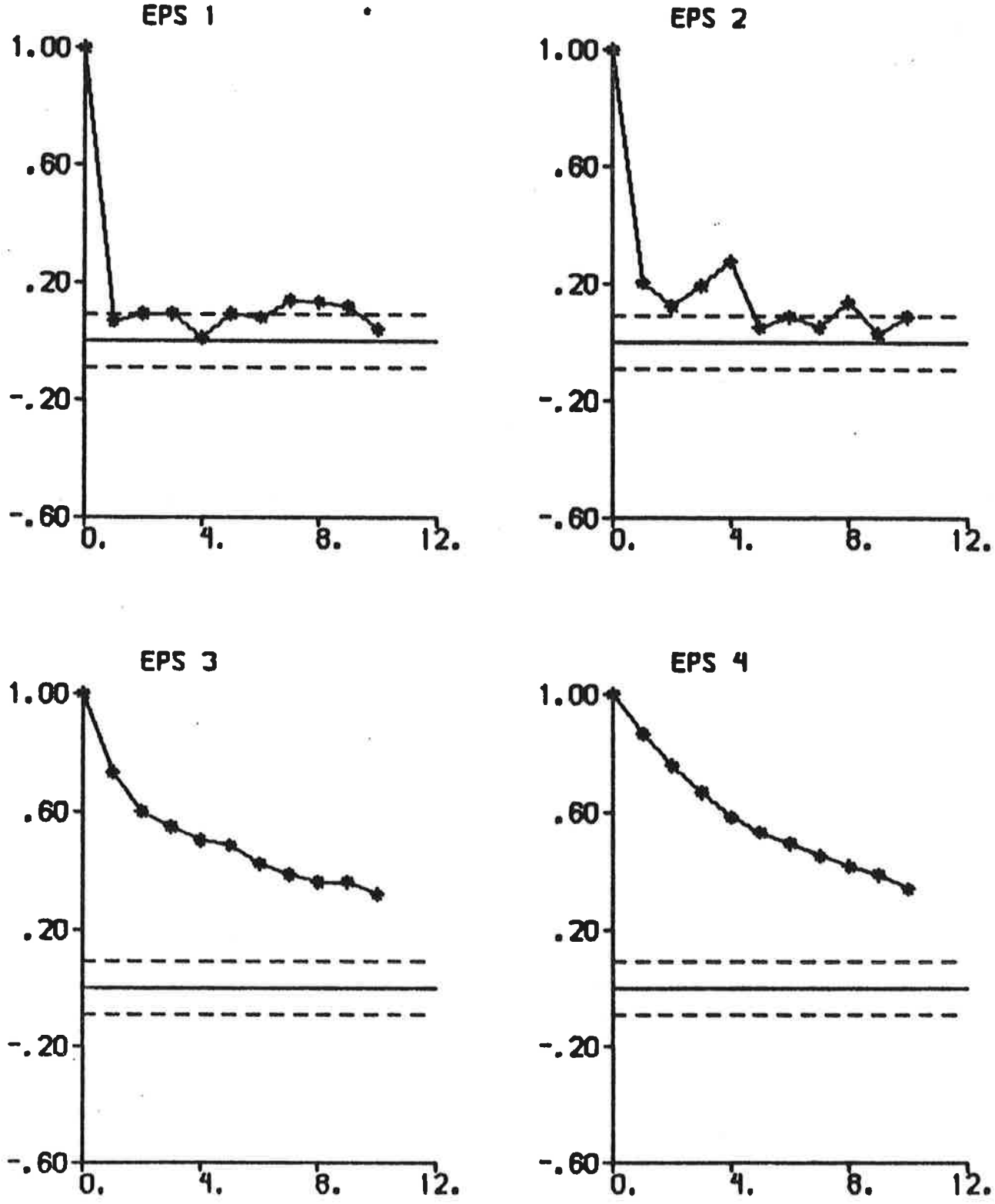

Fig. 4.2c - Autocorrelation functions of prediction errors.

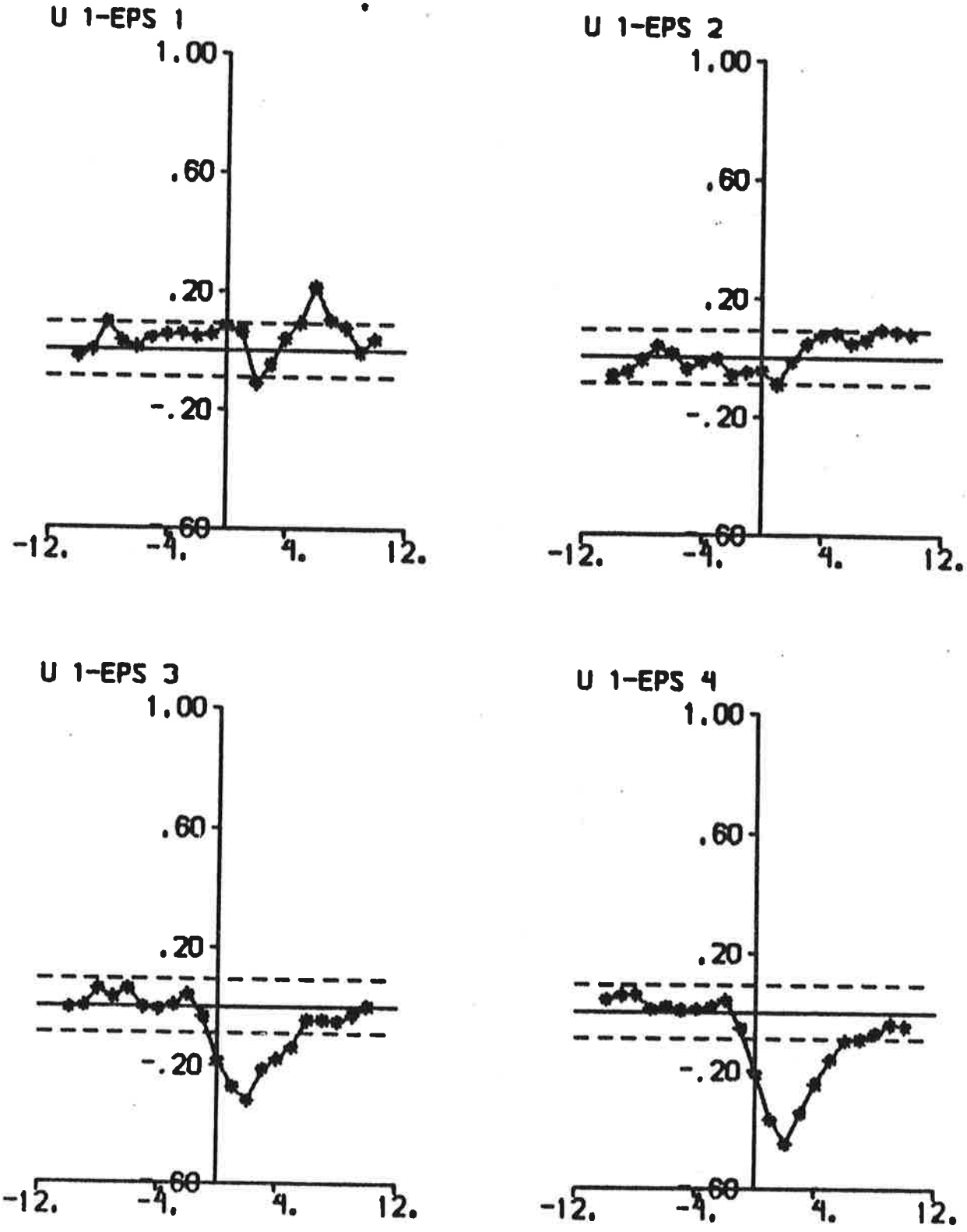

Fig. 4.2d - Cross correlation functions between rudder input and prediction errors.

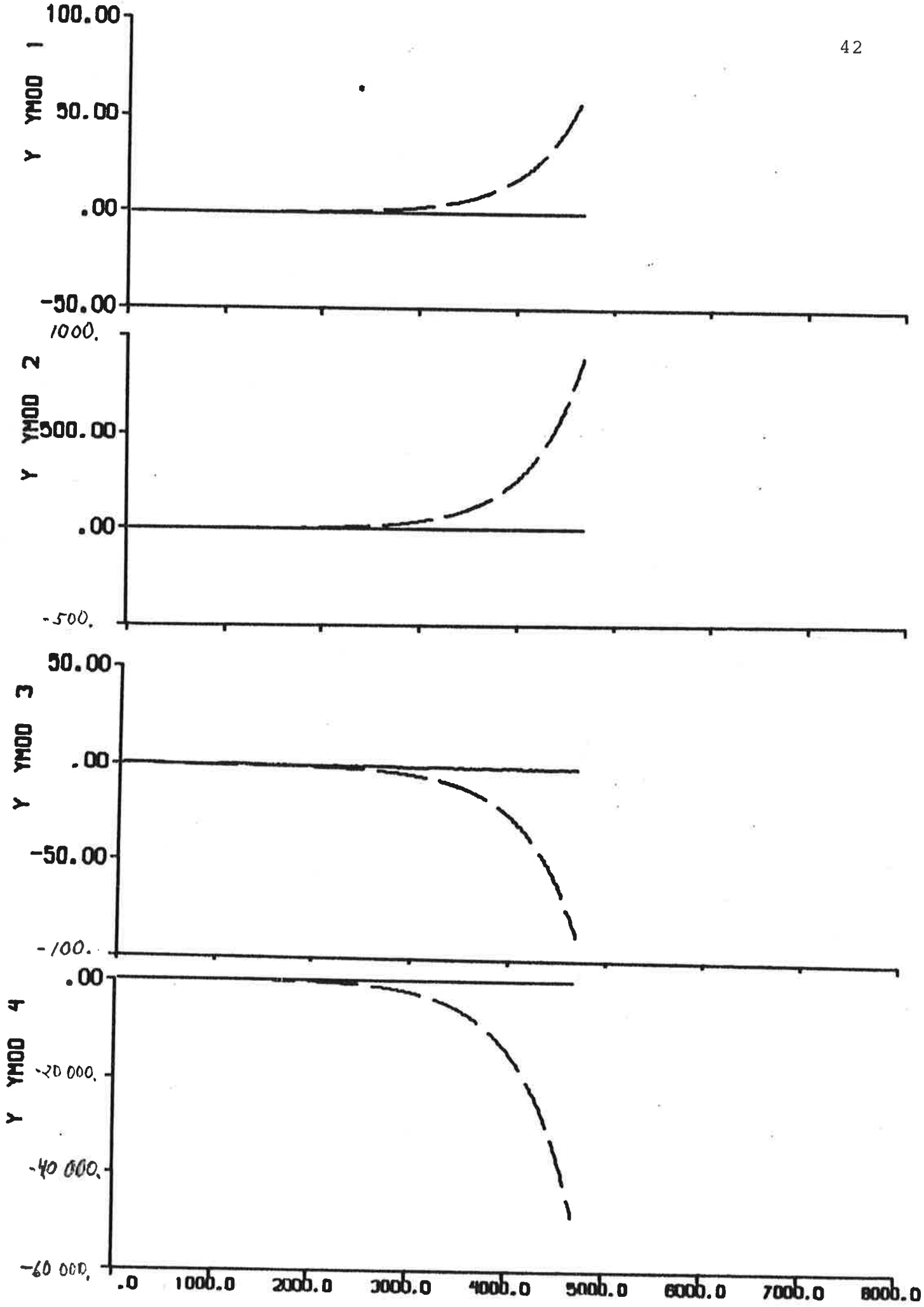

Fig. 4.3a - Result of prediction error identification (p = 4) to data from experiment E1.

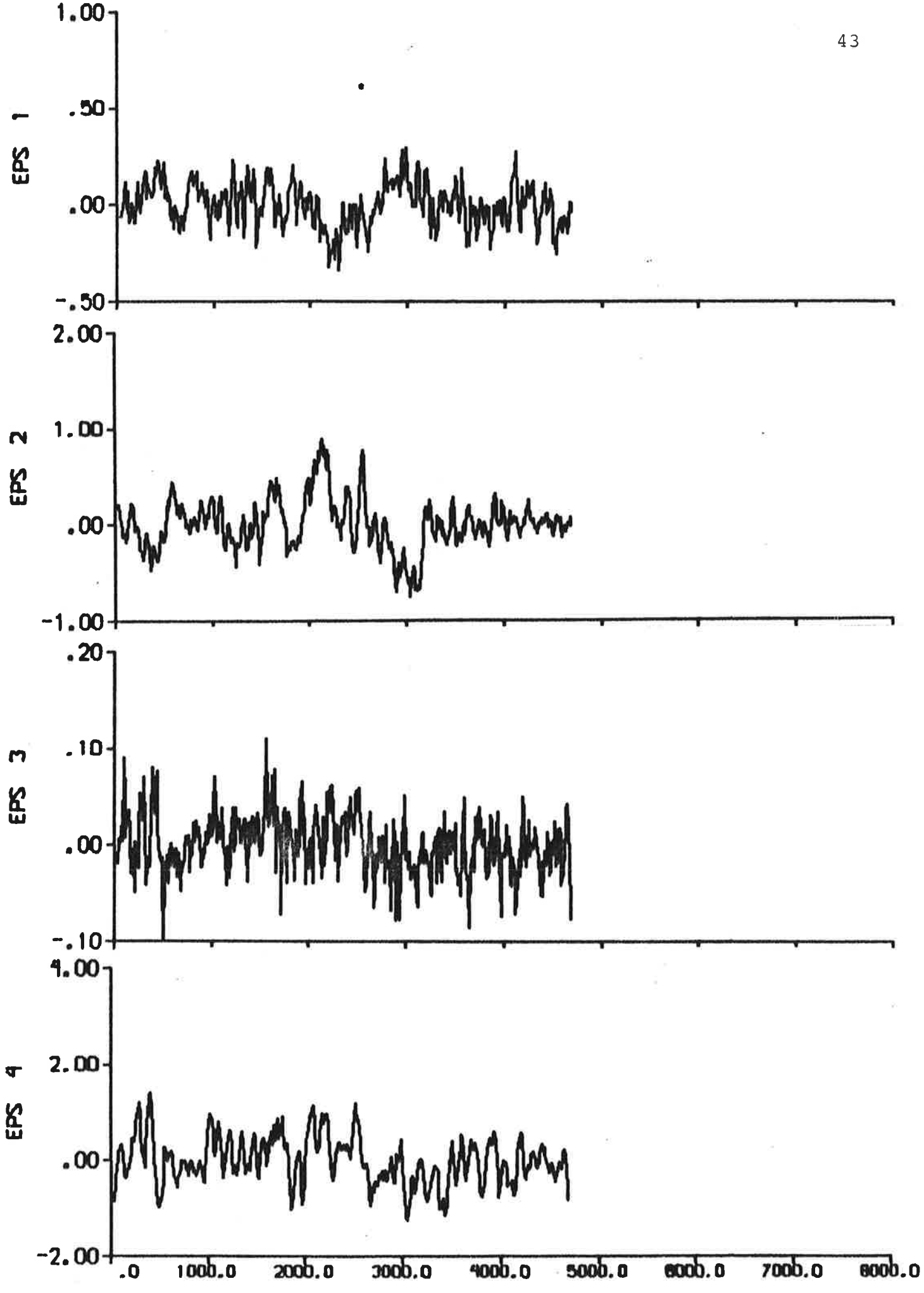

Fig. 4.3b - Prediction errors.

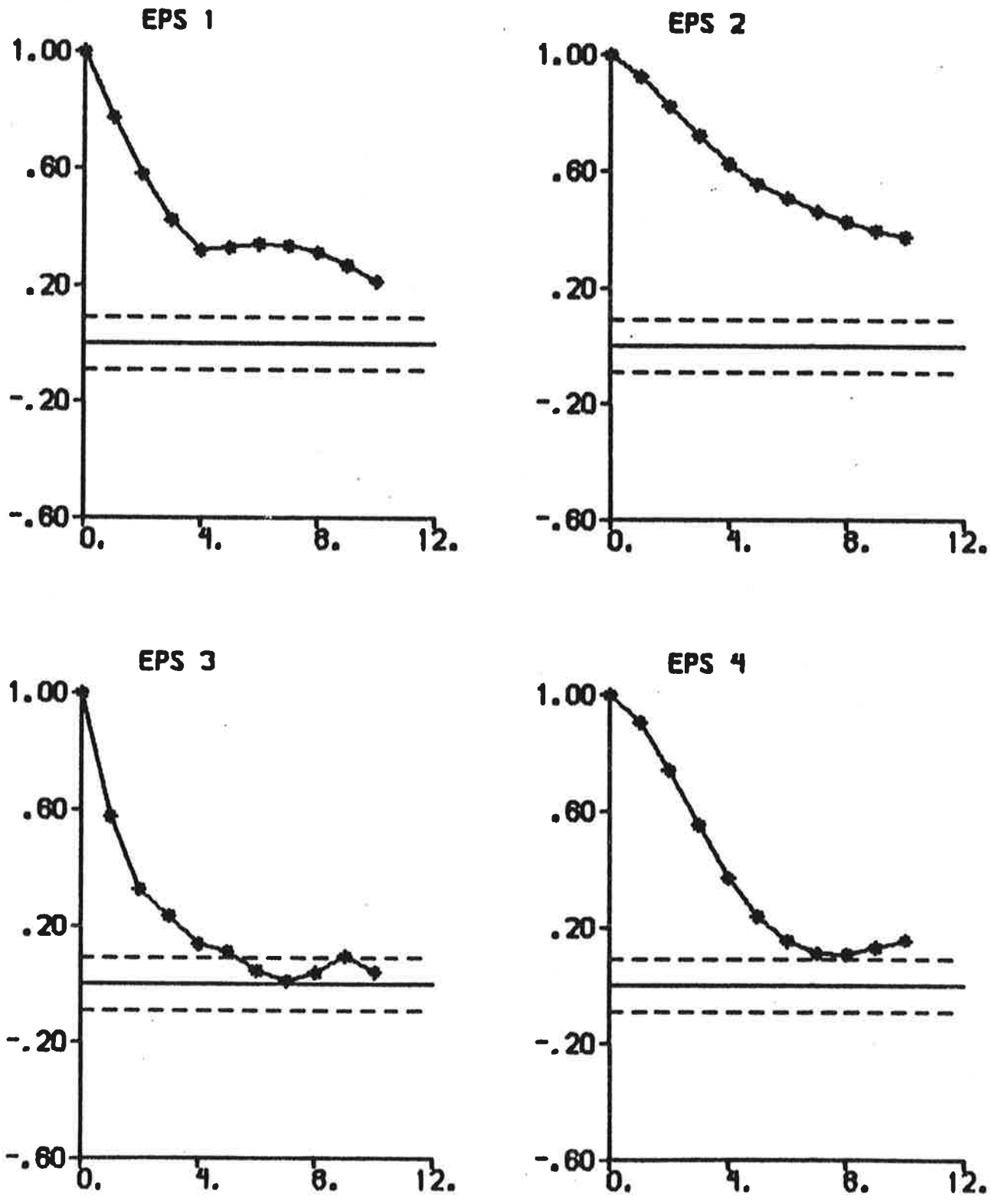

Fig. 4.3c - Autocorrelation functions of prediction errors.

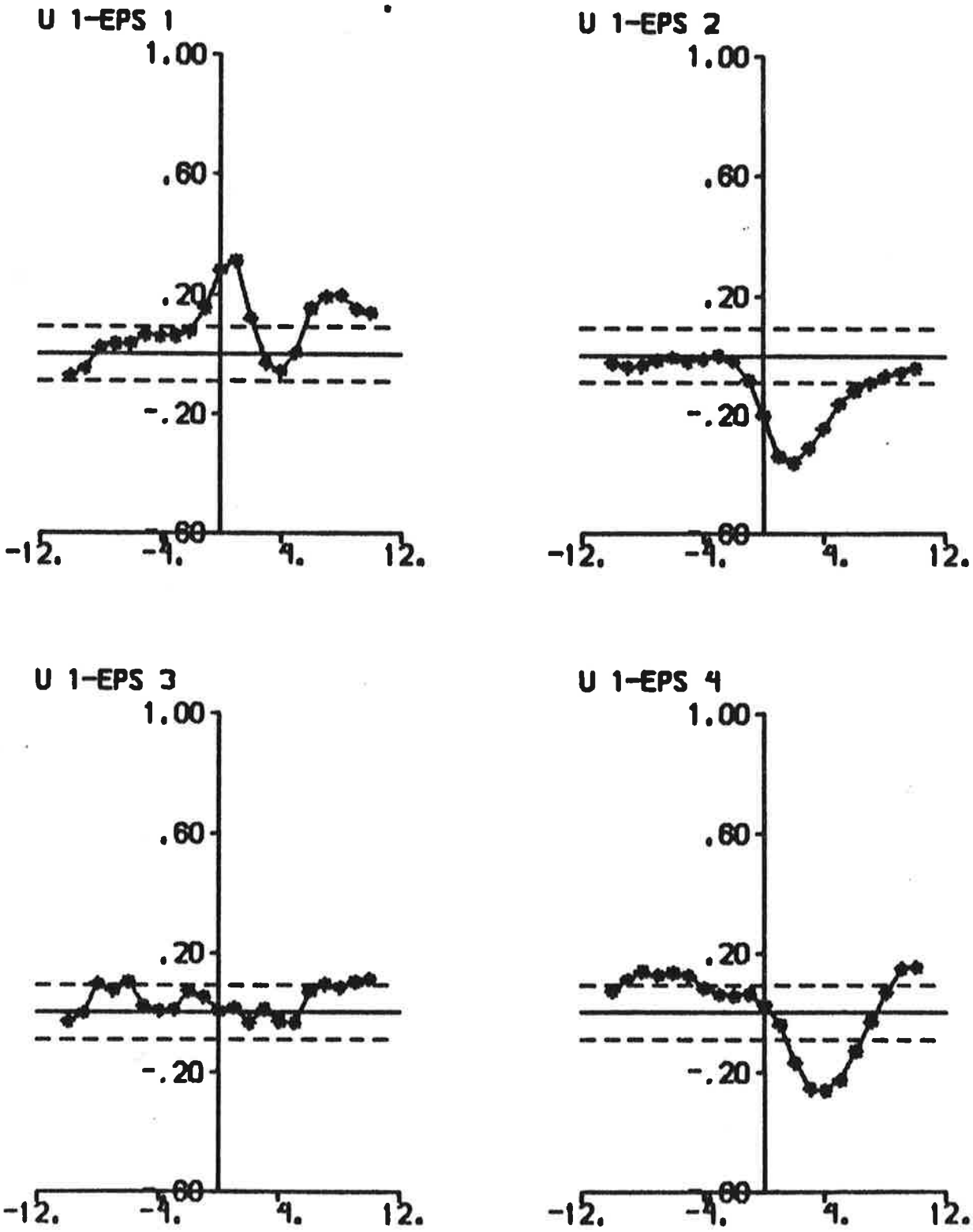

Fig. 4.3d - Cross correlation functions between rudder input and prediction errors.

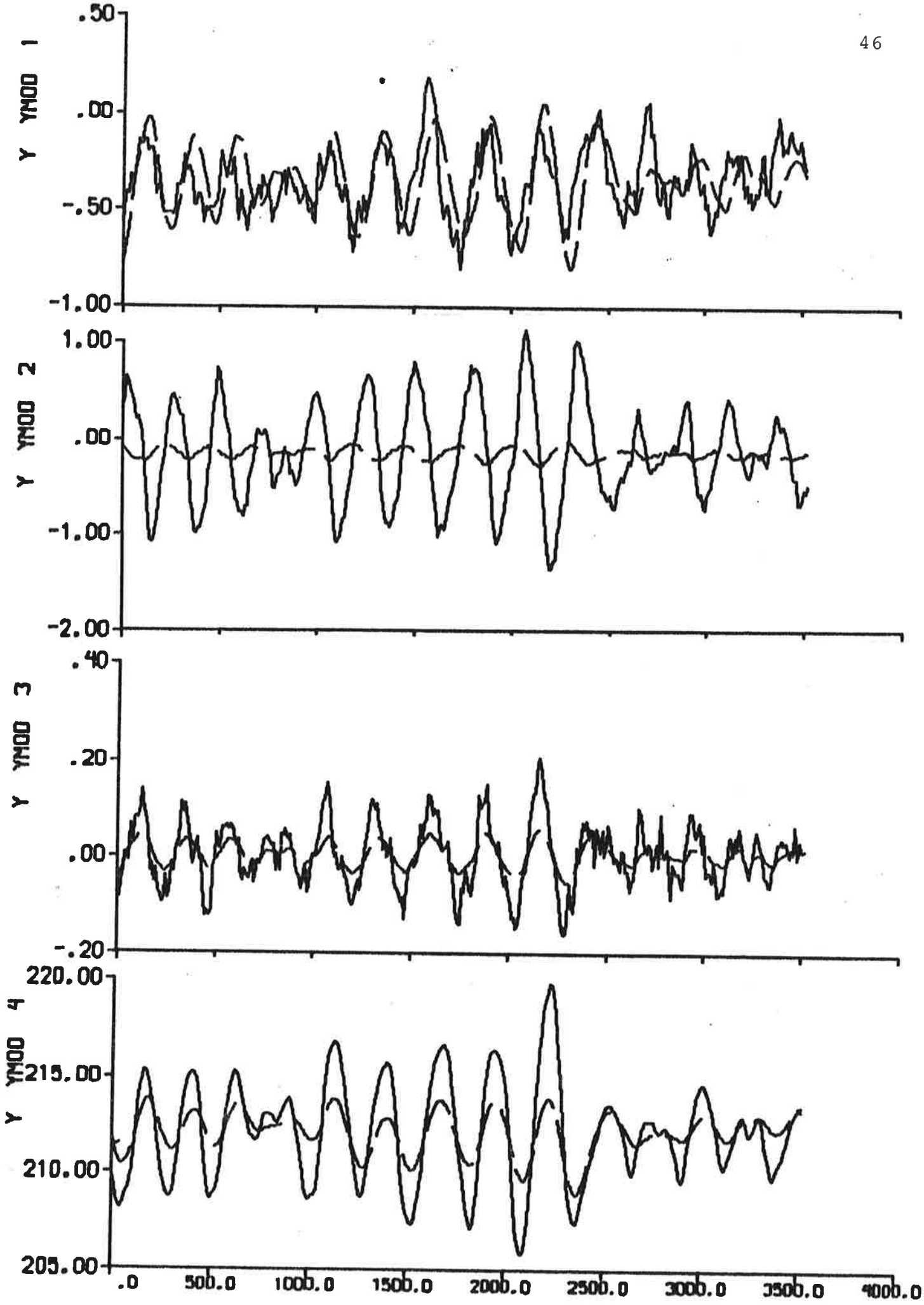

Fig. 4.4a - Result of output error identification to data from experiment E2.

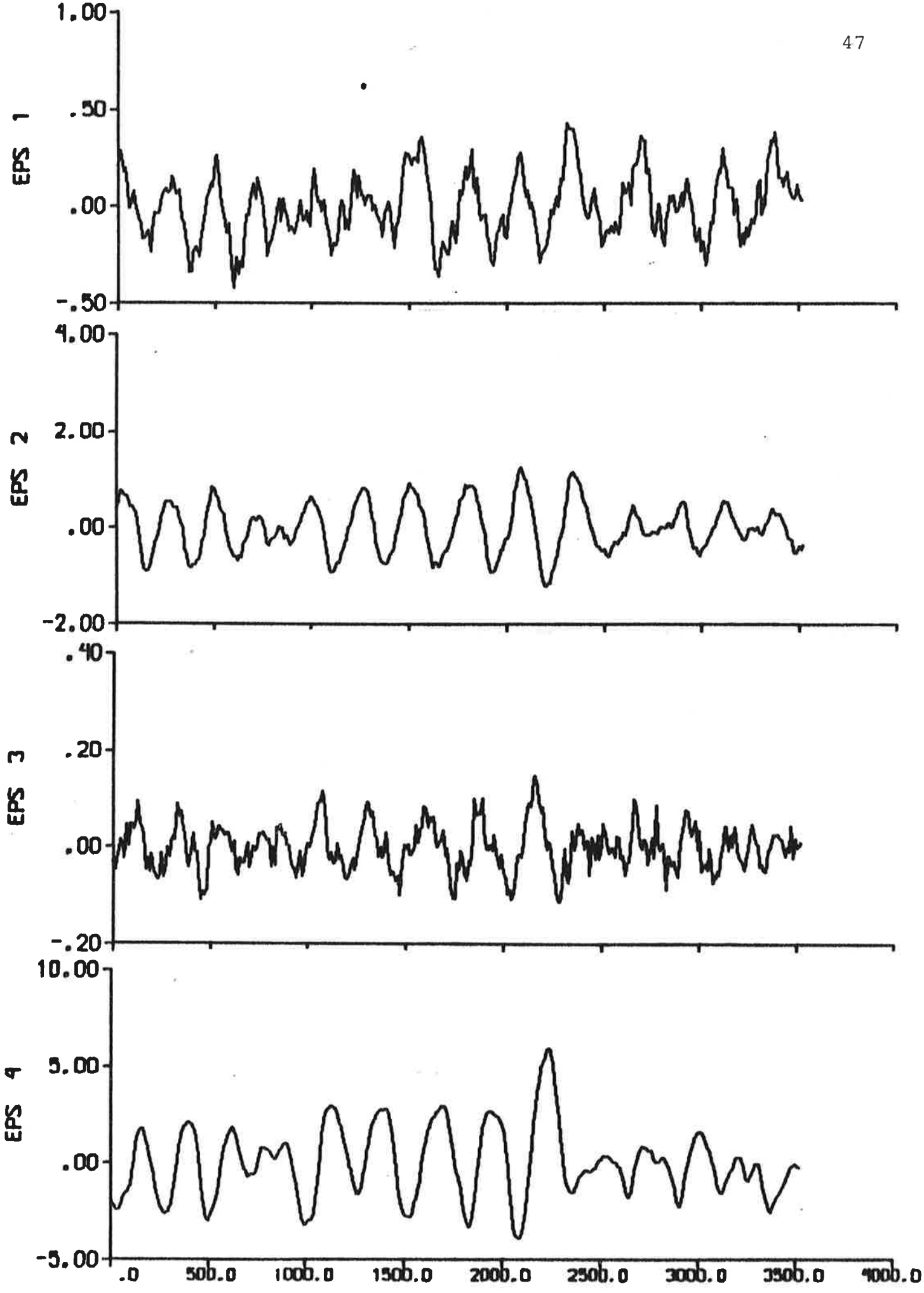

Fig. 4.4b - Prediction errors.

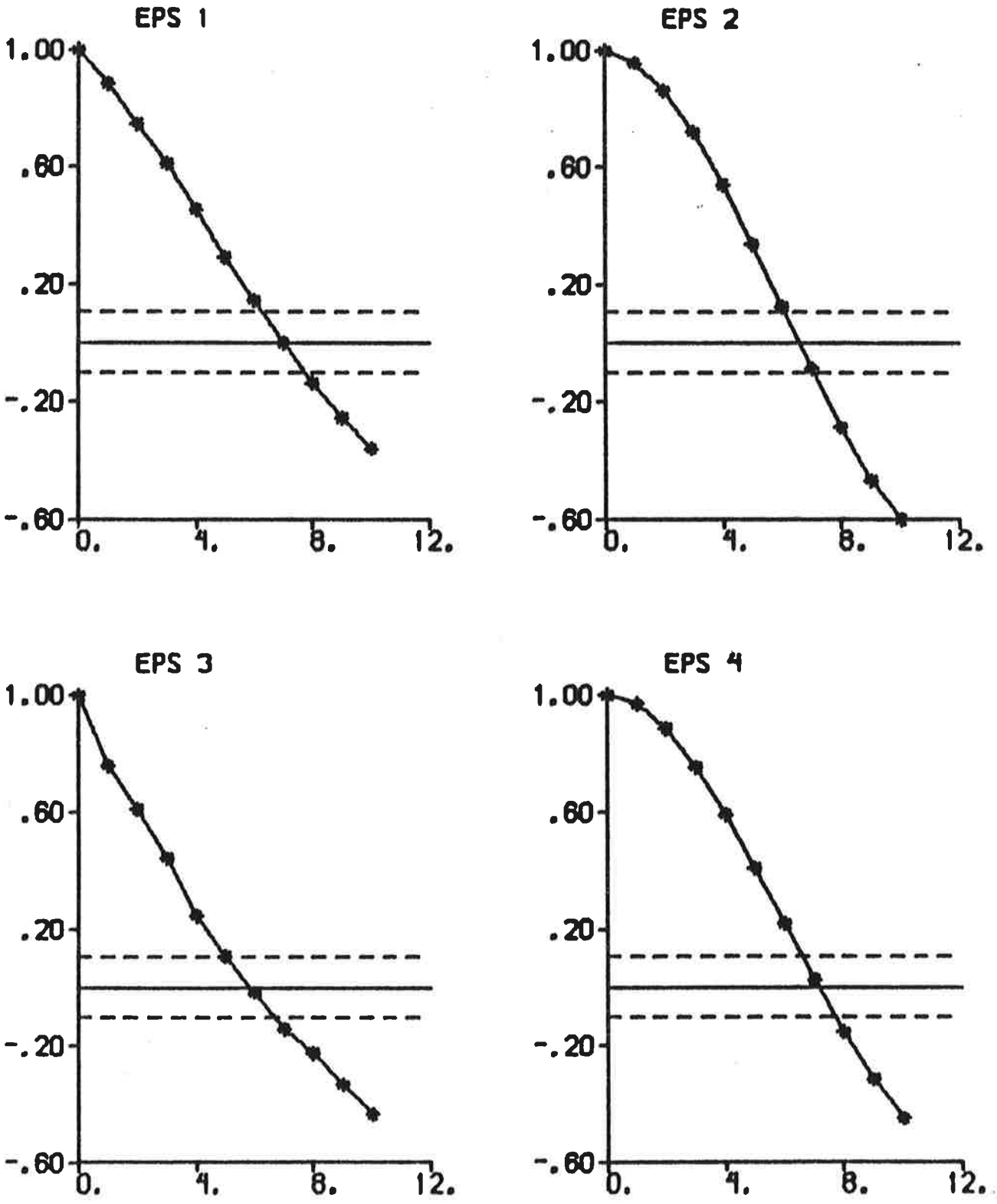

Fig. 4.4c - Autocorrelation functions of prediction errors.

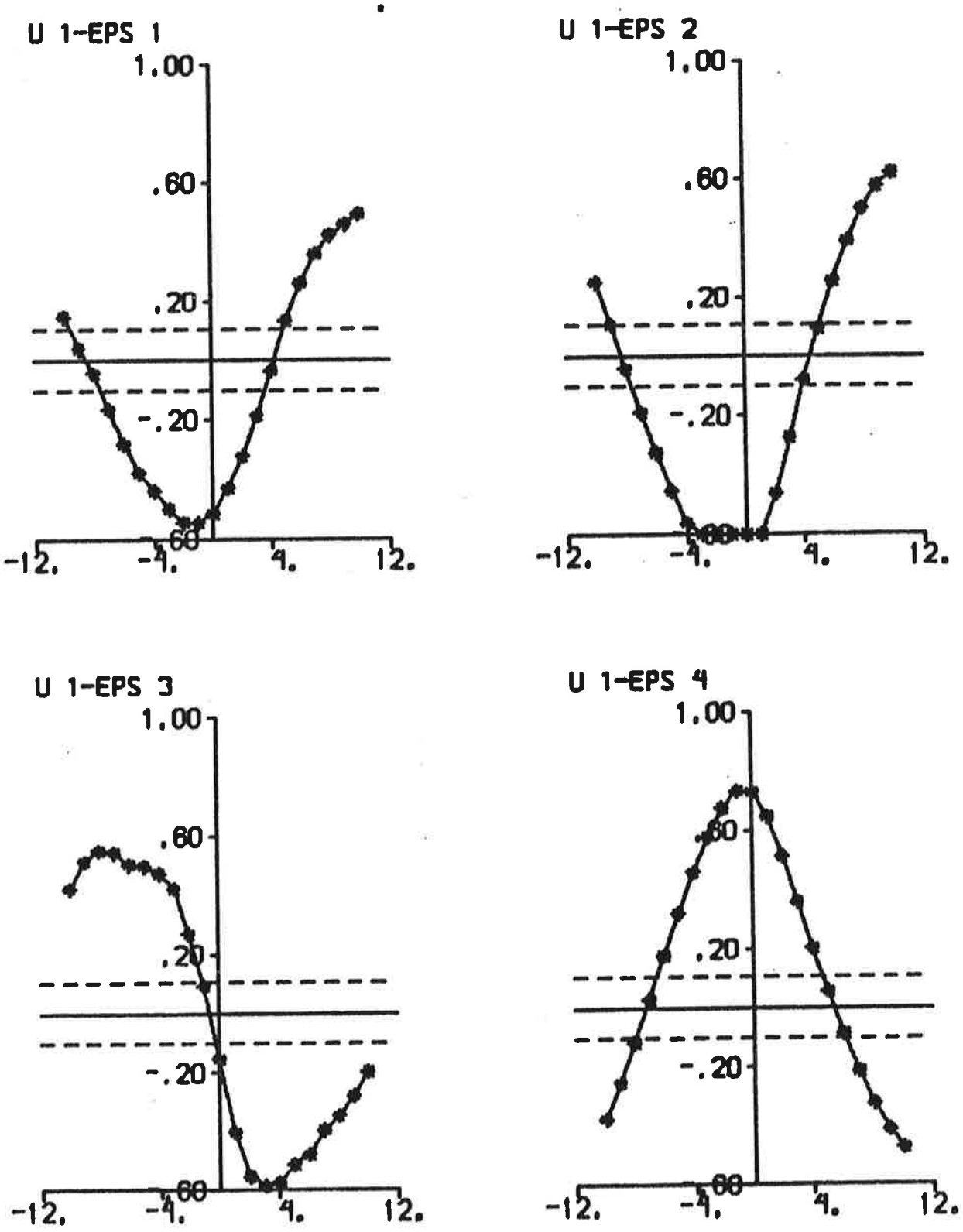

Fig. 4.4d - Cross correlation functions between rudder input and prediction errors.

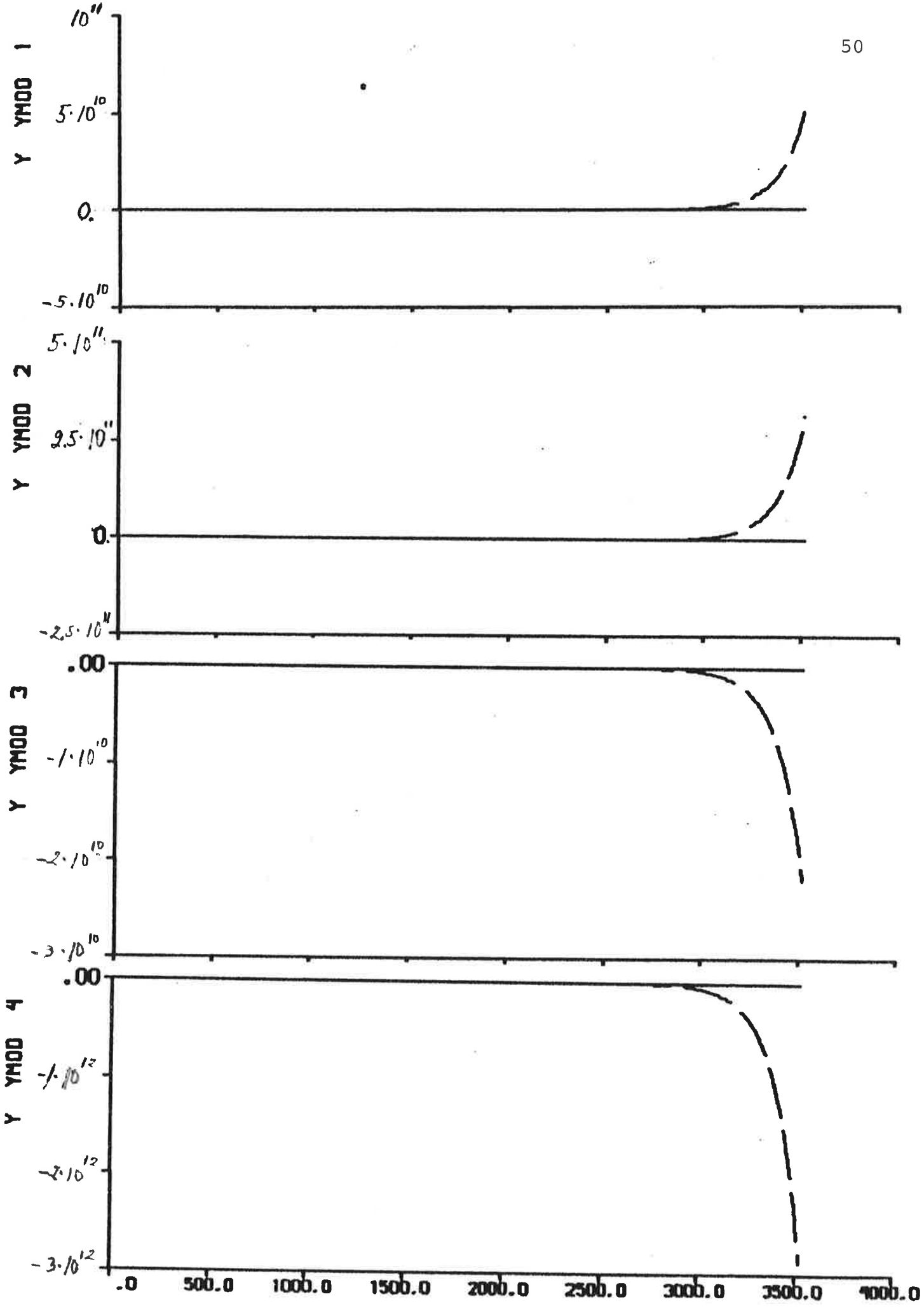

Fig. 4.5a - Result of ML identification to data from experiment E2.

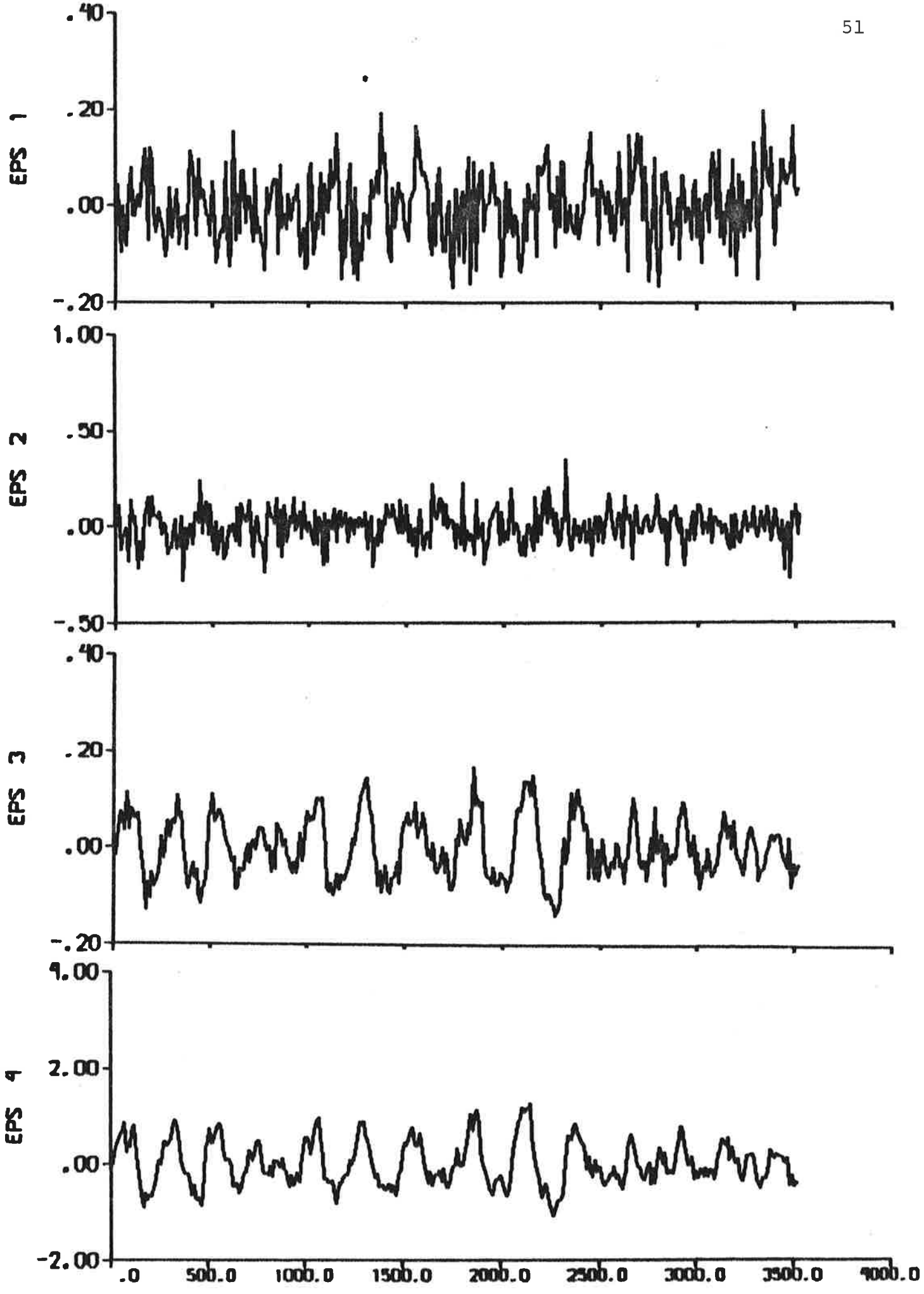

Fig. 4.5b - Prediction errors.

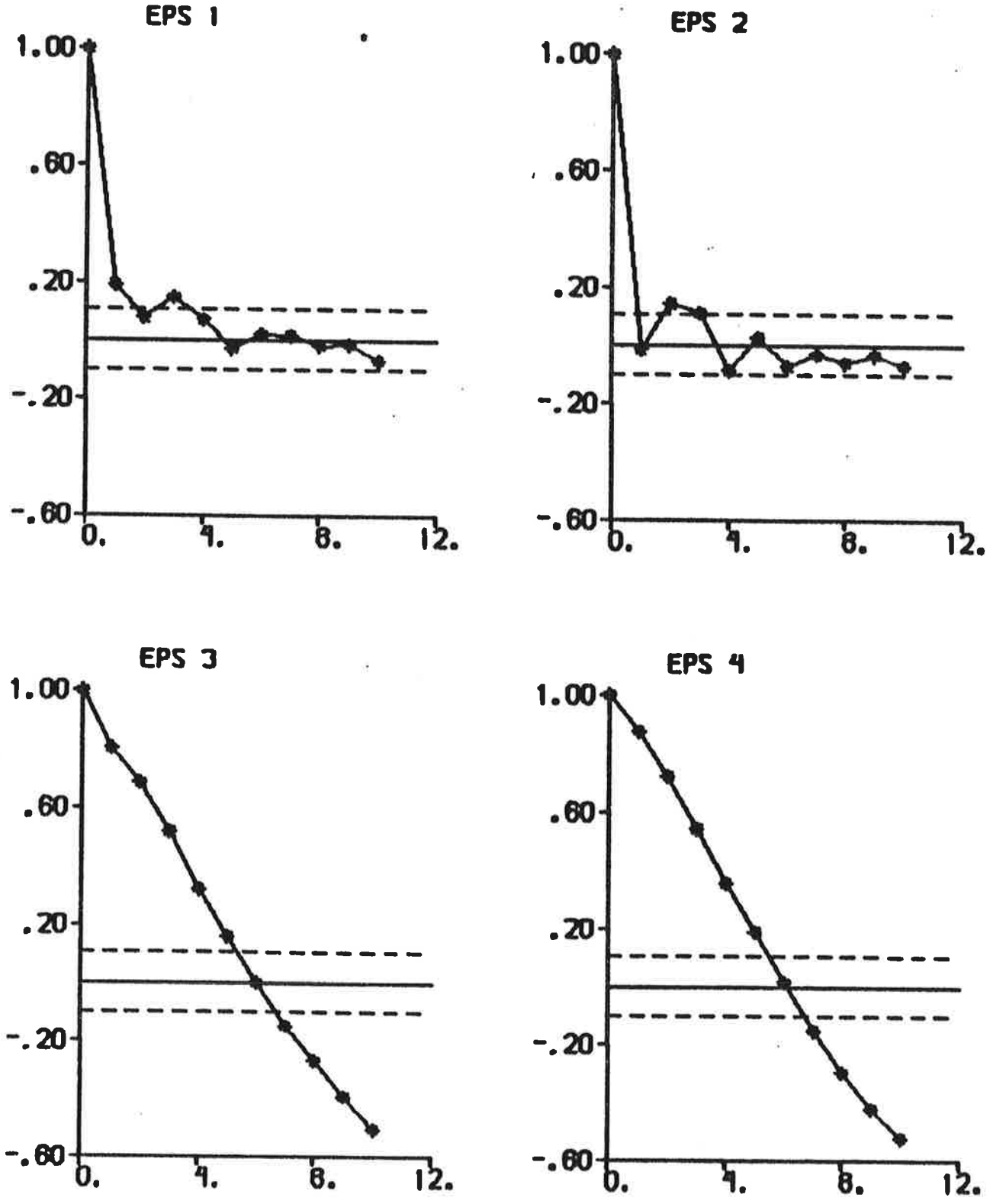

Fig. 4.5c - Autocorrelation functions of prediction errors.

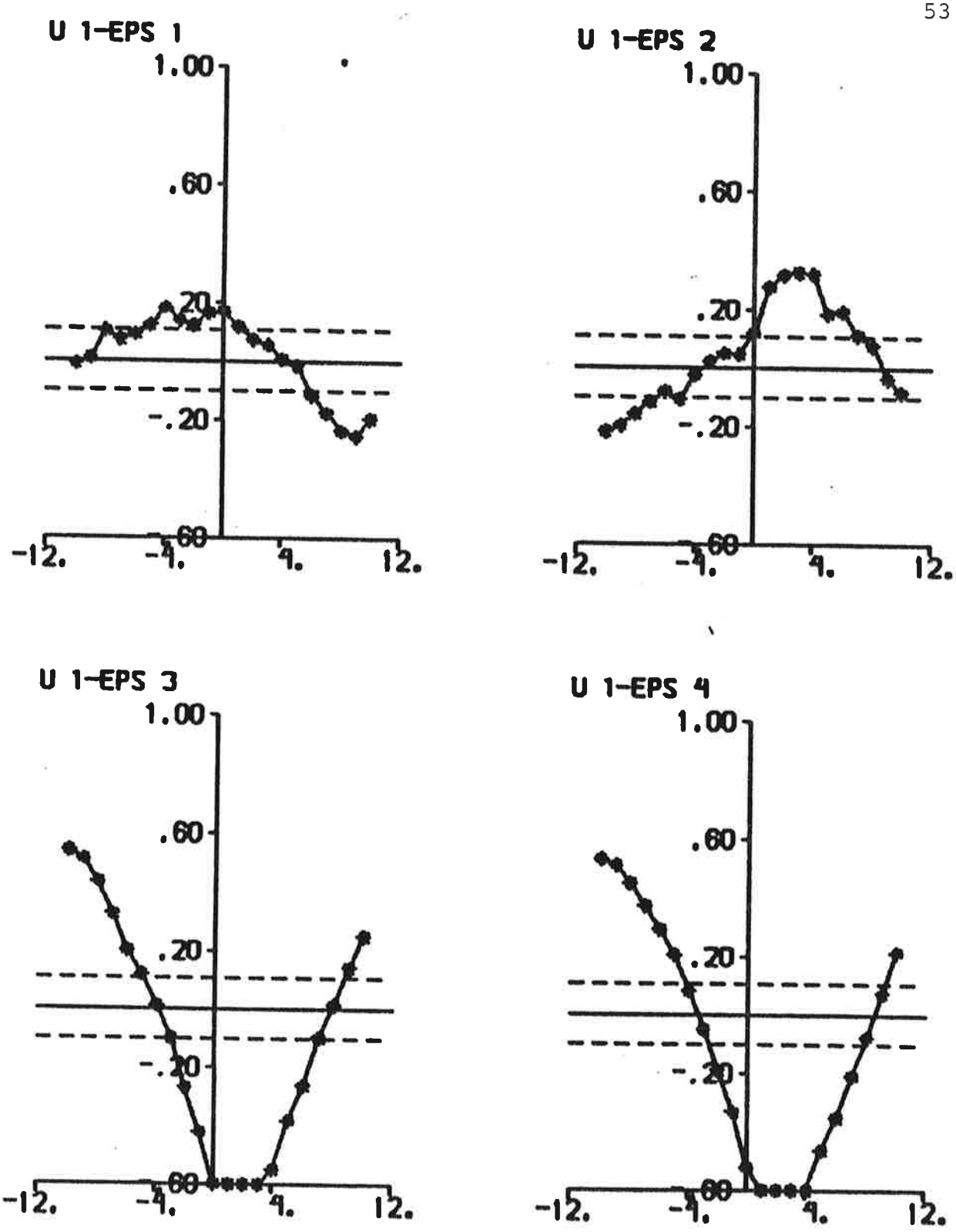

Fig. 4.5d - Cross correlation functions between rudder input and prediction errors.

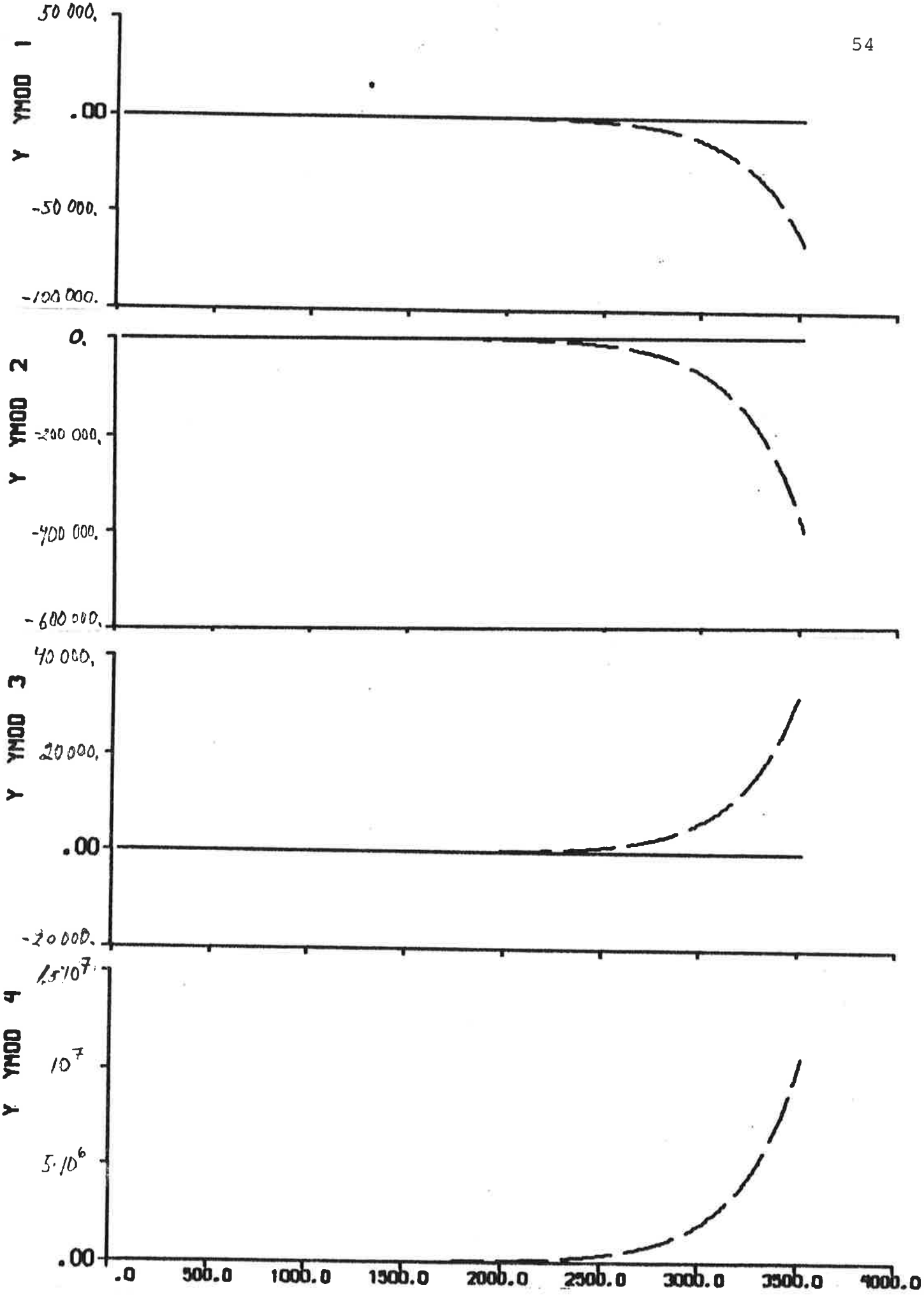

Fig. 4.6a - Result of prediction error identification (p = 4) to data from experiment E2.

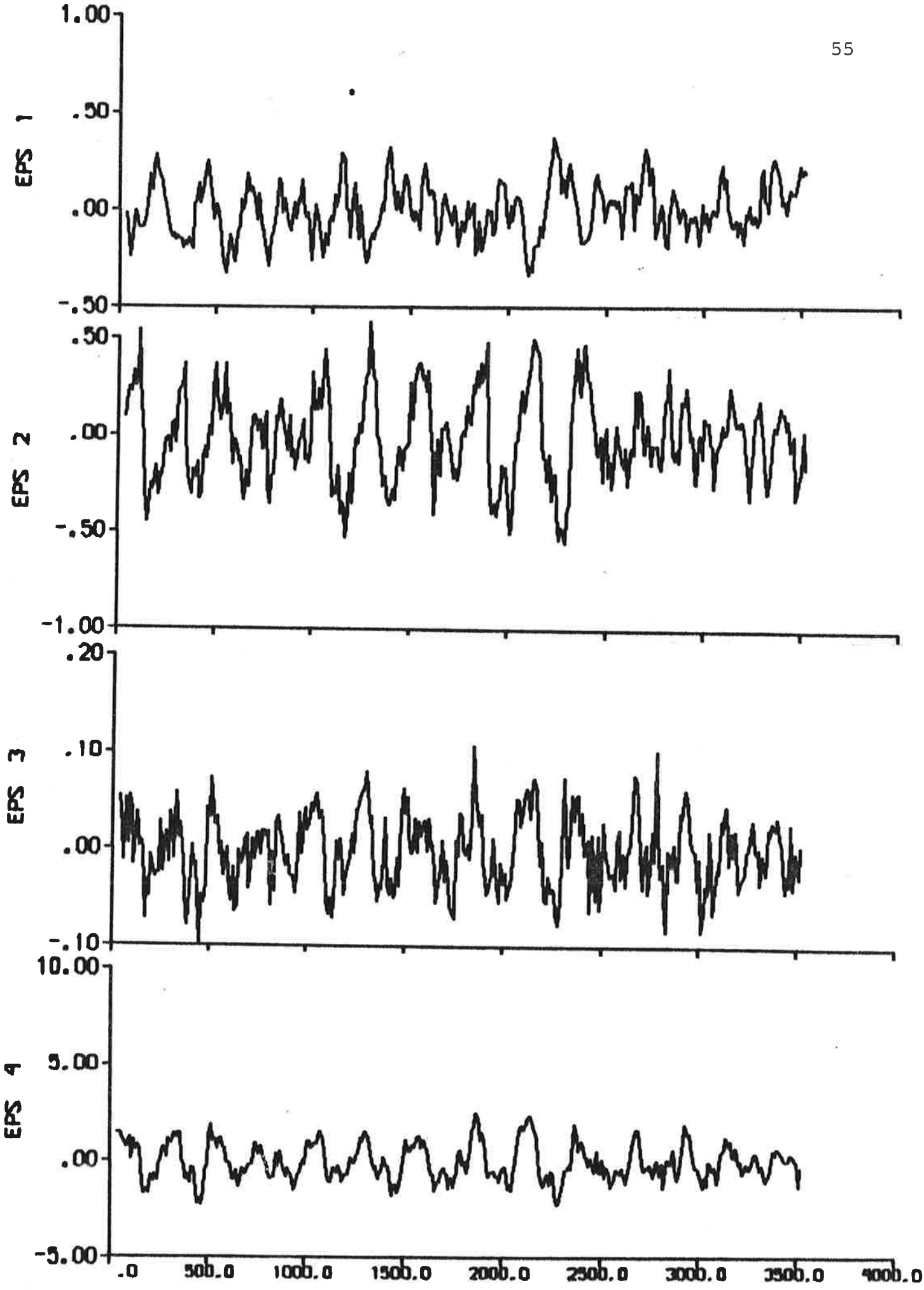

Fig. 4.6b - Prediction errors.

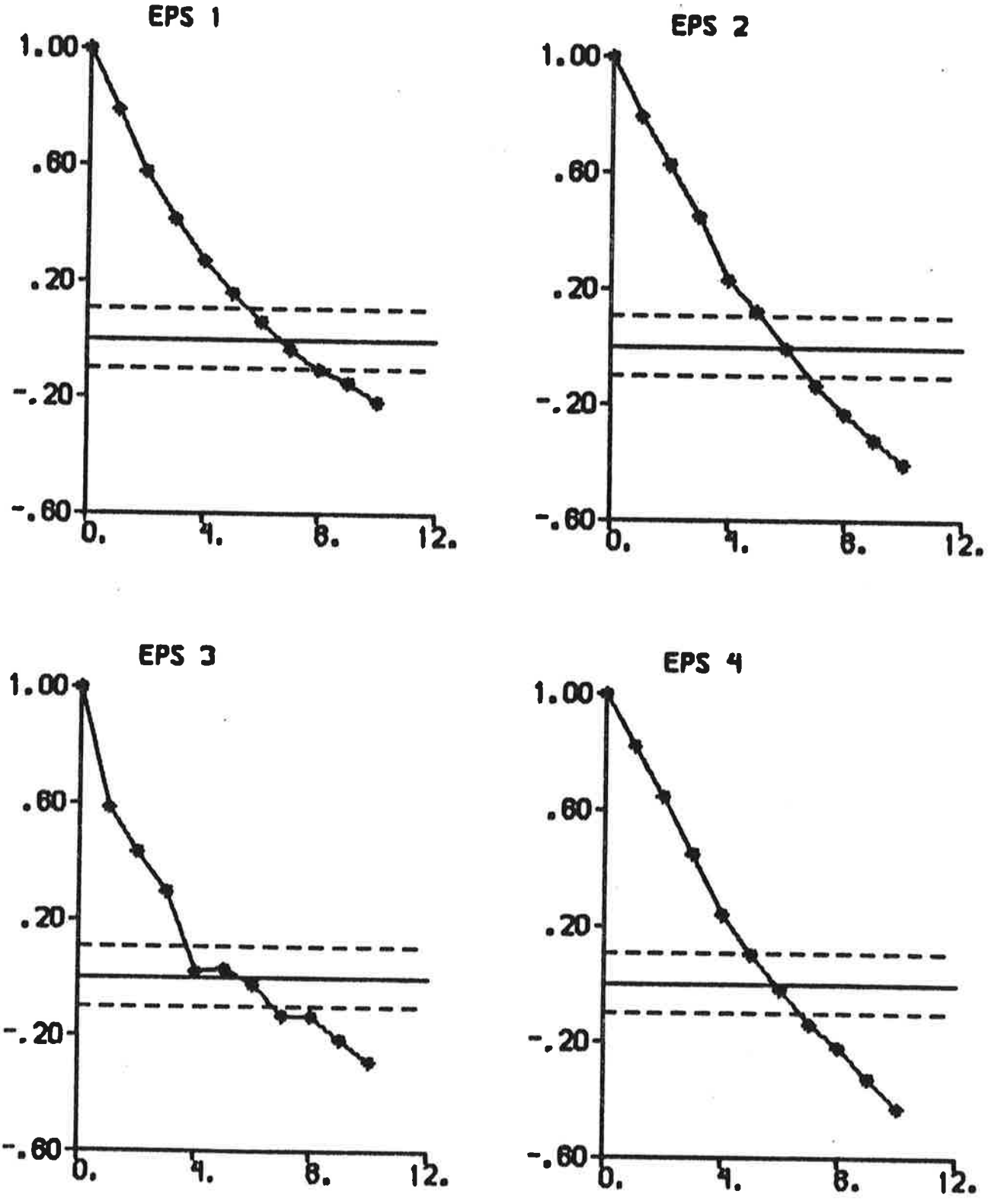

Fig. 4.6c - Autocorrelation functions of prediction errors.

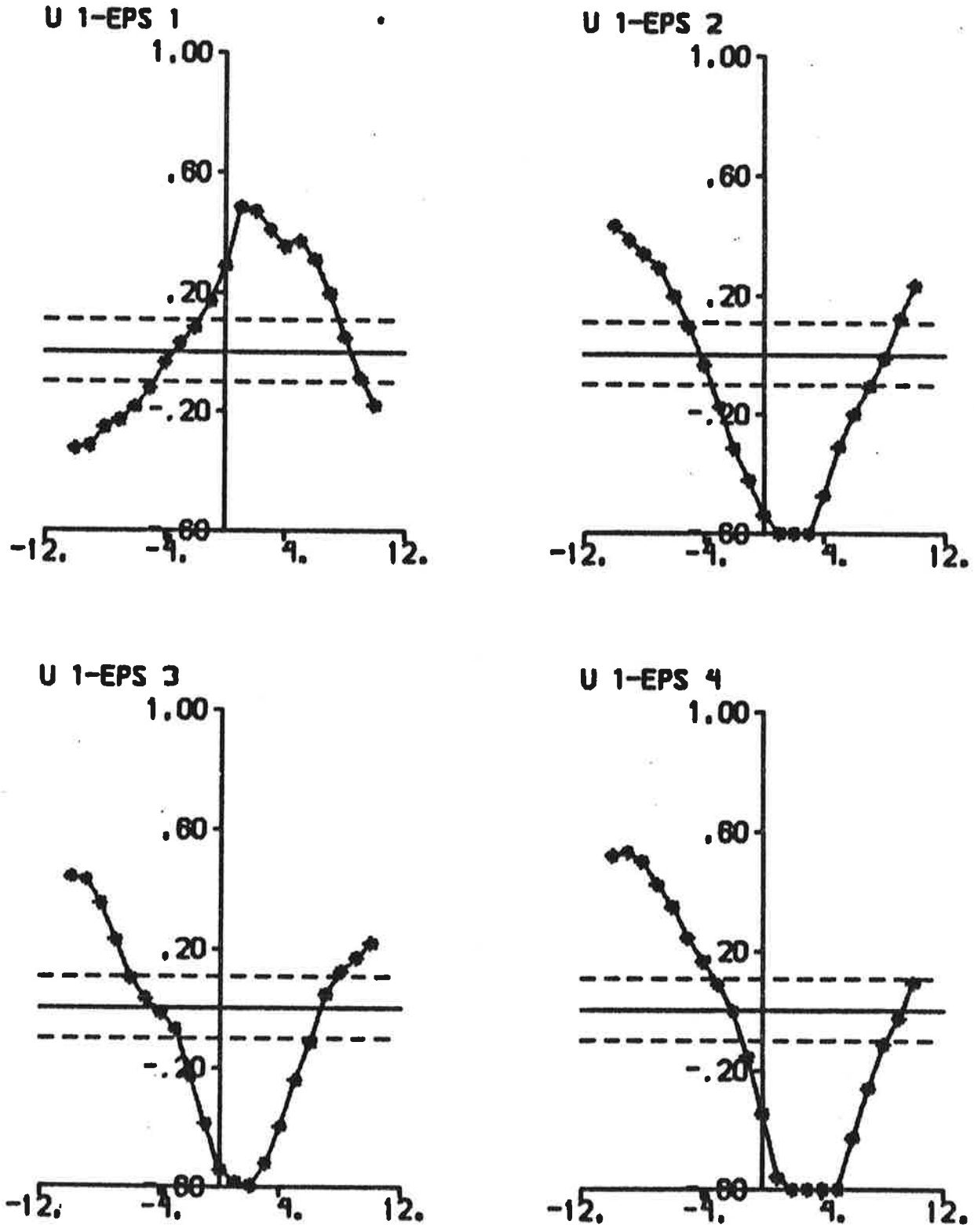

Fig. 4.6d - Cross correlation functions between rudder input and prediction errors.

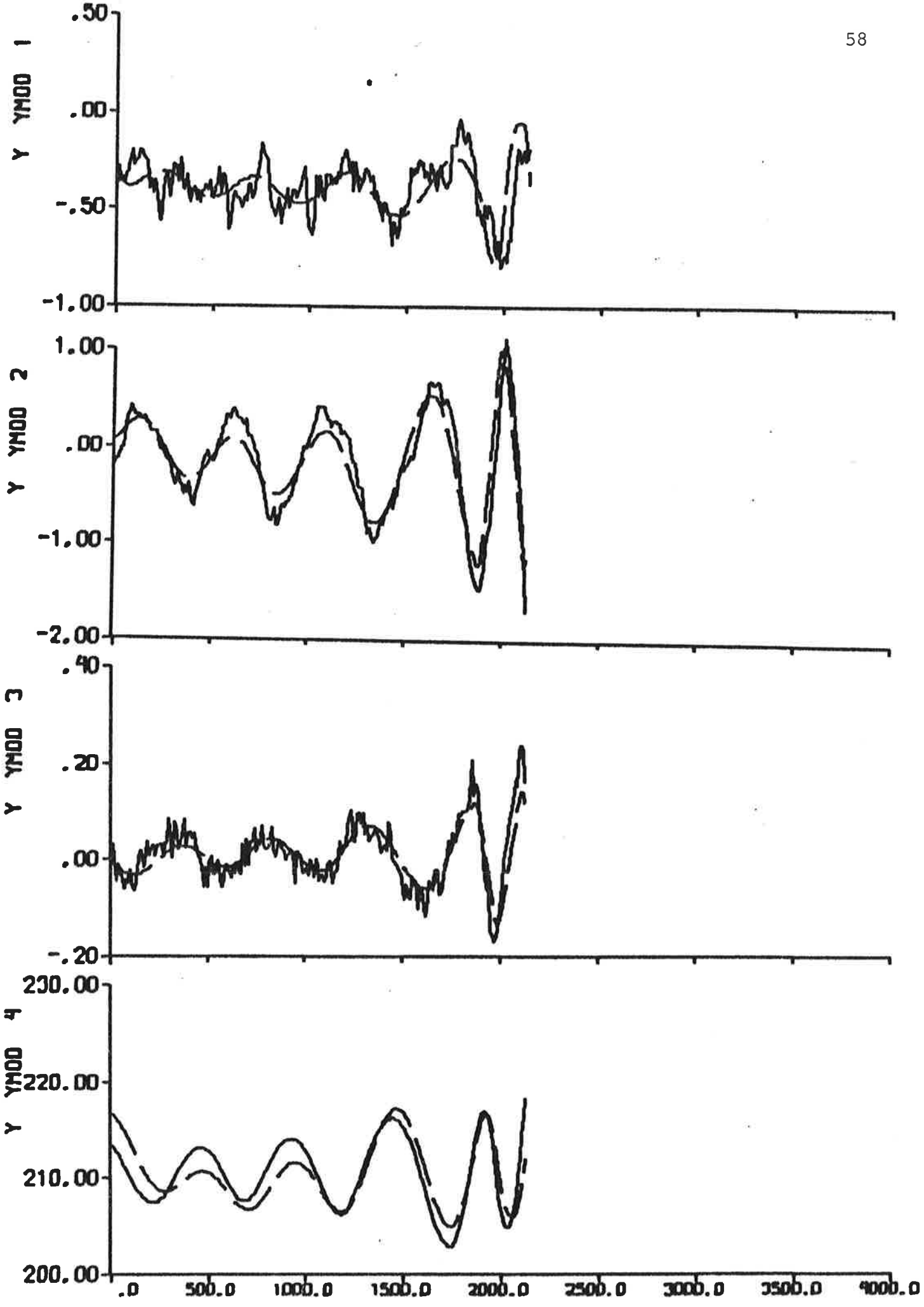

Fig. 4.7a - Result of output error identification to data from experiment E3.

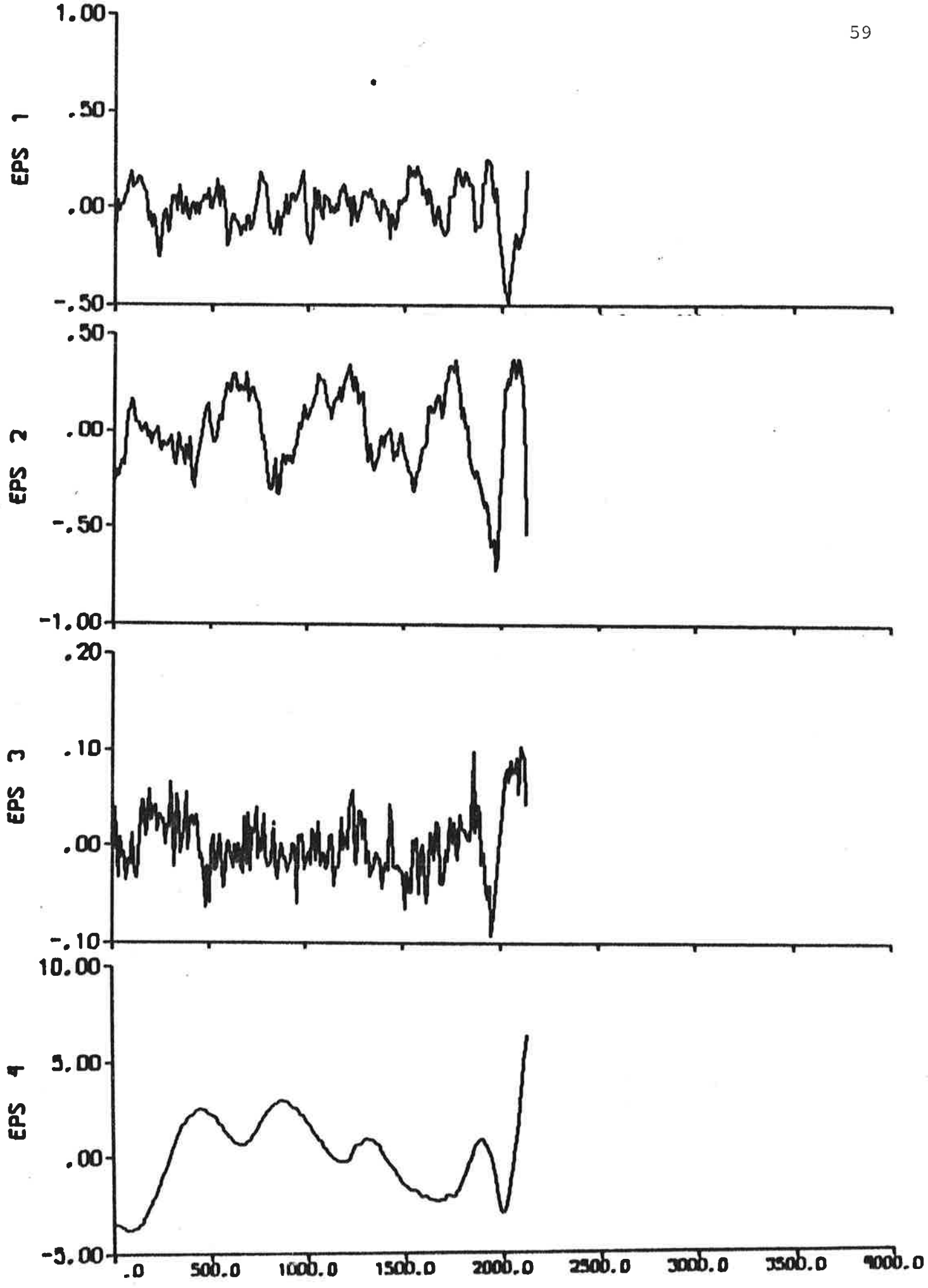

Fig. 4.7b - Prediction errors.

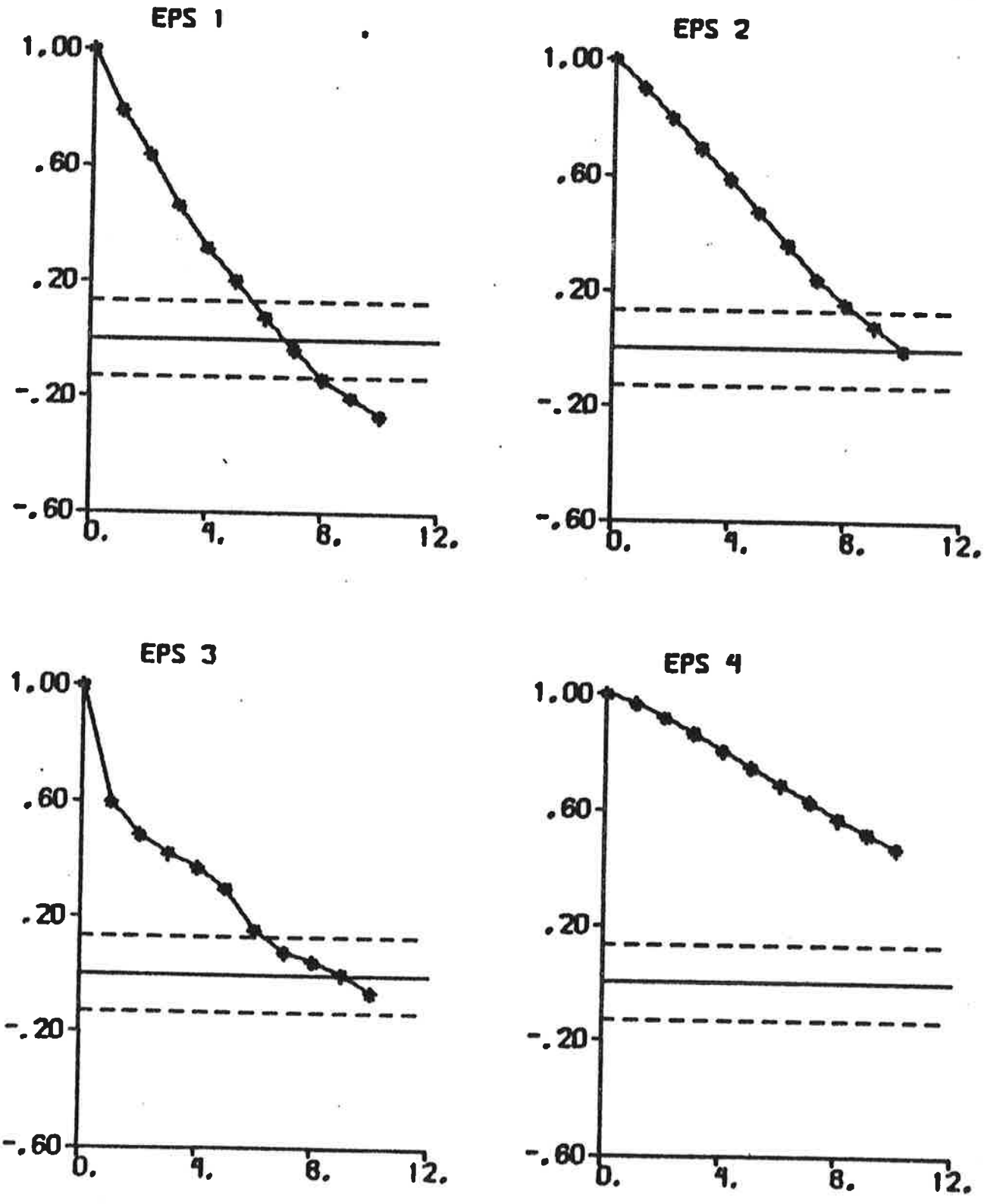

Fig. 4.7c - Autocorrelation functions of prediction errors.

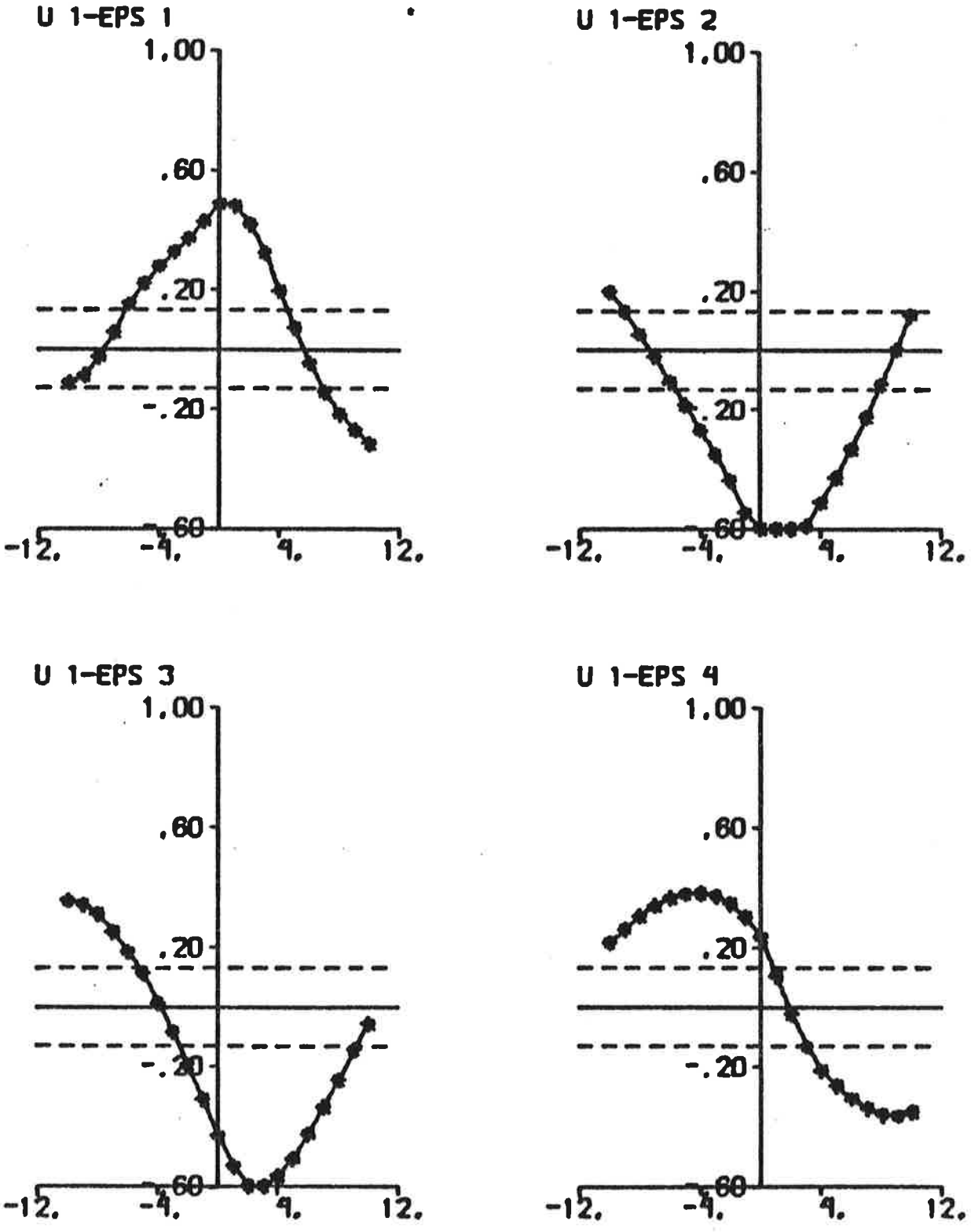

Fig. 4.7d - Cross correlation functions between rudder input and prediction errors.

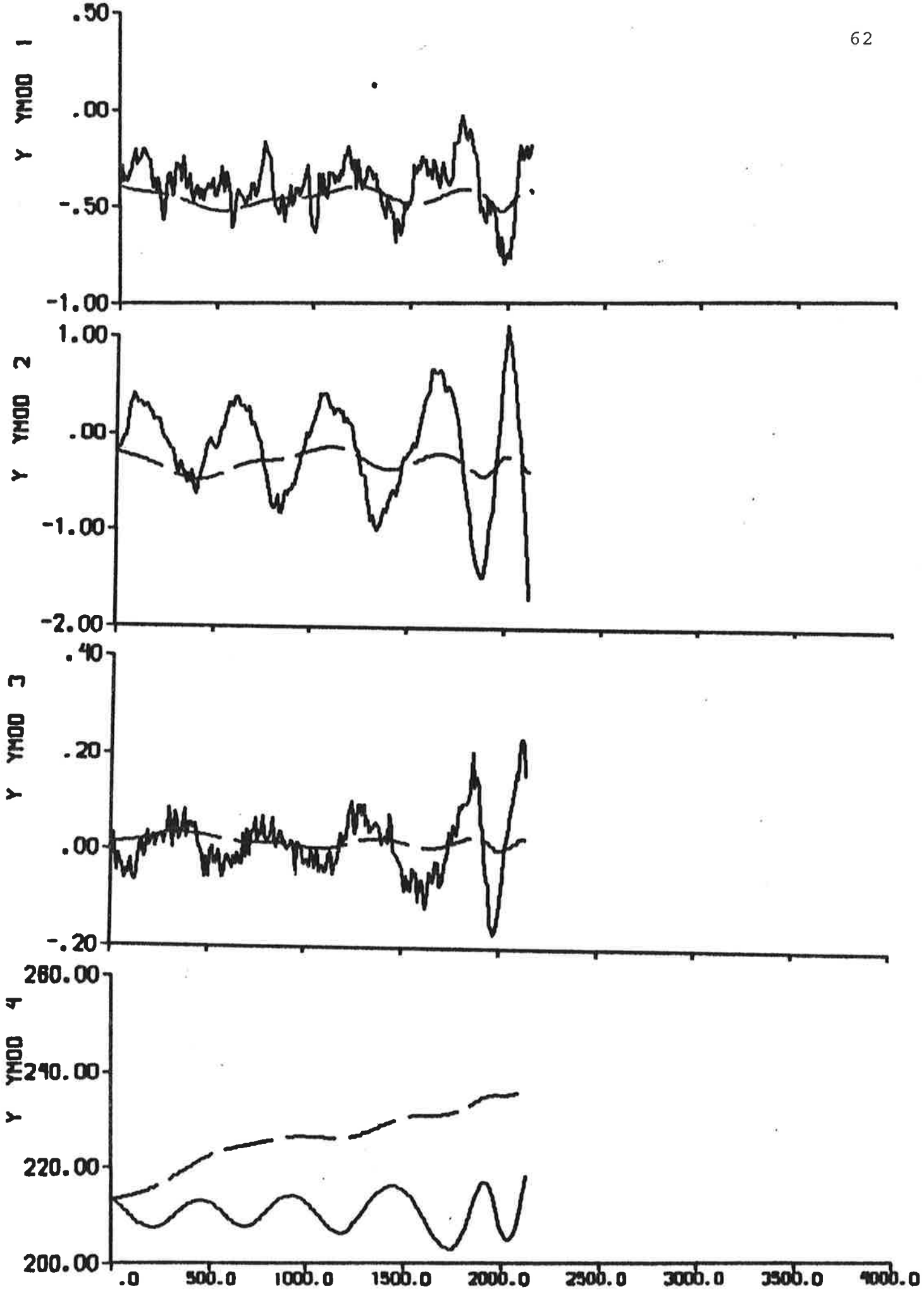

Fig. 4.8a - Result of ML identification to data from experiment E3.

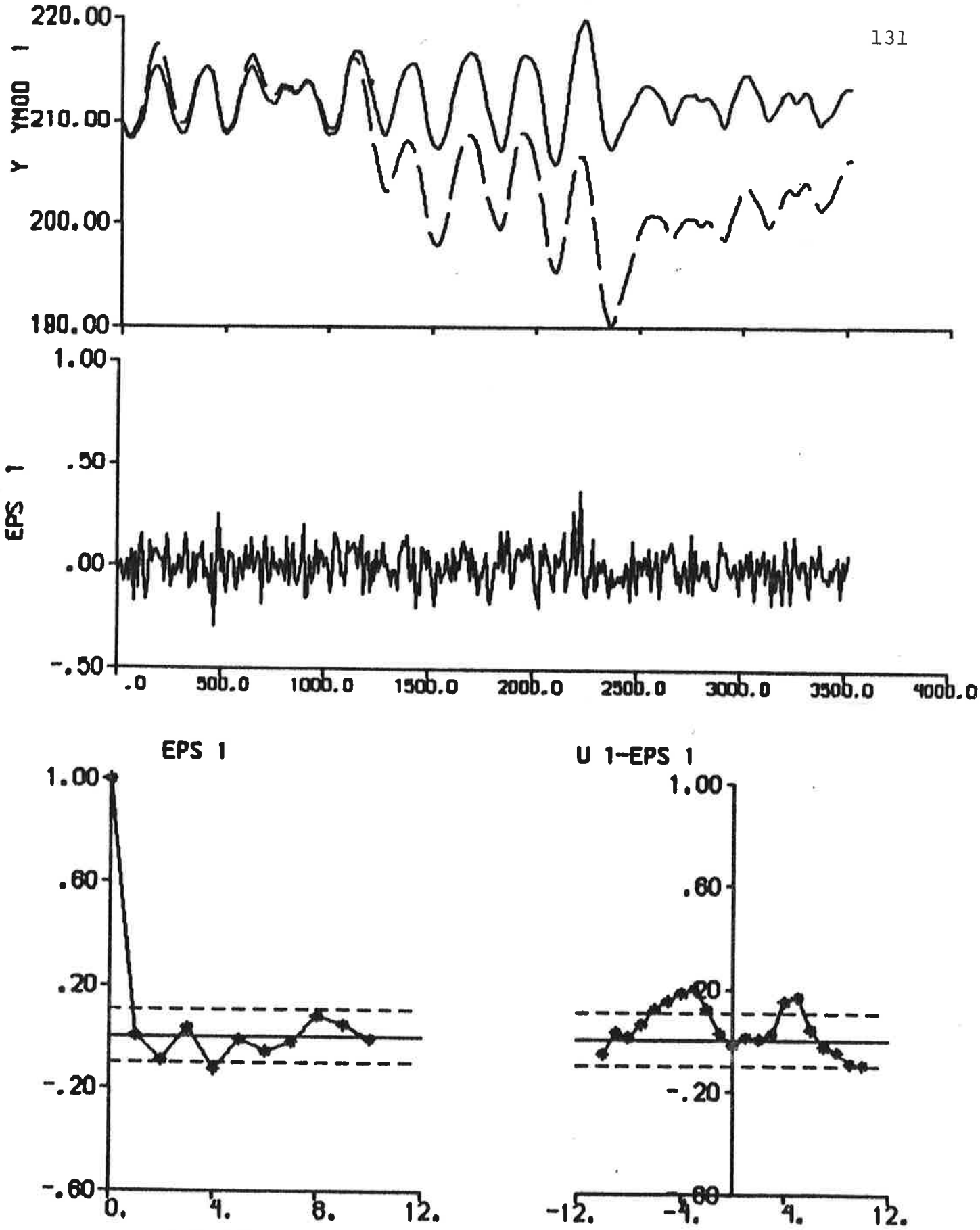

Fig. 6.6 - Result of ML identification to data from experiment E2.

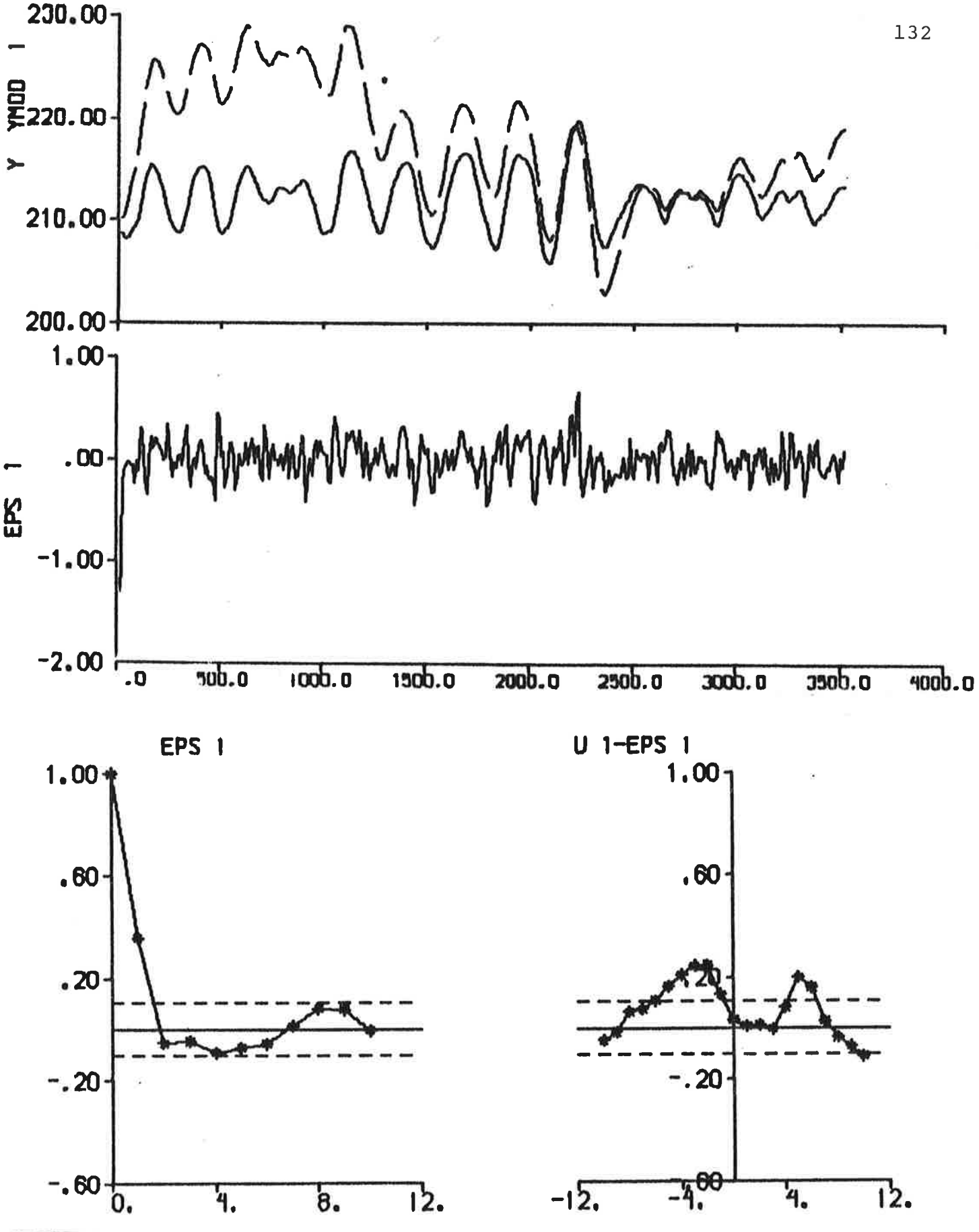

Fig. 6.7 - Result of prediction error identification (p = 2) to data from experiment E2.

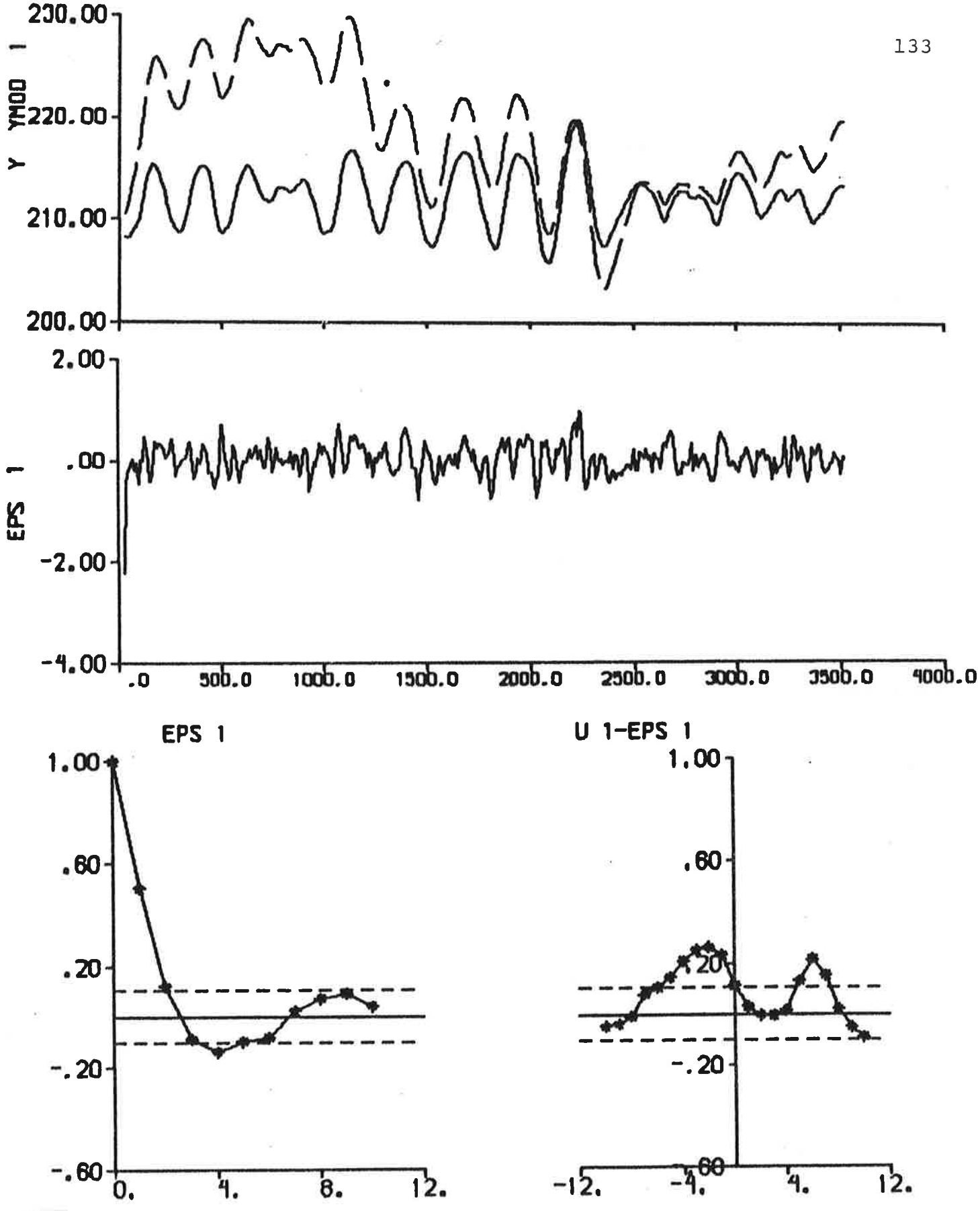

Fig. 6.8 - Result of prediction error identification (p = 3) to data from experiment E2.

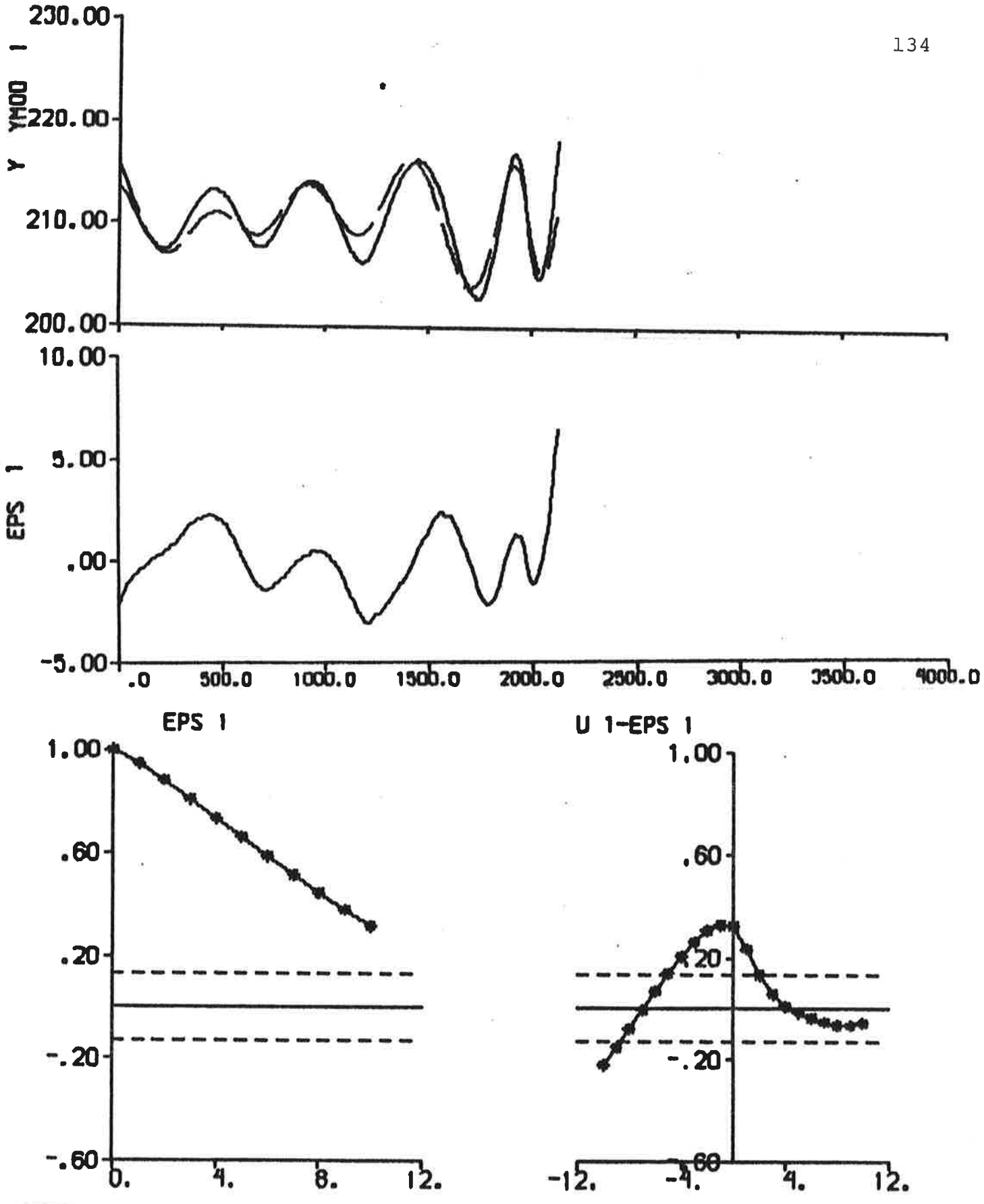

Fig. 6.9 - Result of output error identification to data from experiment E3.

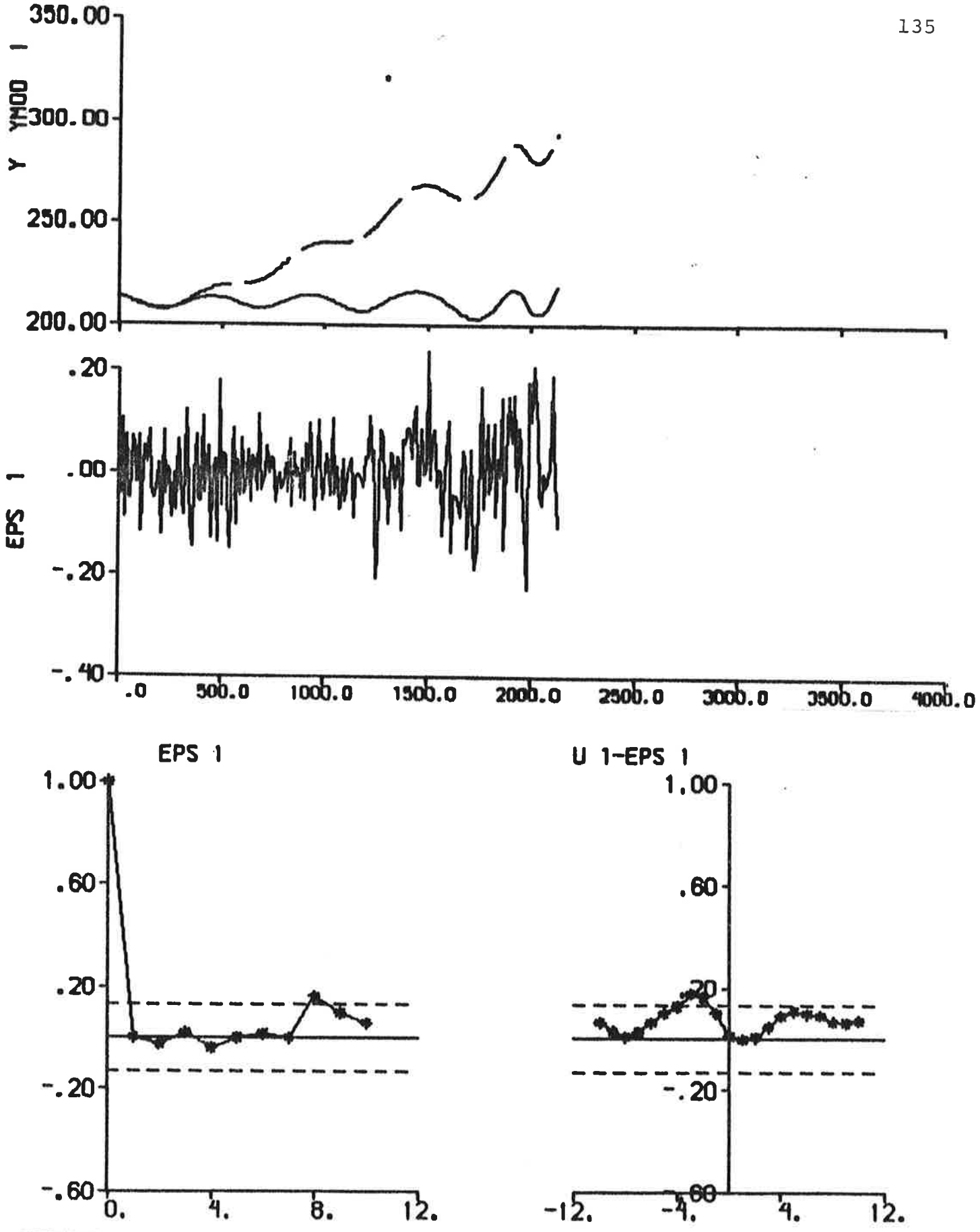

Fig. 6.10 - Result of ML identification to data from experiment E3.

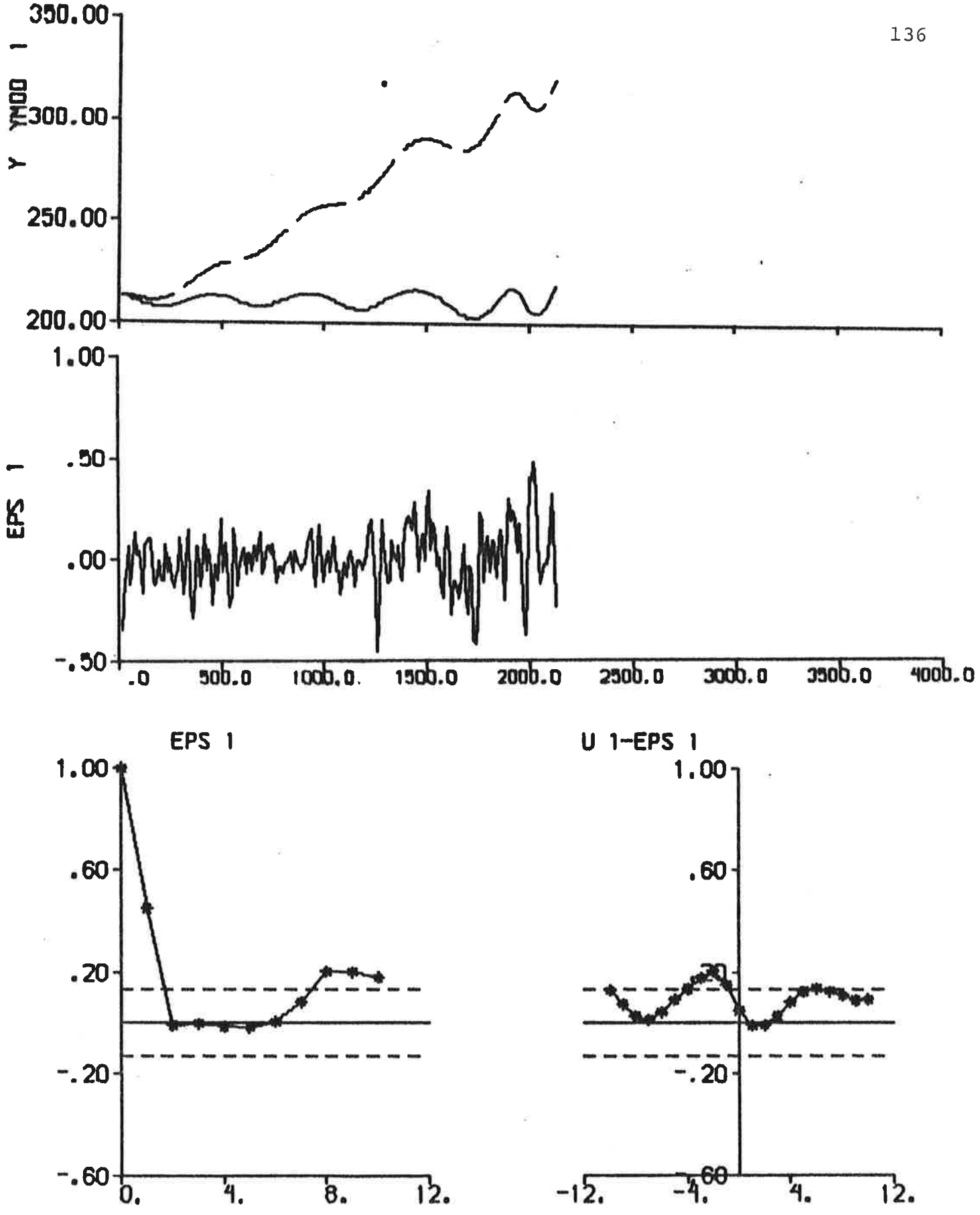

Fig. 6.11 - Result of prediction error identification (p = 2) to data from experiment E3.

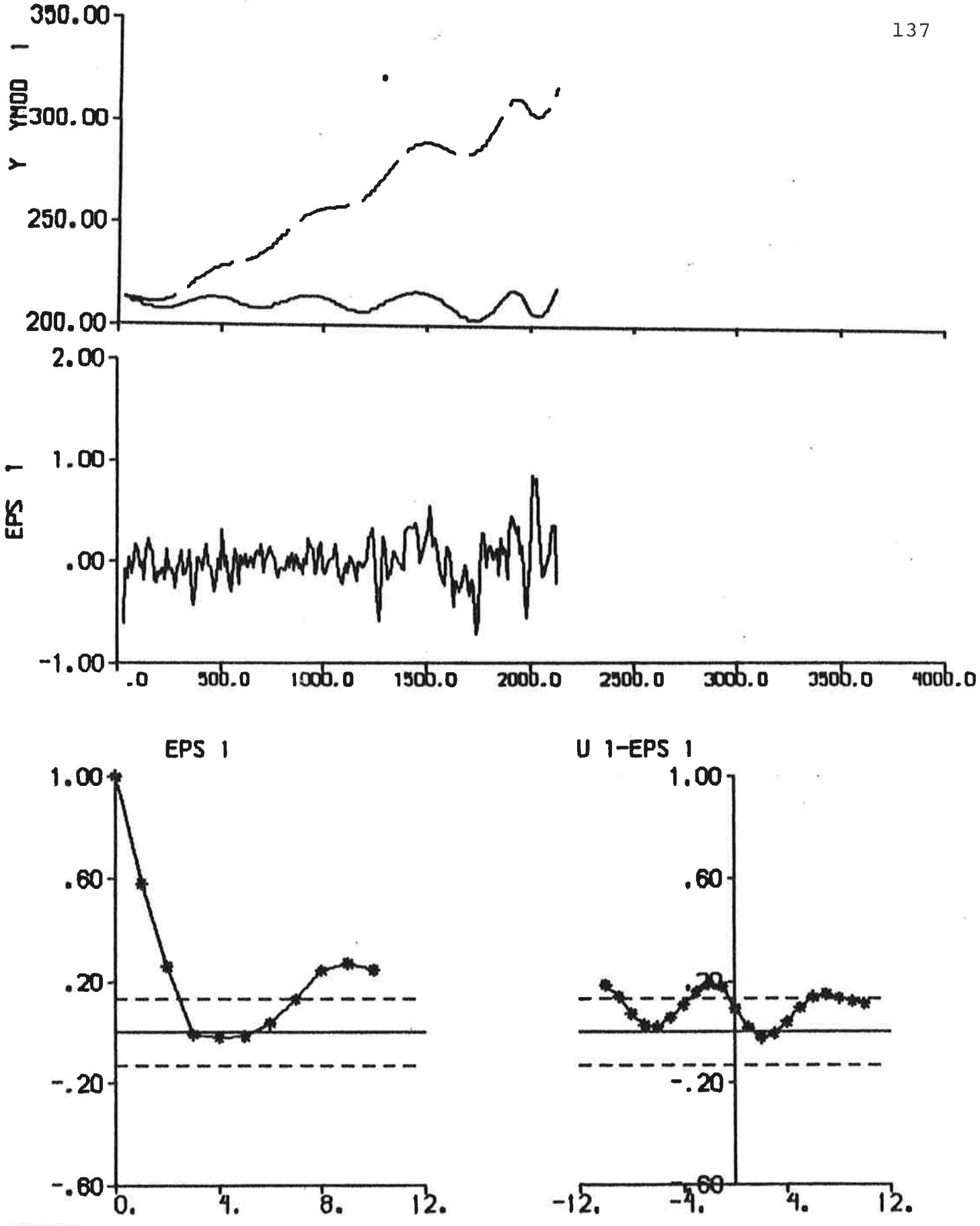

Fig. 6.12 - Result of prediction error identification (p = 3) to data from experiment E3.

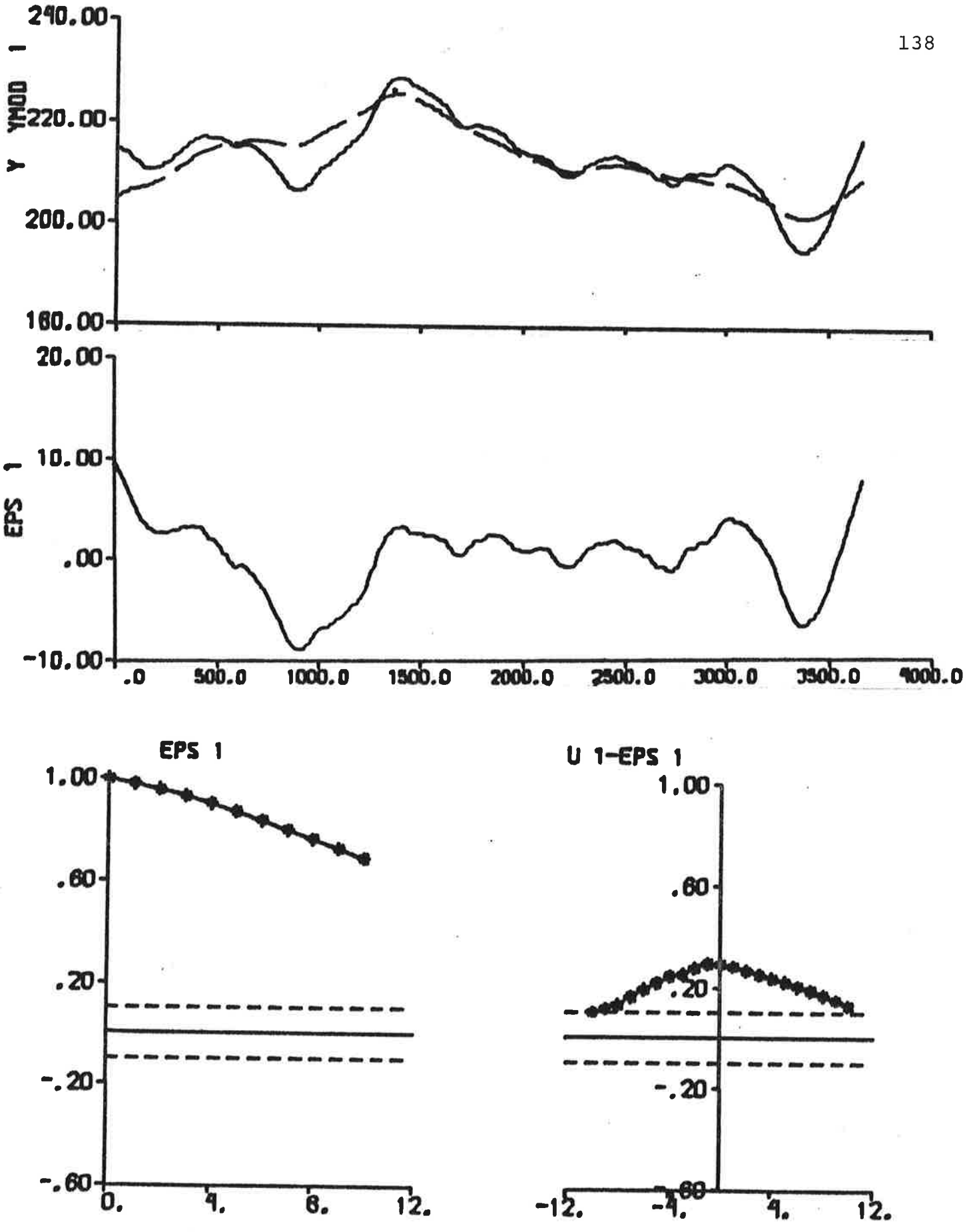

Fig. 6.13 - Result of output error identification to data from experiment E4.

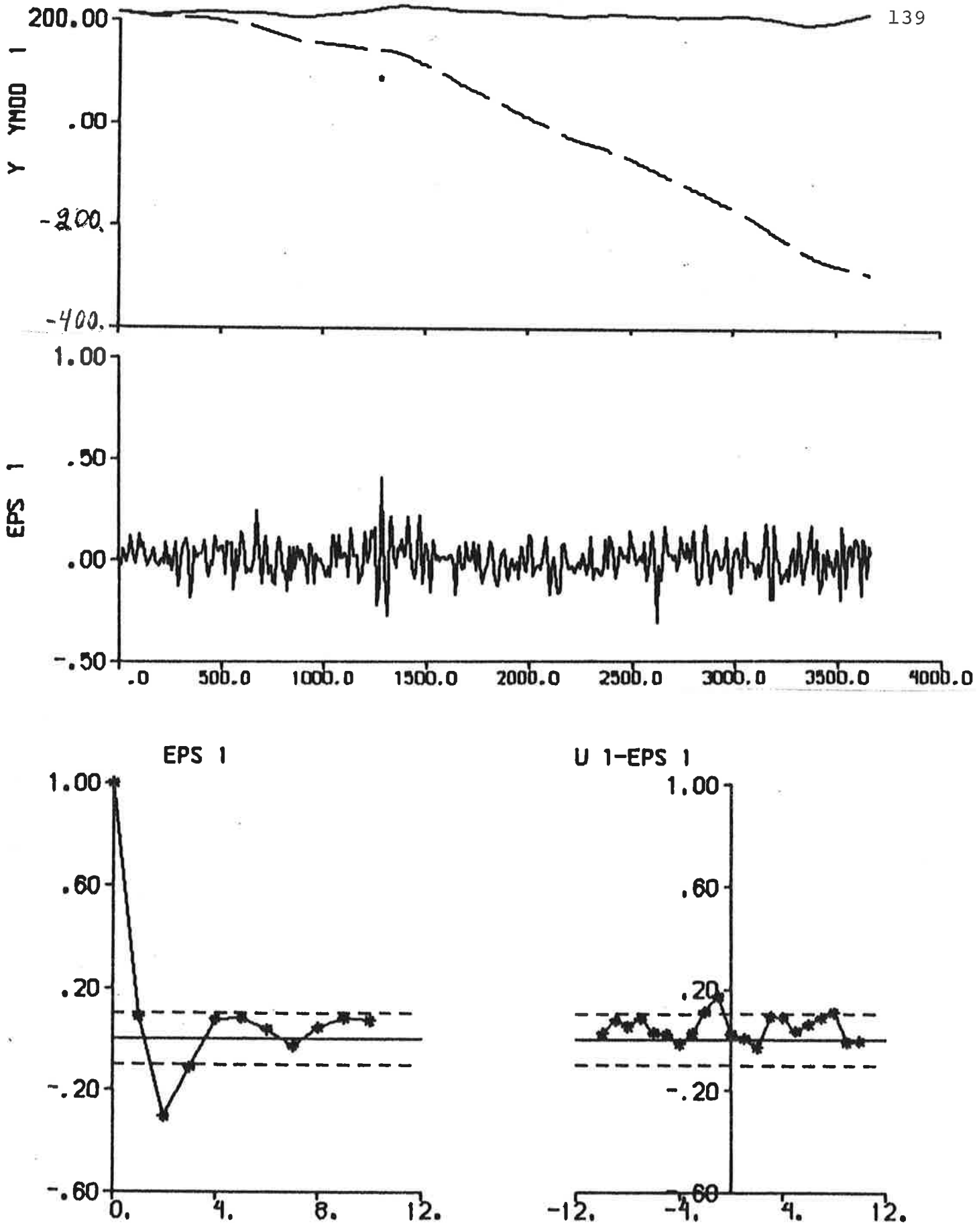

Fig. 6.14 - Result of ML identification to data from experiment E4.

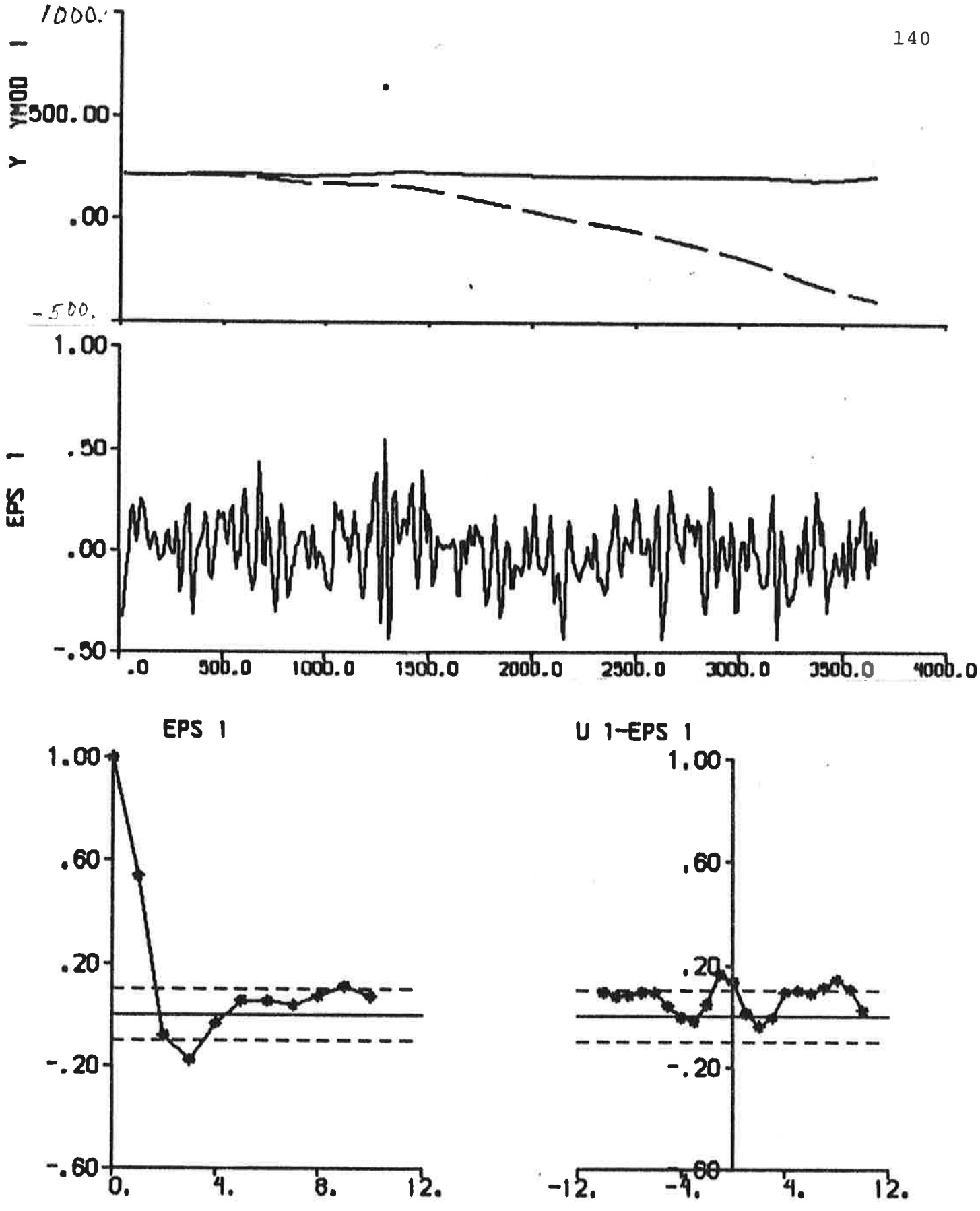

Fig. 6.15 - Result of prediction error identification (p = 2) to data from experiment E4.

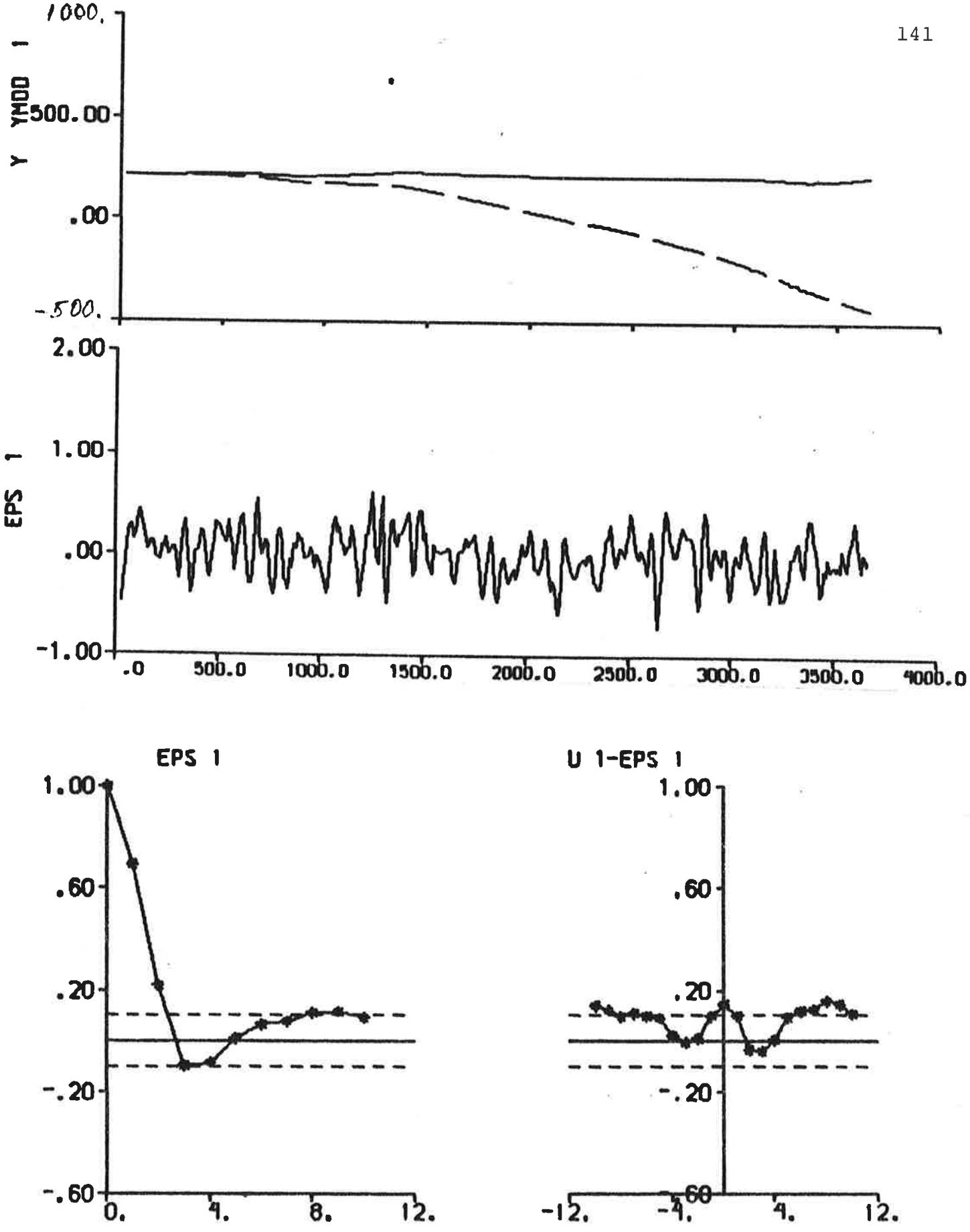

Fig. 6.16 - Result of prediction error identification (p = 3) to data from experiment E4.

Strange models are obtained when the output error method is applied to the data from the 4 experiments. The parameter estimates of φ_2 and φ_5 are very small. Nevertheless Akaike's information criterion selects the third-order transfer function (3.12) instead of Nomoto's model (3.13) in all cases.

The results are improved when the ML method is applied to the data. Notice, however, that T_2' is estimated to 0.03 - 0.07 which corresponds to 1.1 - 2.6 s. Such a short time constant may be originated from the steering engine or the wave motions but probably not from the ship steering dynamics. Akaike's information criterion also indicates in 3 cases that Nomoto's model is appropriate to the data when the ML method is used. The following filter gains K (cf. (3.4)) are obtained from applying the ML method to data from experiments E1, E2, E3 and E4:

$$K = \begin{pmatrix} 8.5\cdot10^{-4} \\ 1.1\cdot10^{-3} \\ 2.9\cdot10^{-2} \end{pmatrix}, \begin{pmatrix} 9.8\cdot10^{-4} \\ 1.2\cdot10^{-3} \\ 3.0\cdot10^{-2} \end{pmatrix}, \begin{pmatrix} 6.4\cdot10^{-4} \\ 0.9\cdot10^{-3} \\ 2.7\cdot10^{-2} \end{pmatrix}, \begin{pmatrix} 2.7\cdot10^{-4} \\ 0.8\cdot10^{-3} \\ 2.7\cdot10^{-2} \end{pmatrix} \qquad (6.8)$$

Cf.(6.4).

The results of prediction error identifications with p = 2 and 3 indicate no significant improvements compared with the ML results. The following filter gains are obtained when p =2:

$$K = \begin{pmatrix} 9.2\cdot10^{-4} \\ 1.1\cdot10^{-3} \\ 2.9\cdot10^{-2} \end{pmatrix}, \begin{pmatrix} 13.4\cdot10^{-4} \\ 1.1\cdot10^{-3} \\ 3.0\cdot10^{-2} \end{pmatrix}, \begin{pmatrix} 9.5\cdot10^{-4} \\ 1.0\cdot10^{-3} \\ 2.7\cdot10^{-2} \end{pmatrix}, \begin{pmatrix} 5.1\cdot10^{-4} \\ 0.7\cdot10^{-3} \\ 2.5\cdot10^{-2} \end{pmatrix} \qquad (6.9)$$

The corresponding filter gains for p = 3 are:

$$K = \begin{pmatrix} 3.4\cdot10^{-4} \\ 1.0\cdot10^{-3} \\ 2.9\cdot10^{-2} \end{pmatrix}, \begin{pmatrix} 13.1\cdot10^{-4} \\ 1.1\cdot10^{-3} \\ 3.0\cdot10^{-2} \end{pmatrix}, \begin{pmatrix} 9.7\cdot10^{-4} \\ 1.0\cdot10^{-3} \\ 2.8\cdot10^{-2} \end{pmatrix}, \begin{pmatrix} 5.4\cdot10^{-4} \\ 0.7\cdot10^{-3} \\ 2.6\cdot10^{-2} \end{pmatrix} \qquad (6.10)$$

It is thus concluded that the filter gains are remarkably similar for the different models.

		E 1				E 2				E 3				E 4			
	Init. estim.	Output error	ML	Pred. error		Output error	ML	Pred. error		Output error	ML	Pred. error		Output error	ML	Pred. error	
				p=2	p=3			p=2	p=3			p=2	p=3			p=2	p=3
Figure		6.17	6.18	6.19	6.20	6.21	6.22	6.23	6.24	6.25	6.26	6.27	6.28	6.29	6.30	6.31	6.32
ν		10	12	9	9	10	12	9	9	10	12	9	9	10	12	9	9
V		10.22	0.0066	0.0239	0.0520	1.77	0.0080	0.0320	0.0759	0.74	0.0061	0.0184	0.0429	5.09	0.0069	0.0226	0.0458
AIC		2447	-1002	-	-	1224	-678	-	-	563	-460	-	-	1659	-760	-	-
φ_1	2.23	-0.014	29.63	31.46	13.11	0.46	27.70	38.78	39.02	-0.038	28.60	36.94	36.92	-0.038	14.06	28.55	28.66
φ_2	-0.82	-0.0006	-0.36	-0.31	-0.50	0.0002	5.91	7.58	7.55	0.0002	-0.71	0.03	0.02	-0.00009	-0.56	-1.14	-1.14
φ_4	-0.82	-0.20	0.01	-0.83	-1.43	-0.42	-1.71	-2.46	-2.61	-0.39	-4.45	-5.18	-5.18	-0.24	-0.55	-2.64	-2.68
φ_5	-0.82	0.0004	-12.50	-13.25	-4.92	0.0005	-14.05	-19.77	-19.83	0.001	-13.54	-17.70	-17.71	-0.0006	-5.83	-11.13	-11.21
$\varphi_6 \cdot 10^9$ [s^{-3}]		-0.4	1661	1774	663.7	-0.6	-72.1	-101.7	-101.5	1.3	-2600	-3395	-3395	-0.5	-768.5	-14 18	-1435
$\varphi_7 \cdot 10^6$ [s^{-2}]		-1.3	169.6	-1151	-13 94	0.2	3272	18095	17999	-7.1	1.3	-193.2	-199.9	-1.1	-225.8	-3265	-3247
$R_1(1,1)$ [s^{-5}]		-	0.69	1.55	1.56	-	1.04	2.30	3.15	-	0.58	3.61	3.58	-	0.06	0.18	0.19
$R_1(2,2)$ [s^{-3}]		-	97.8	205.8	383.7	-	80.8	201.5	292.8	-	169.4	584.2	574.4	-	31.8	87.2	82.2
$\varphi_{15} \cdot 10^6$ [s^{-2}]		1.7	-1443	0*	0*	1.1	10976	0*	0*	3.6	-2071	0*	0*	0.4	-1332	0*	0*
φ_{16} [deg/s]		-0.009	-0.141	0*	0*	-0.086	-0.087	0*	0*	-0.008	-0.079	0*	0*	-0.001	-0.046	0*	0*
φ_{17} [deg]		219.75	214.41	214.41*	214.41*	210.20	209.86	209.86*	209.86*	213.08	213.35	213.35*	213.35*	213.36	214.41	214.41*	214.41*
T_D [s]		9.2	3.2	5.3	10.0	10.0	10.0	10.0	10.0	3.9	10.0	10.0	10.0	10.0	3.6	10.0	10.0
K'	0.99	-0.66	34.77	43.02	9.88	26.06	-2.38	-2.61	-2.63	4.59	18.98	-652	-741	6.38	10.41	9.74	9.80
K_1'	-0.82	-0.20	0.01	-0.84	-1.36	-0.42	-1.54	-205	-2.22	-0.40	-5.20	-4.63	-4.64	-0.24	-0.59	-3.12	-3.12
T_1'	-3.09	-31.37	-82.50	-102	-26.39	24600	4.65	5.09	5.14	-32.52	-40.13	1360	1544	-24.80	-25.16	-25.00	-25.10
T_2'	0.39	56.72	0.03	0.03	0.08	2.17	0.04	0.03	0.03	-143	0.03	0.03	0.03	455	0.07	0.03	0.03
T_3'	1.00	-548	-0.0006	0.06	0.29	-856	0.12	0.12	0.13	-401	0.33	0.29	0.29	428	0.10	0.24	0.24

* = fixed value

Table 6.2 - Parameter values from identifications of the transfer function (3.12).

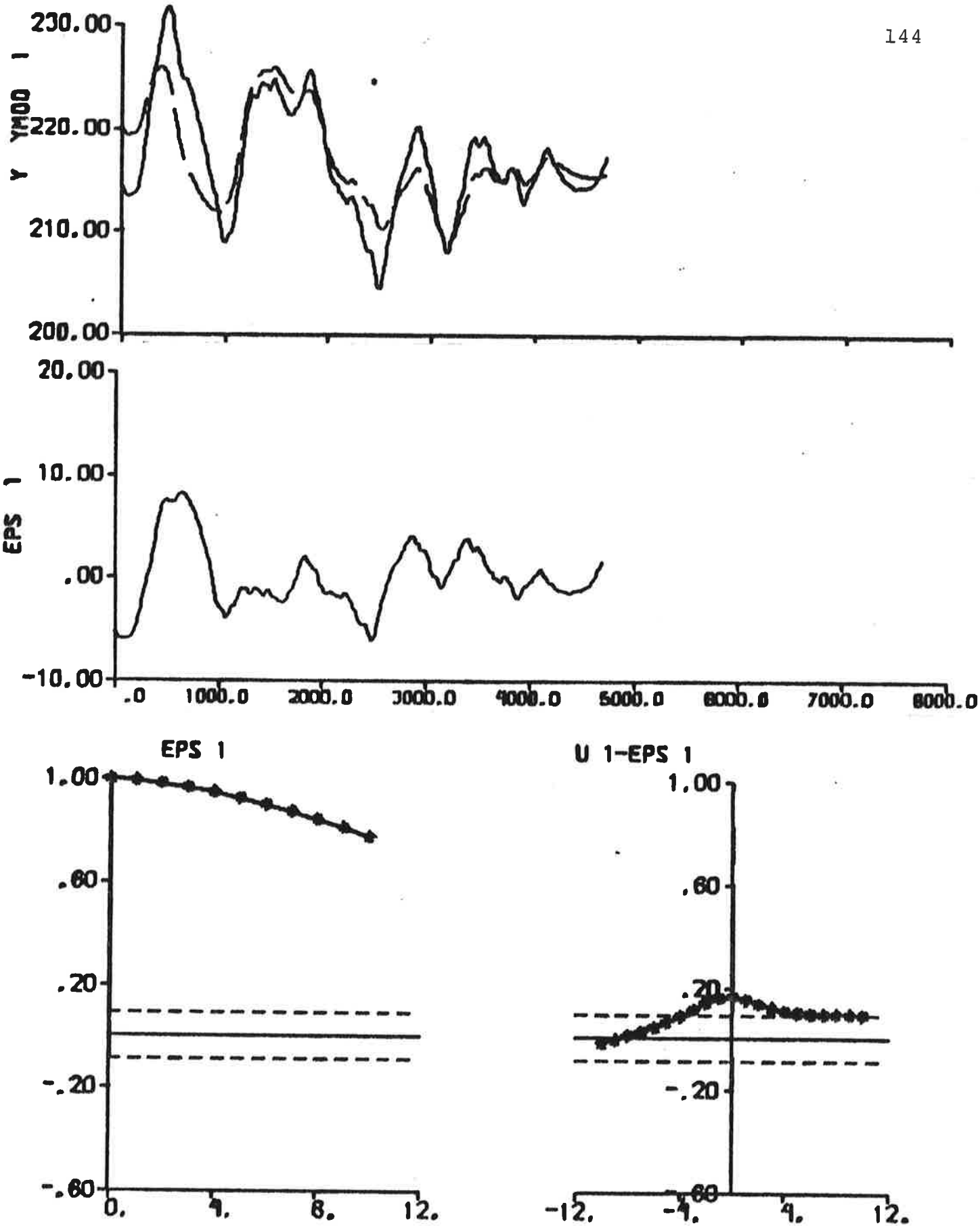

Fig. 6.17 - Result of output error identification to data from experiment E1.

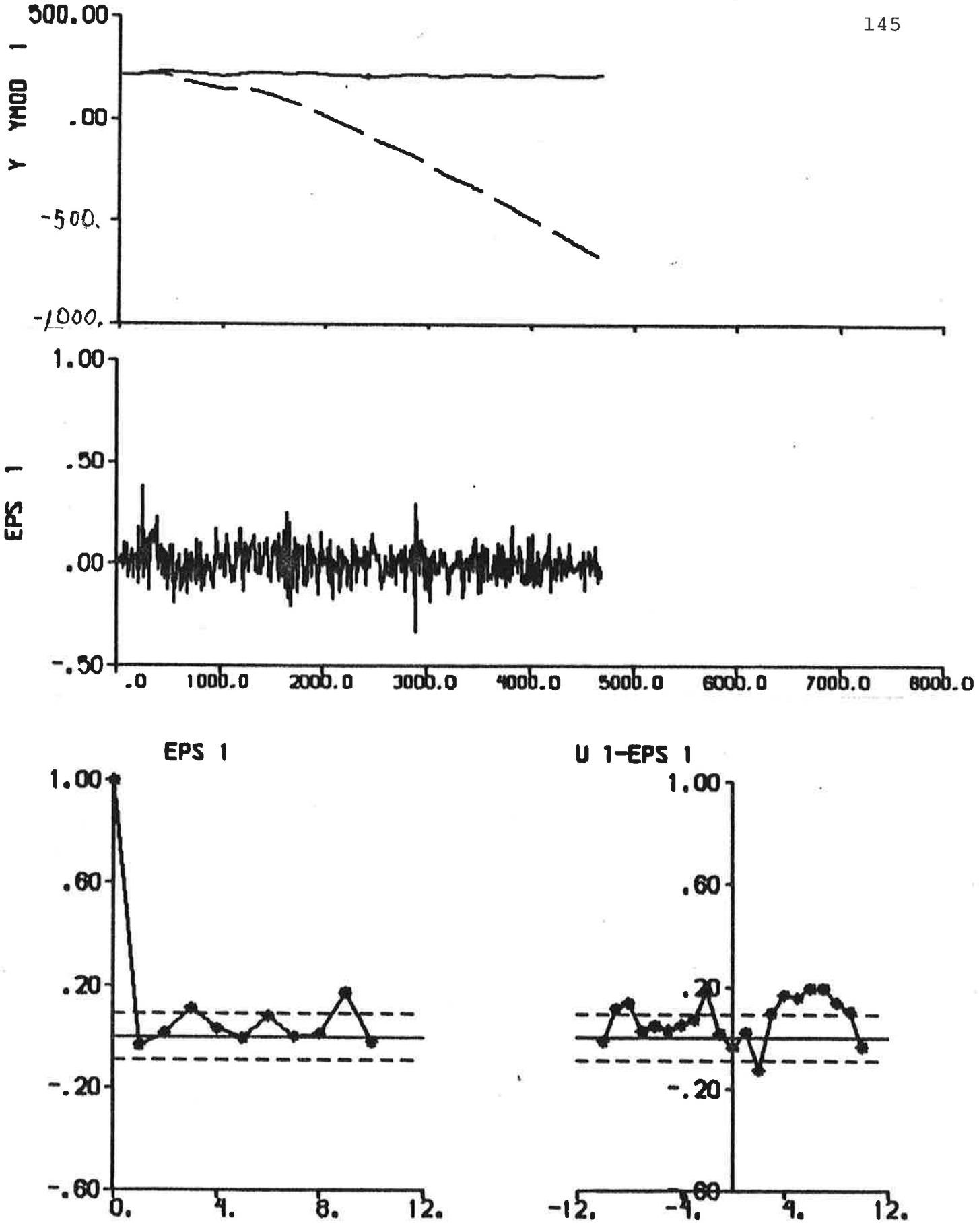

Fig. 6.18 - Result of ML identification to data from experiment E1.

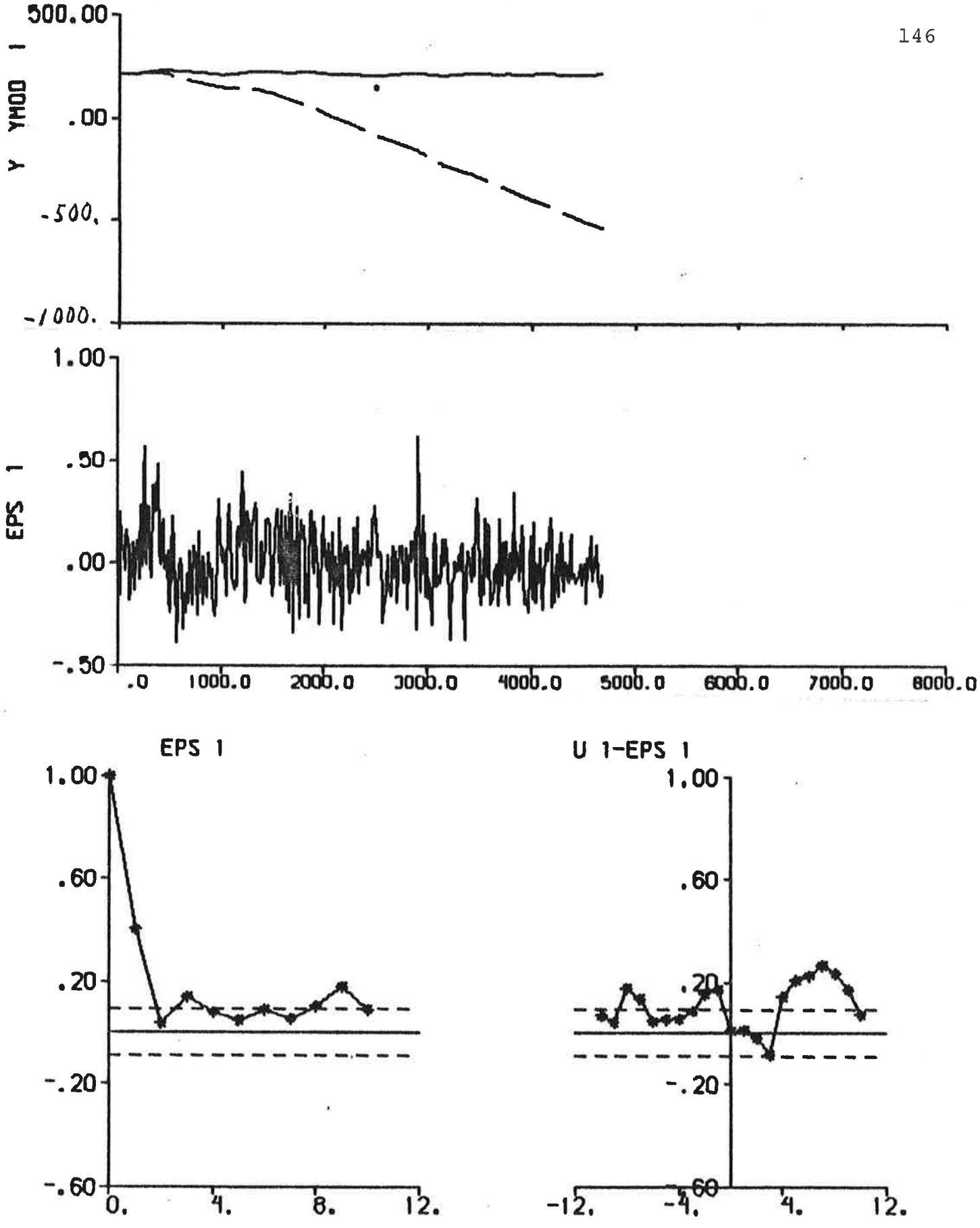

Fig. 6.19 - Result of prediction error identification (p = 2) to data from experiment E1.

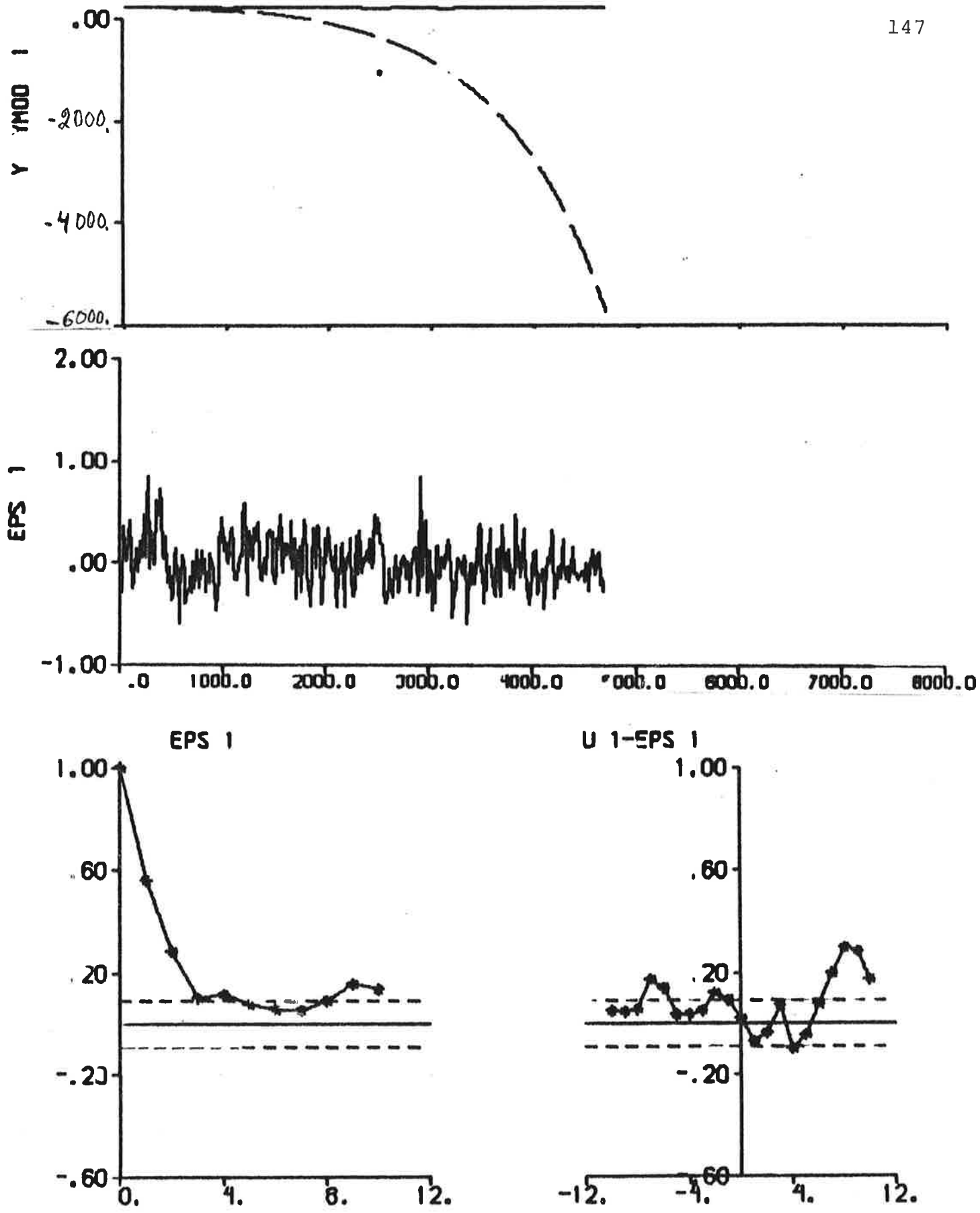

Fig. 6.20 - Result of prediction error identification (p = 3) to data from experiment E1.

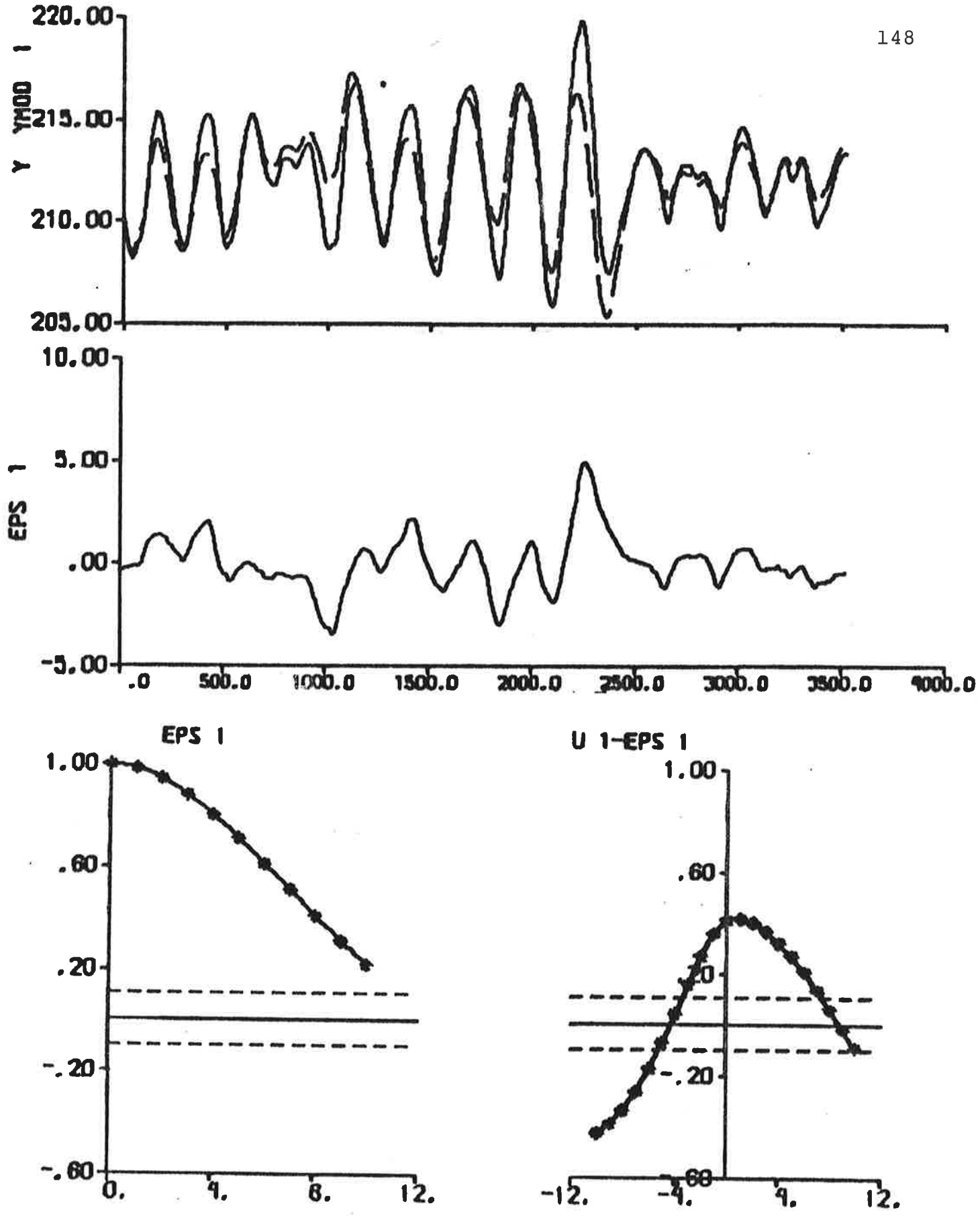

Fig. 6.21 - Result of output error identification to data from experiment E2.

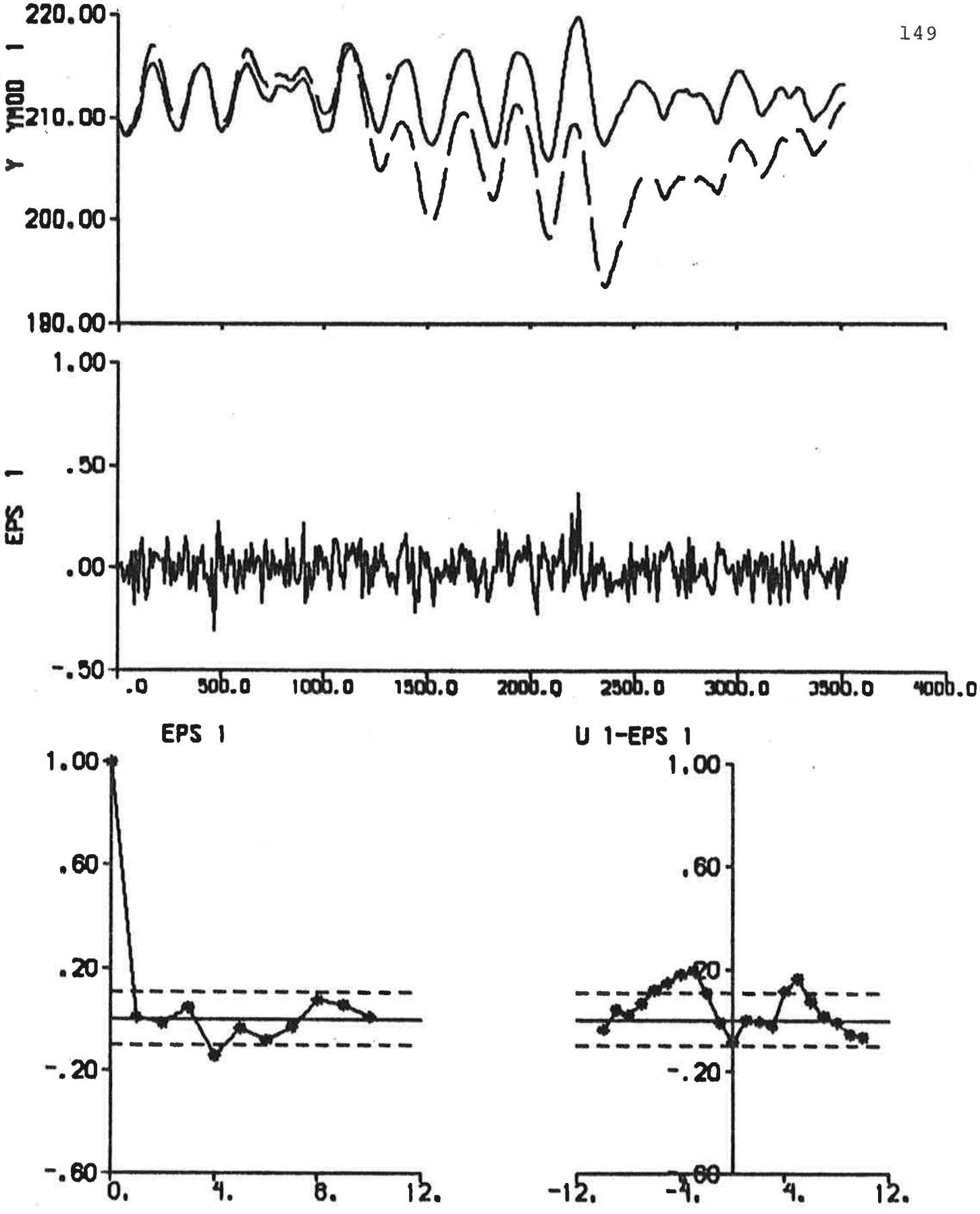

Fig. 6.22 - Result of ML identification to data from experiment E2.

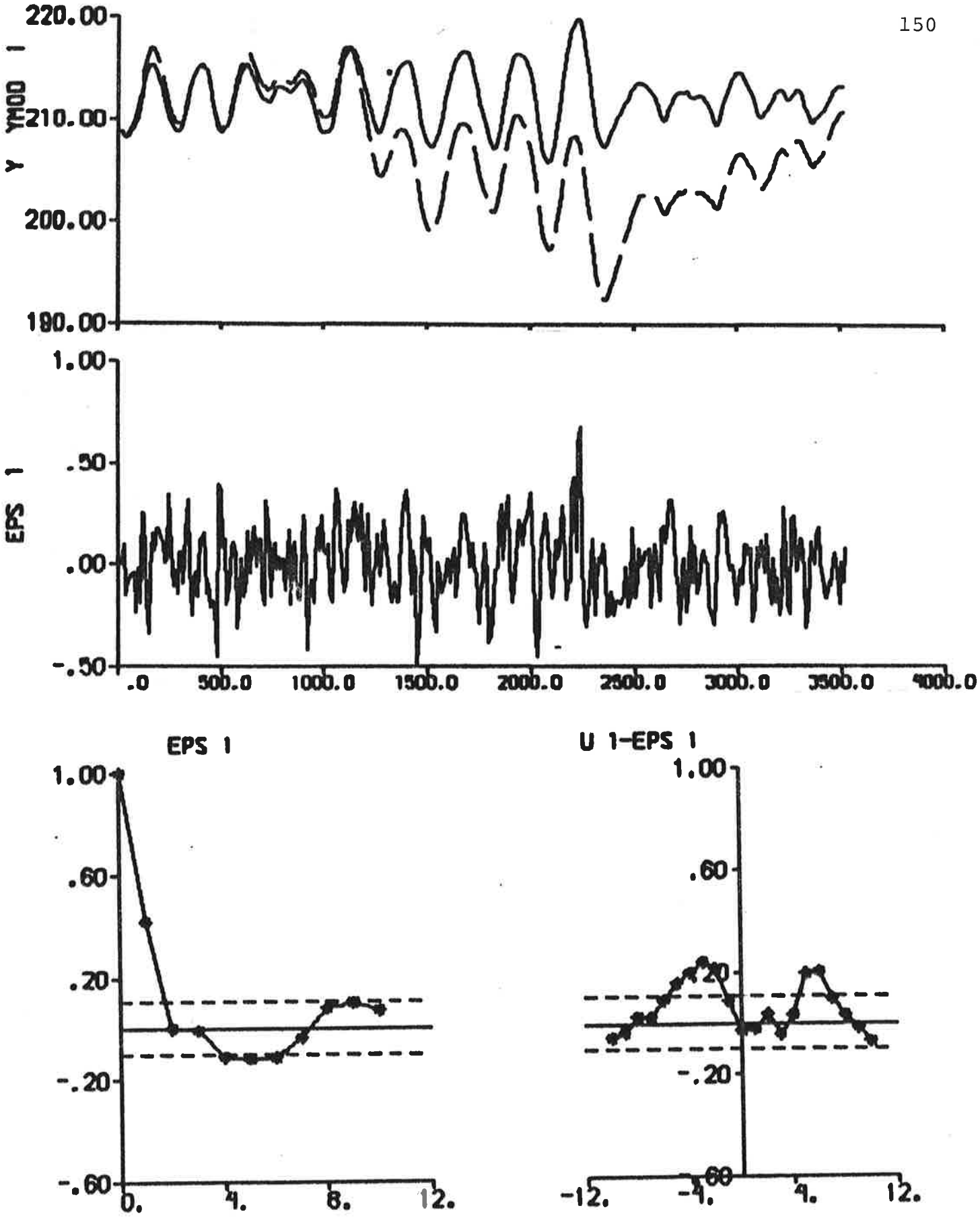

Fig. 6.23 - Result of prediction error identification (p = 2) to data from experiment E2.

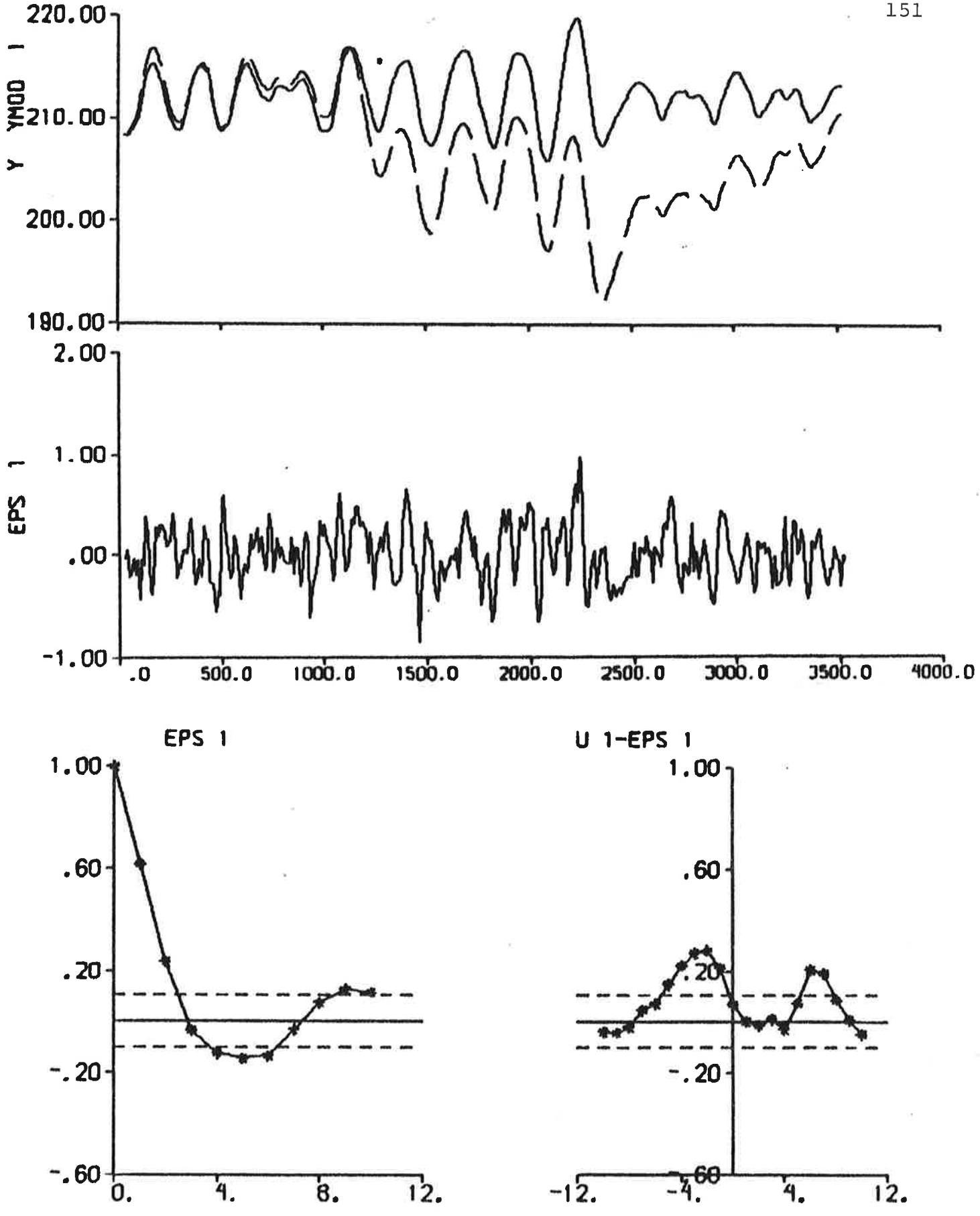

Fig. 6.24 - Result of prediction error identification (p = 3) to data from experiment E2.

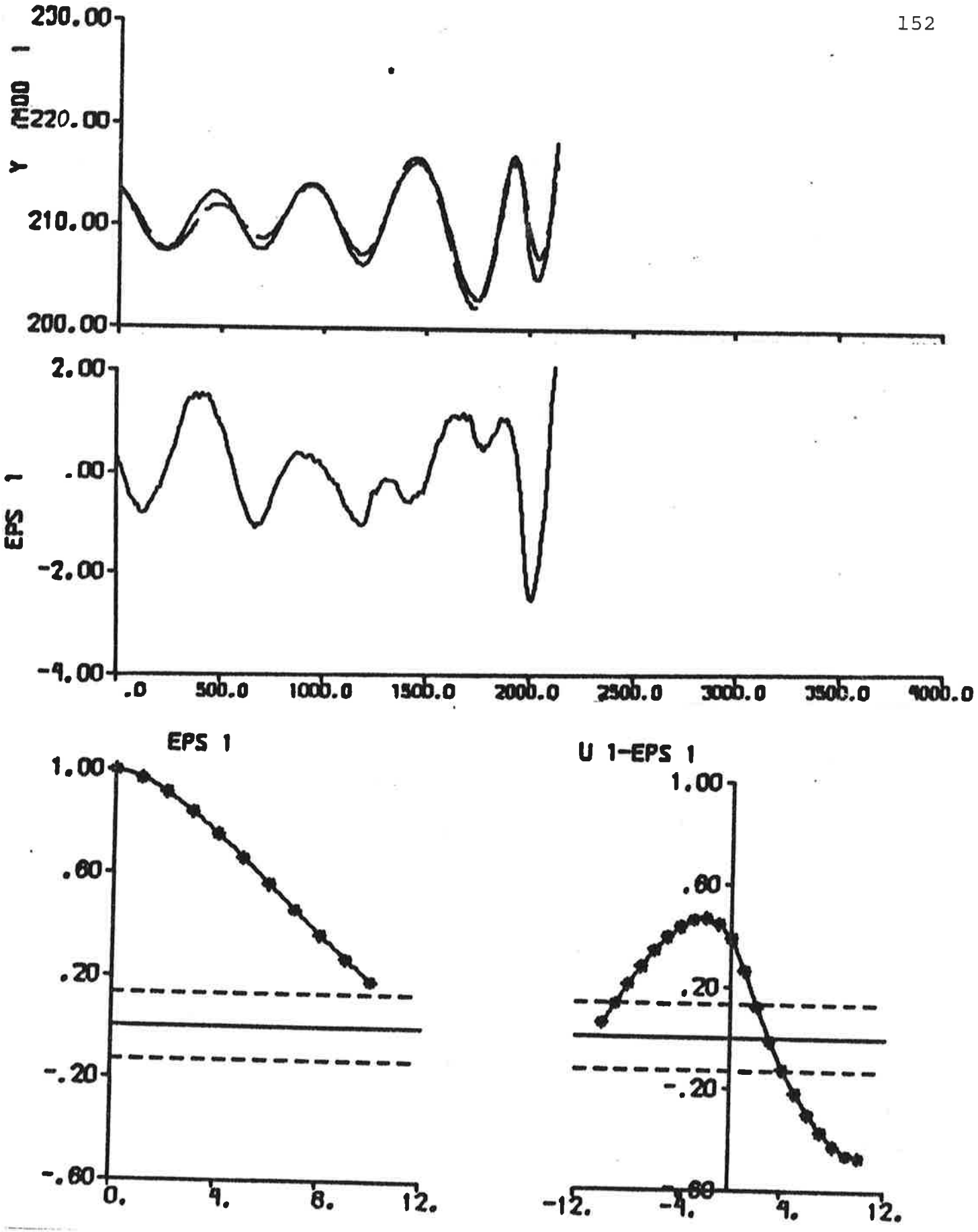

Fig. 6.25 - Result of output error identification to data from experiment E3.

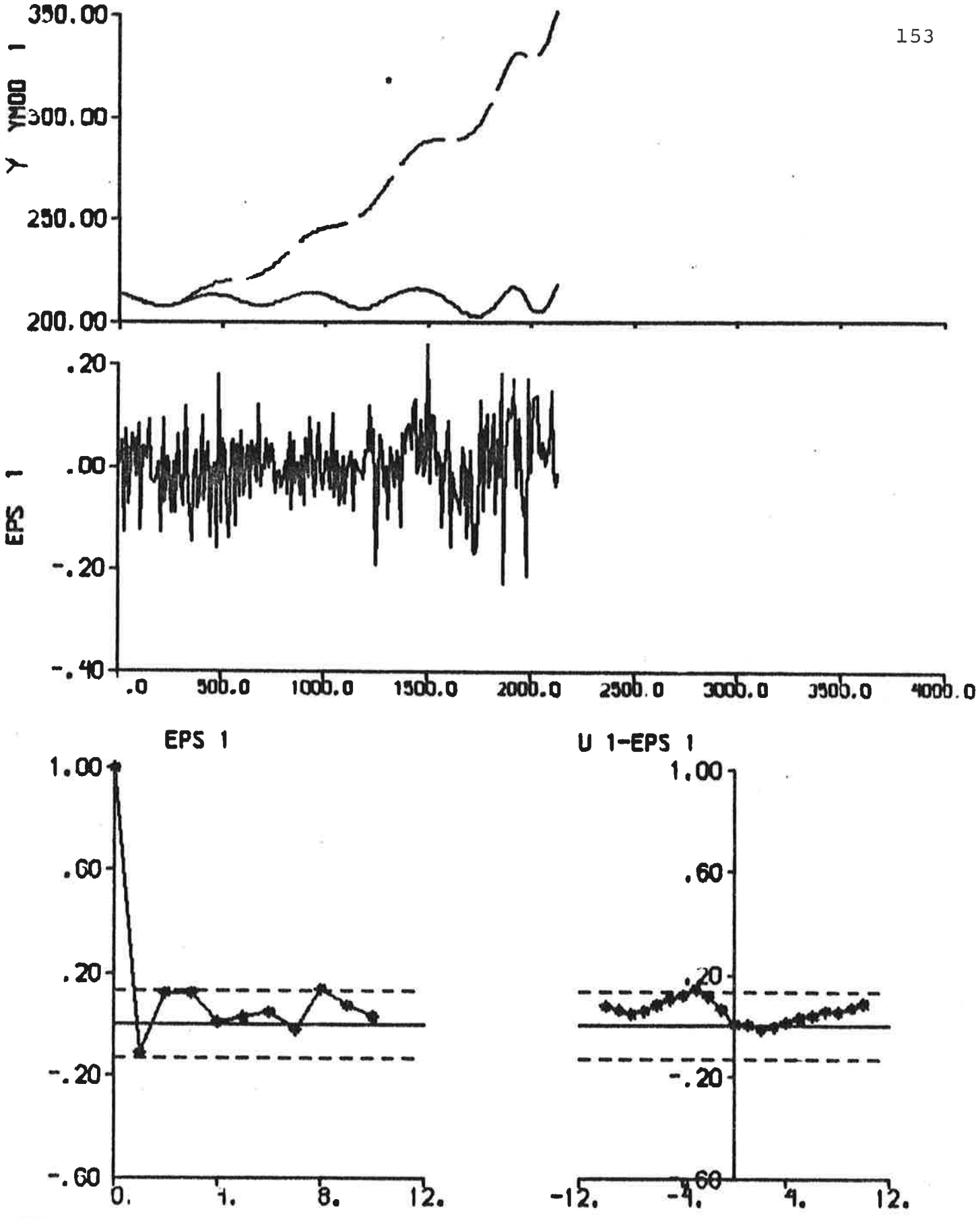

Fig. 6.26 - Result of ML identification to data from experiment E3.

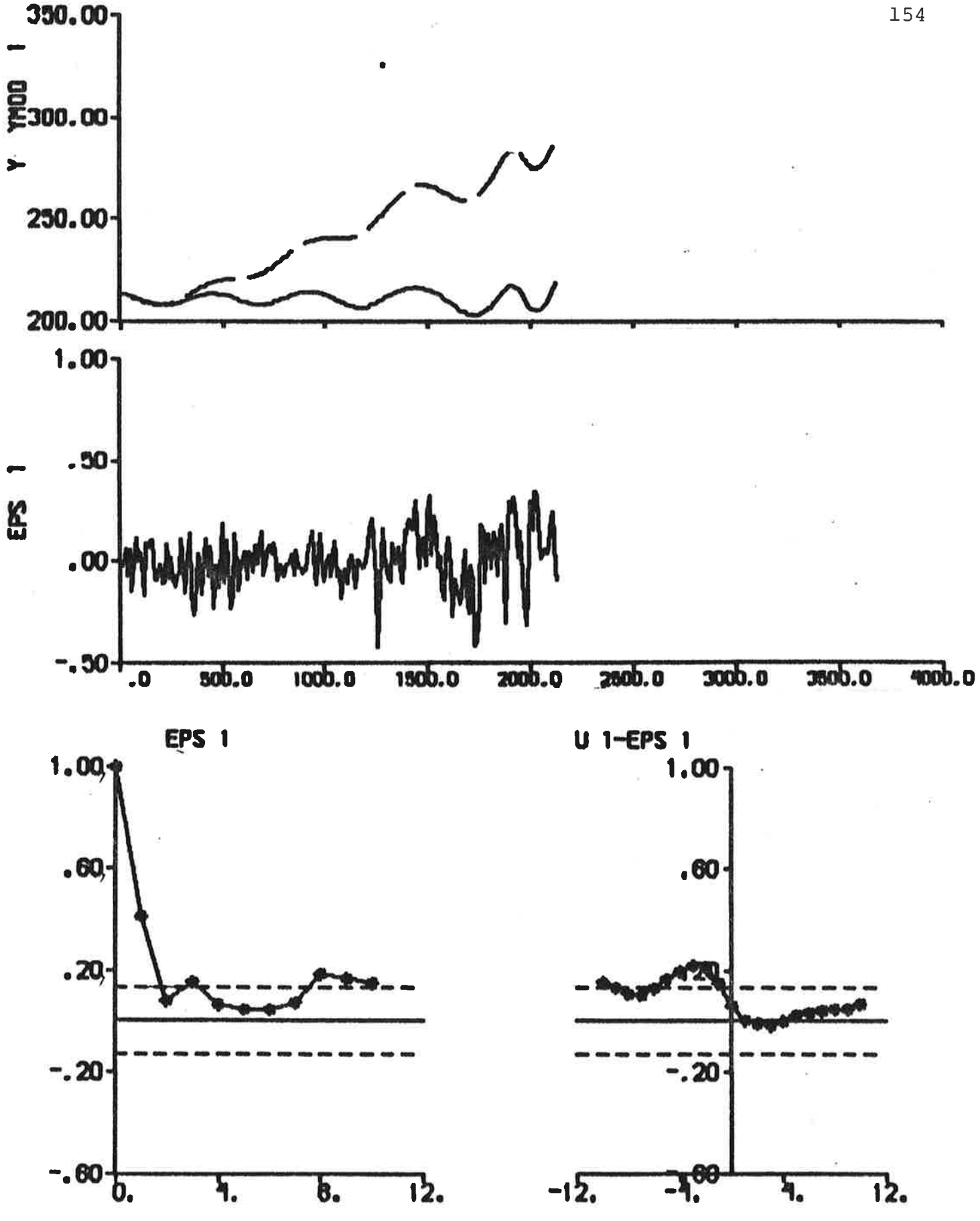

Fig. 6.27 - Result of prediction error identification (p = 2) to data from experiment E3.

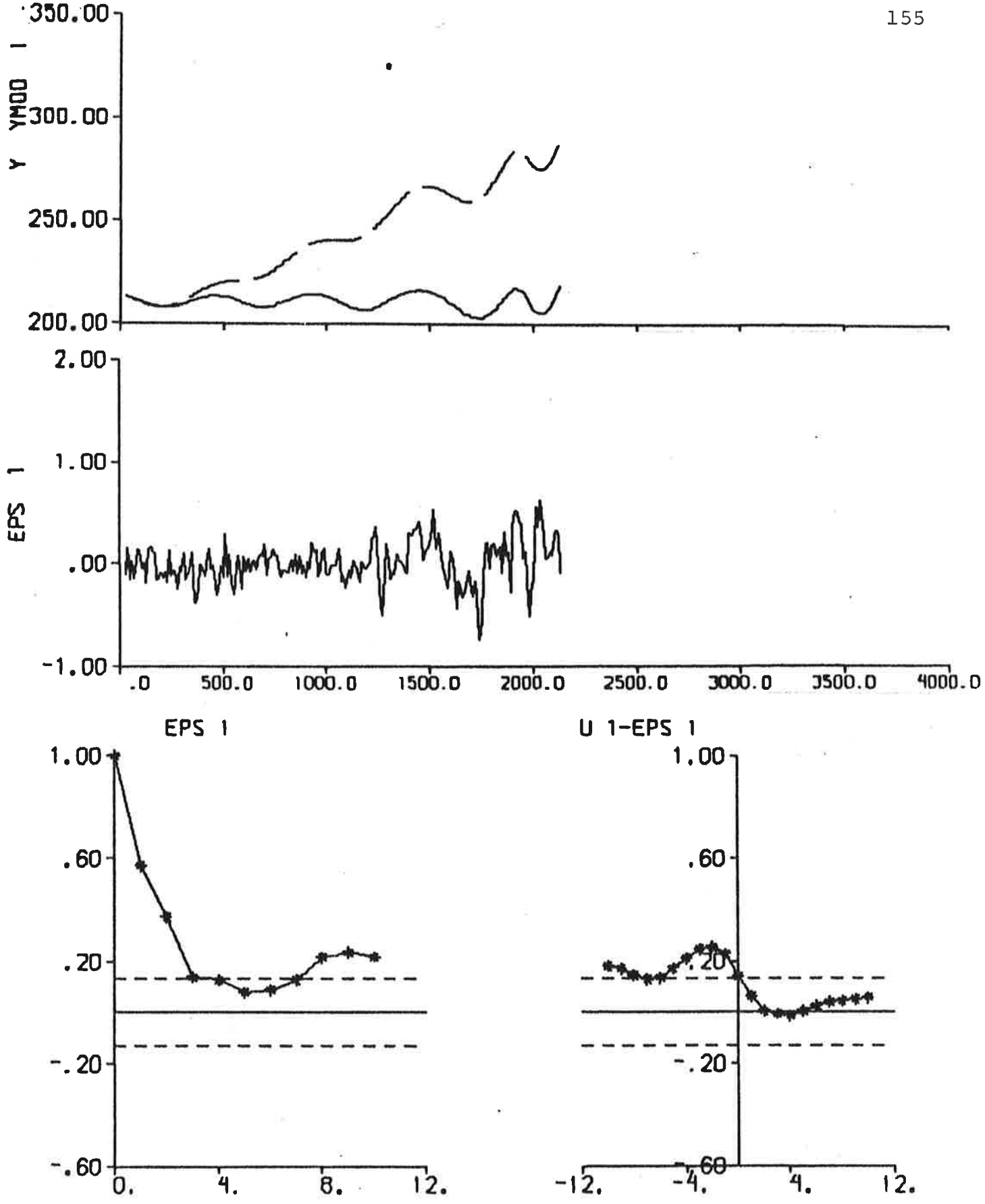

Fig. 6.28 - Result of prediction error identification (p = 3) to data from experiment E3.

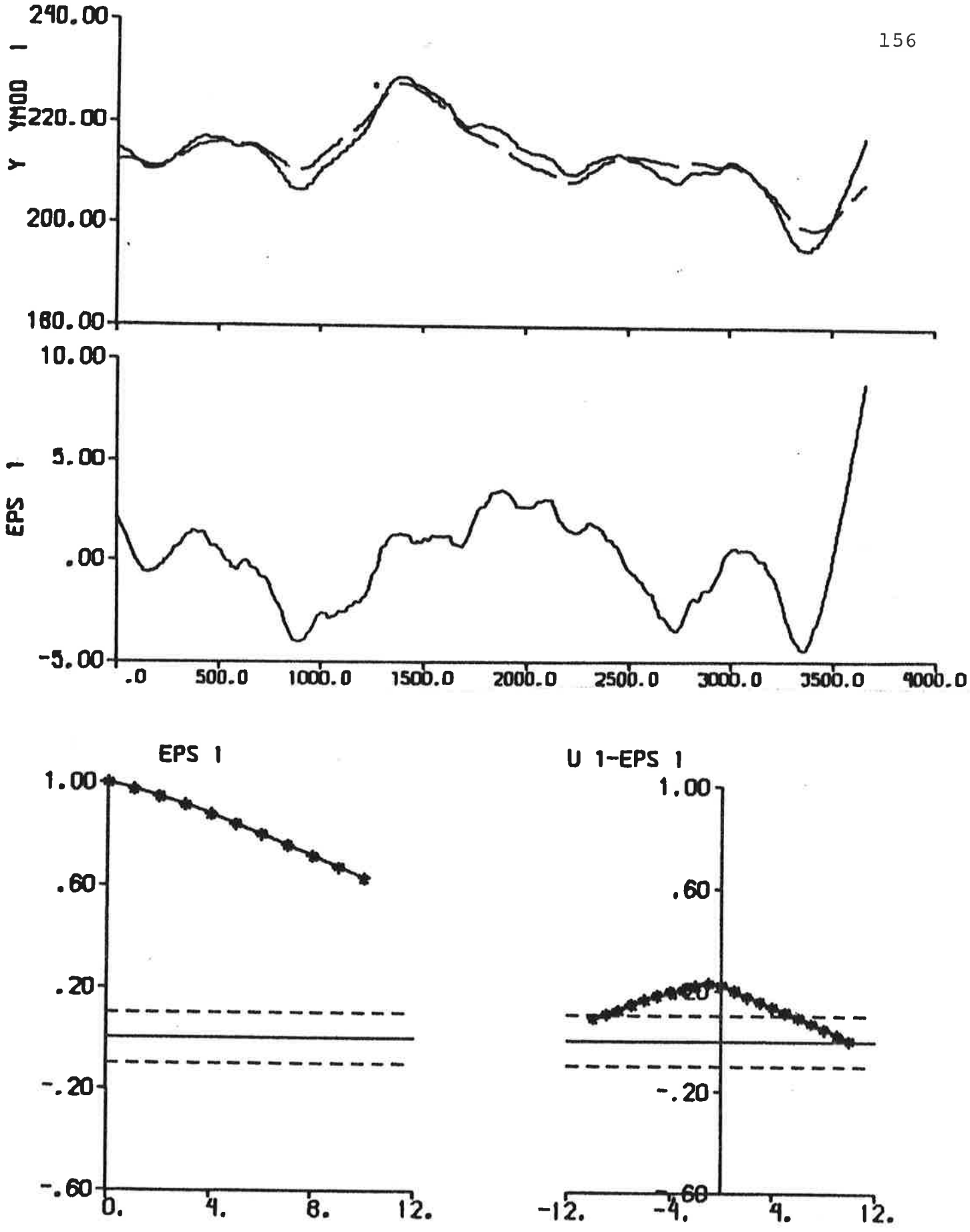

Fig. 6.29 - Result of output error identification to data from experiment E4.

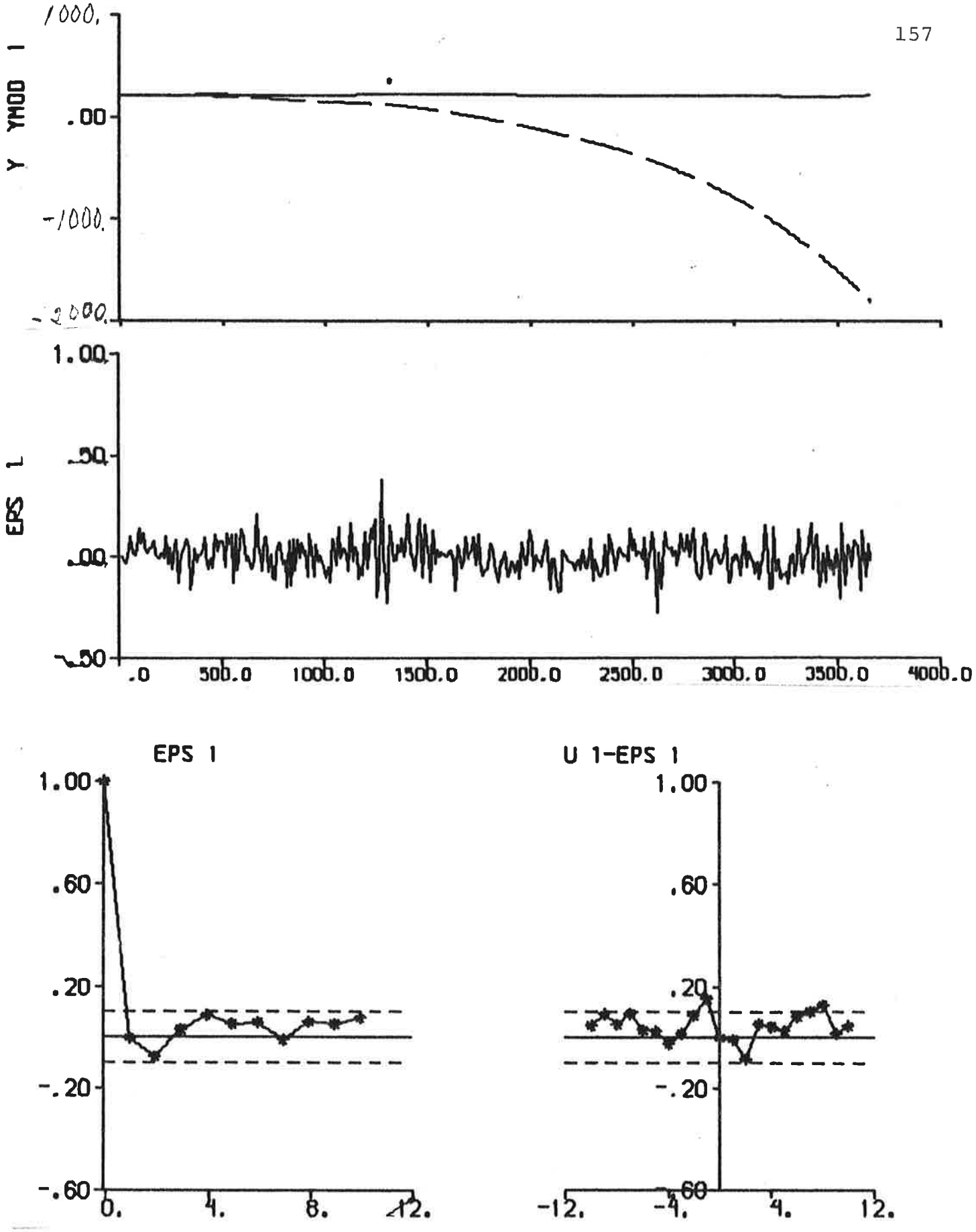

Fig. 6.30 - Result of ML identification to data from experiment E4.

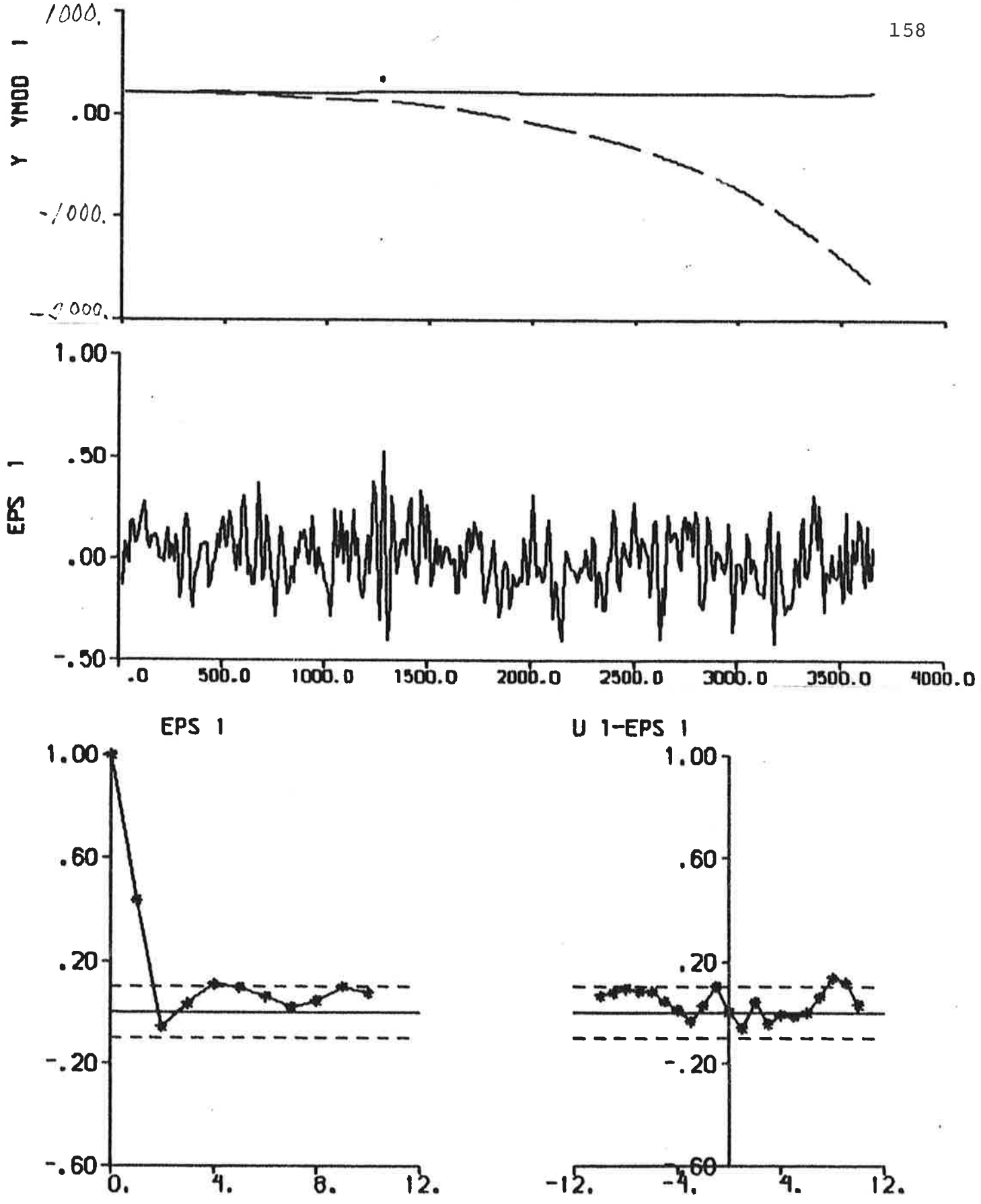

Fig. 6.31 - Result of prediction error identification (p = 2) to data from experiment E4.

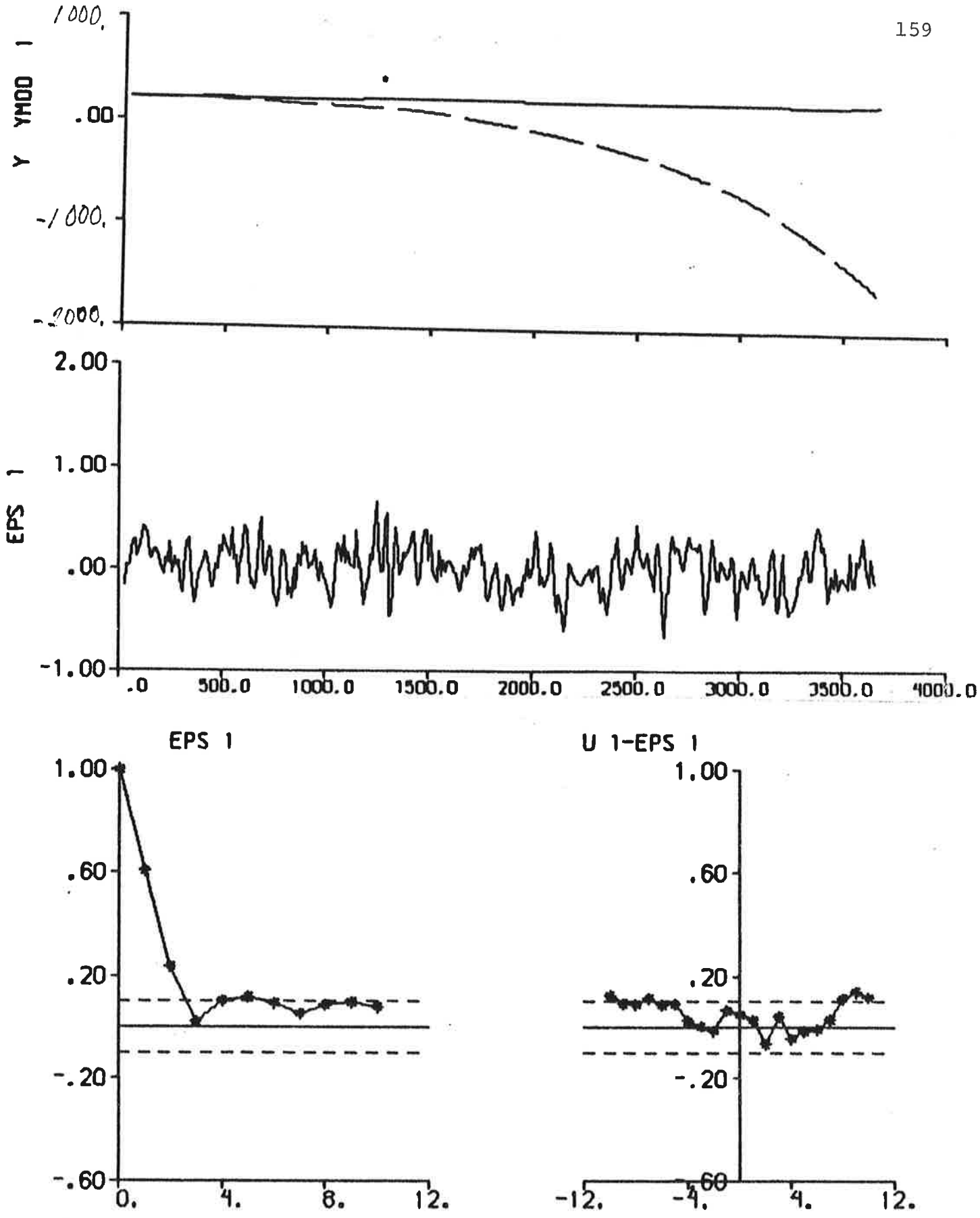

Fig. 6.32 - Result of prediction error identification (p = 3) to data from experiment E4.

Results of fitting the model (3.15) to data from experiments E1 and E2 by use of IDPAC are summarized in Table 6.3. The maximum likelihood method is used and parameters d_1 and d_2 for the initial state are also estimated. Mean values and linear trends are removed from both the rudder inputs and the heading measurements before the data are analysed. A pure integrator is almost obtained in all cases, since $1 + a_1 + a_2$ is approximately equal to zero. The parameters of Nomoto's model (3.17) are computed from the models in Table 6.3 by use of (3.20). The time delay T_D should be zero when $b_3 = 0$, if the model (3.13) is appropriate to the data. It can be concluded from Table 6.3 that T_D is different from zero, which means that the model (3.17) including a time delay should be used. The proper way of including a time delay is to also estimate b_3 (cf. (3.17) and (3.18)). See Table 6.3. It is also concluded that b_3 should be estimated according to Akaike's information criterion, since -372 and -648 should be compared with -1021 and -707. Notice that the models obtained when b_3 is estimated do not differ much from the corresponding models obtained with LISPID (cf. Table 6.1). All models of Table 6.3, except the model obtained from experiment E1 when $b_3 = 0$, are non-minimum phase. This is a consequence of the fact that a model including a time delay describing the steering engine is sampled, and has nothing to do with the ship steering dynamics.

The autocorrelation functions of residuals and the cross correlation functions between rudder inputs and residuals are shown in Figs. 6.33 - 6.36. Figures 6.34 and 6.36 can be compared with the corresponding results from LISPID (Figs. 6.2 and 6.6). It is concluded that the consistency between the results from IDPAC and LISPID is very good.

A third-order model (3.15) is also fitted to the data from the 2 experiments by use of IDPAC (cf. (3.12)). The maximum likelihood method is used and parameters d_1, d_2 and d_3 for the initial state are also estimated. Convergence difficulties

		E 1		E 2	
	Initial estimates	$b_3 = 0$	b_3 estim.	$b_3 = 0$	b_3 estim.
Figure		6.33	6.34	6.35	6.36
ν		8	9	8	9
V		0.0256*	0.0064	0.0089	0.0075
AIC		-372	-1021	-648	-707
a_1		-1.218	-2.003±0.007	-1.973±0.007	-1.956±0.007
a_2		0.226	1.002±0.007	0.968±0.006	0.941±0.007
b_1		0.006	-0.007±0.001	-0.004±0.002	-0.006±0.001
b_2		0.001	-0.019±0.002	-0.032±0.001	-0.027±0.001
b_3		-	-0.006±0.001	-	-0.011±0.001
c_1		1.07	-0.38 ± 0.05	-0.28 ± 0.06	-0.26 ± 0.05
c_2		0.57	0.03 ± 0.05	-0.17 ± 0.06	-0.05 ± 0.06
d_1		-6.39	-6.26 ± 0.08	-2.24 ± 0.10	-2.24 ± 0.09
d_2		0.77	5.94 ± 0.10	1.44 ± 0.10	1.41 ± 0.09
K'	0.99	0.03	60.19	-4.25	-2.82
K_1'	-0.27	0.17	-0.45	-0.52	-0.65
T'	-3.70	0.18	-133.04	8.17	4.37
T_D [s]	-	-2.4	4.7	3.9	6.2

* = minimum point not found (maximum number of iterations (50) reached)

Table 6.3 - Parameter values from ML identifications using IDPAC. Nomoto's model (see (3.13) and (3.17)) is determined. Parameters d_1 and d_2 for the initial state are estimated. The estimated standard deviations are given in some cases.

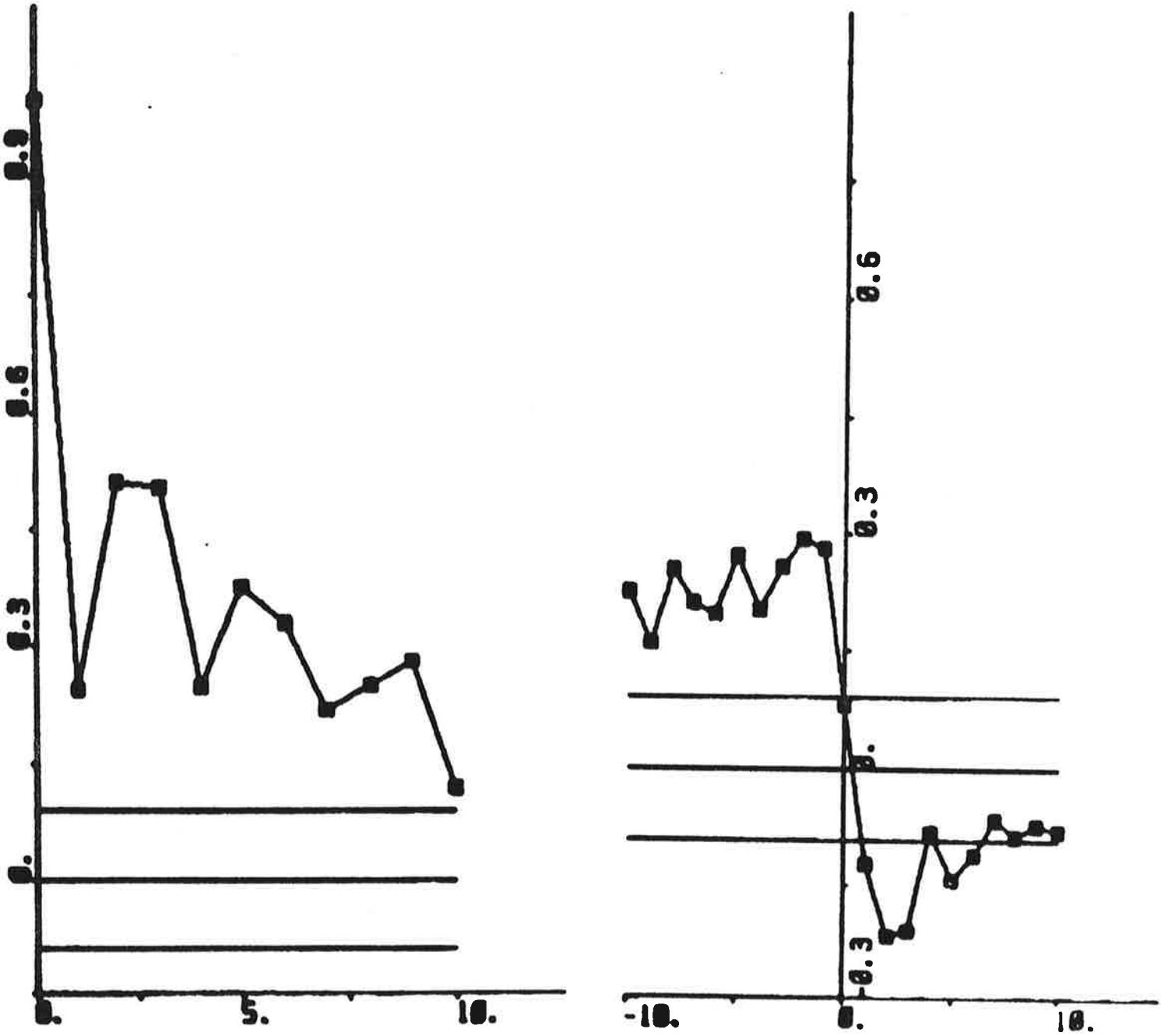

Fig. 6.33 - Autocorrelation function of residuals and cross correlation function between rudder input and residuals, where the residuals are obtained from ML identification using IDPAC to data from experiment E1 ($b_3 = 0$).

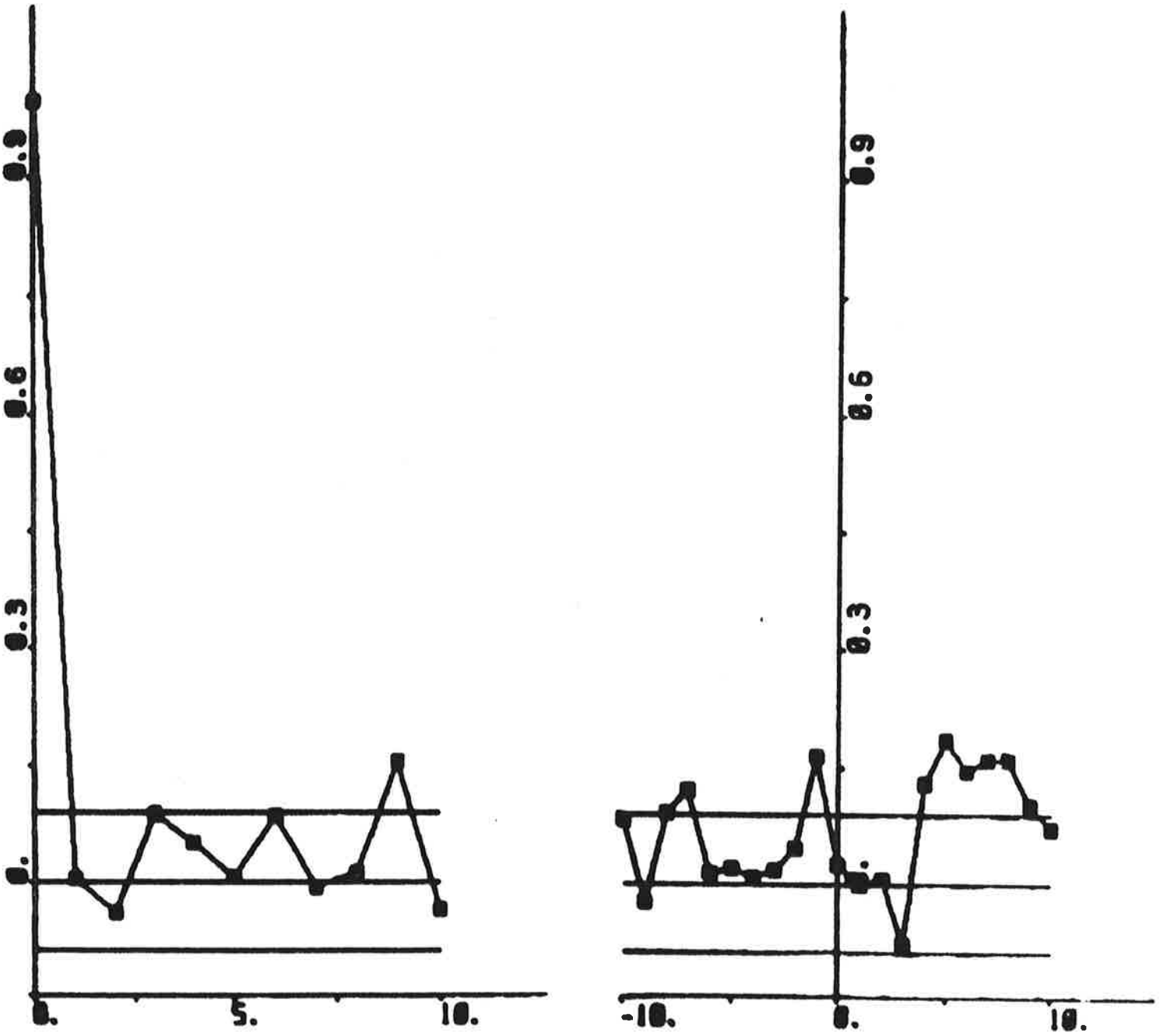

Fig. 6.34 - Autocorrelation function of residuals and cross correlation function between rudder input and residuals, where the residuals are obtained from ML identification using IDPAC to data from experiment E1 (b_3 estimated).

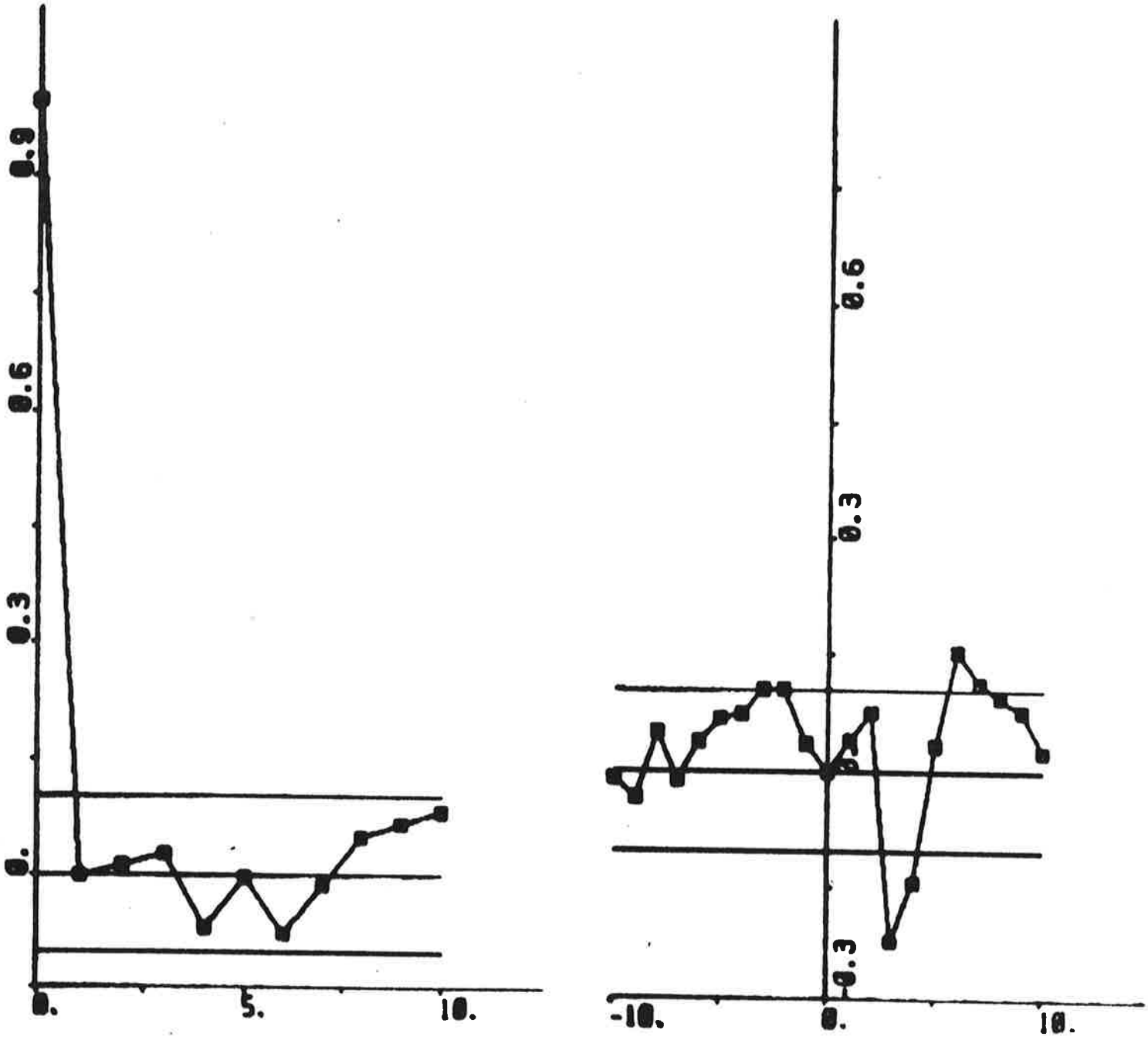

Fig. 6.35 - Autocorrelation function of residuals and cross correlation function between rudder input and residuals, where the residuals are obtained from ML identification using IDPAC to data from experiment E 2 ($b_3 = 0$).

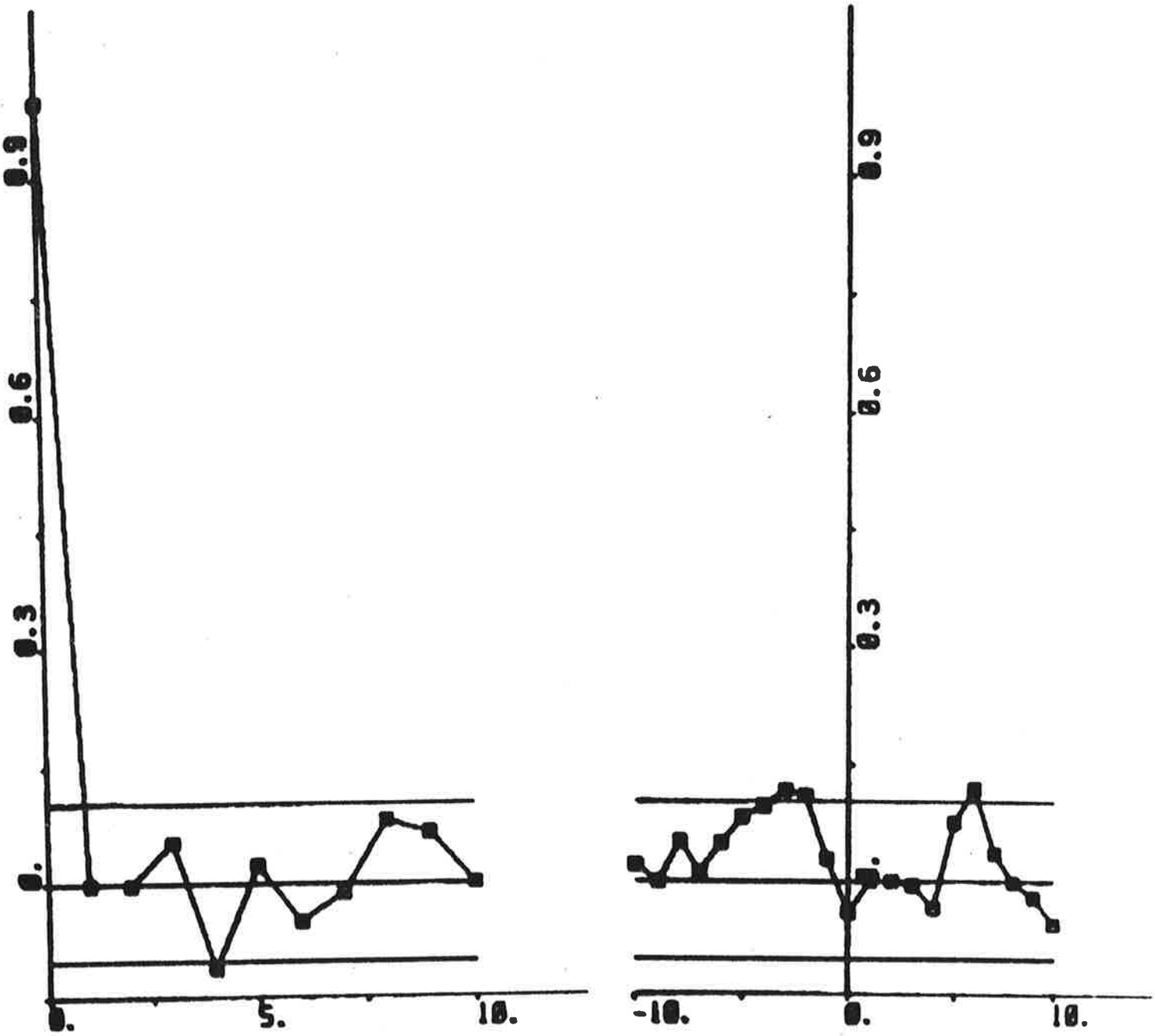

Fig. 6.36 - Autocorrelation function of residuals and cross correlation function between rudder input and residuals, where the residuals are obtained from ML identification using IDPAC to data from experiment E 2 (b_3 estimated).

were obtained. The results are shown in Table 6.4 and Figs. 6.37 and 6.38. A pure integrator is almost obtained since $1 + a_1 + a_2 + a_3$ is approximately equal to zero. Notice that the models of Table 6.4, as well as the models of Table 6.3, are non-minimum phase. It can be concluded by analysing the models in Table 6.4 that a pole on the negative real axis is obtained. This problem was discussed in Åström, Källström, Norrbin and Byström (1975) and in Åström and Källström (1976). It was concluded that a first-order model with a negative pole is typical for a case where round-off noise occurs. However, this will probably not explain the negative pole, since the autocorrelation functions obtained with Nomoto's model (Figs. 6.34 and 6.36) indicate no oscillatory behaviour.

The following input - output relations are obtained for the models in Table 6.4:

$$H(q) = \frac{-0.006q^2 - 0.027q - 0.024}{(q+ 0.925)(q^2 - 2.007q + 1.006)} \qquad (6.11)$$

$$H(q) = \frac{-0.005q^2 - 0.030q - 0.022}{(q + 0.410)(q^2 - 1.964q + 0.954)} \qquad (6.12)$$

These input - output relations can be compared with the models shown in Table 6.3, where b_3 is estimated, provided that the pole on the negative real axis is neglected. It can be concluded that the parameter values of (6.11) and (6.12) are close to the corresponding values of Table 6.3. However, the magnitude of the parameter b_3 is increased in (6.11) and (6.12). By using (3.20) the parameters of Nomoto's model (3.17) can be computed from (6.11) and (6.12). The results are shown in Table 6.4.

Based on Akaike's information criterion and analysis of the residuals it is concluded that Nomoto's models of Table 6.3 are better than the corresponding third-order models of Table 6.4. LISPID and IDPAC thus give the same model order. However, an analysis of experiments E1 and E2 performed by Gustavsson, Ljung and Söderström (1977) indicated that a third-order transfer function relating yaw rate to rudder angle was appropriate to

the data. They used IDPAC to determine a relation between the differenced heading angle and the requested rudder angle, which is not exactly the same as the rudder command used here.

It is thus possible to determine the parameters K_1 and T of Nomoto's model (3.13) by using either LISPID or IDPAC. It is difficult to determine the time constants T_2 and T_3 of (3.12) when the only measurement signal used is the heading angle. Remember, however, that good results were obtained from LISPID when measurements of sway velocities and yaw rates also were used. The difficulties obtained when estimating T_2 and T_3 of the transfer function (3.12) are possibly due to an approximate pole - zero cancellation. If the true values of T_2 and T_3 are close to each other, it is, of course, extremely difficult to detect this mode from an input-output experiment, where the rudder command is the input and the heading angle the output. The improved results obtained when measurements of sway velocities also are used in the identification procedure (see Section 4) are due to the fact that it is possible to get information about T_2 through the transfer function (3.8) in this case. Another explanation is that the heading measurements, but not the measurements of sway velocities, are influenced by disturbances from, for example, waves. The wave periods are typically of the order of 5 - 10 s and it is thus quite possible that they i interact with the time constant T_2.

7. CONCLUSIONS

Four experiments performed with the 255 000 tdw oil tanker Sea Swift were analysed. The tanker was fully loaded and the speed was approximately 17 knots during the experiments. A PRBS was approximately used as rudder perturbations during experiments E1 and E4, which were performed in open loop. Experiments E2 and E3 were carried out in closed loop. Fore and aft sway velocities, yaw rates and heading angles were measured and recorded with a precise, constant sampling interval. The sampling interval was chosen to 10 s.

	Initial estimates	E 1	E 2
Figure		6.37	6.38
ν		12	12
V		0.0070*	0.0078
AIC		-973	-687
a_1		-1.082	-1.554
a_2		-0.850	0.149
a_3		0.931	0.391
b_1		-0.006	-0.005
b_2		-0.027	-0.030
b_3		-0.024	-0.022
c_1		0.54	0.14
c_2		-0.37	-0.23
c_3		0.01	0.02
d_1		-5.79	-2.20
d_2		0.31	0.48
d_3		5.30	0.62
K'	0.99	35.74	-4.66
K_1'	-0.27	-0.80	-0.83
T'	-3.70	-44.43	5.64
T_D [s]	-	8.2	8.0

* = minimum point not found (maximum number of iterations (50) reached).

Table 6.4 - Parameter values from ML identifications using IDPAC. Parameters d_1, d_2 and d_3 for the initial state are estimated.

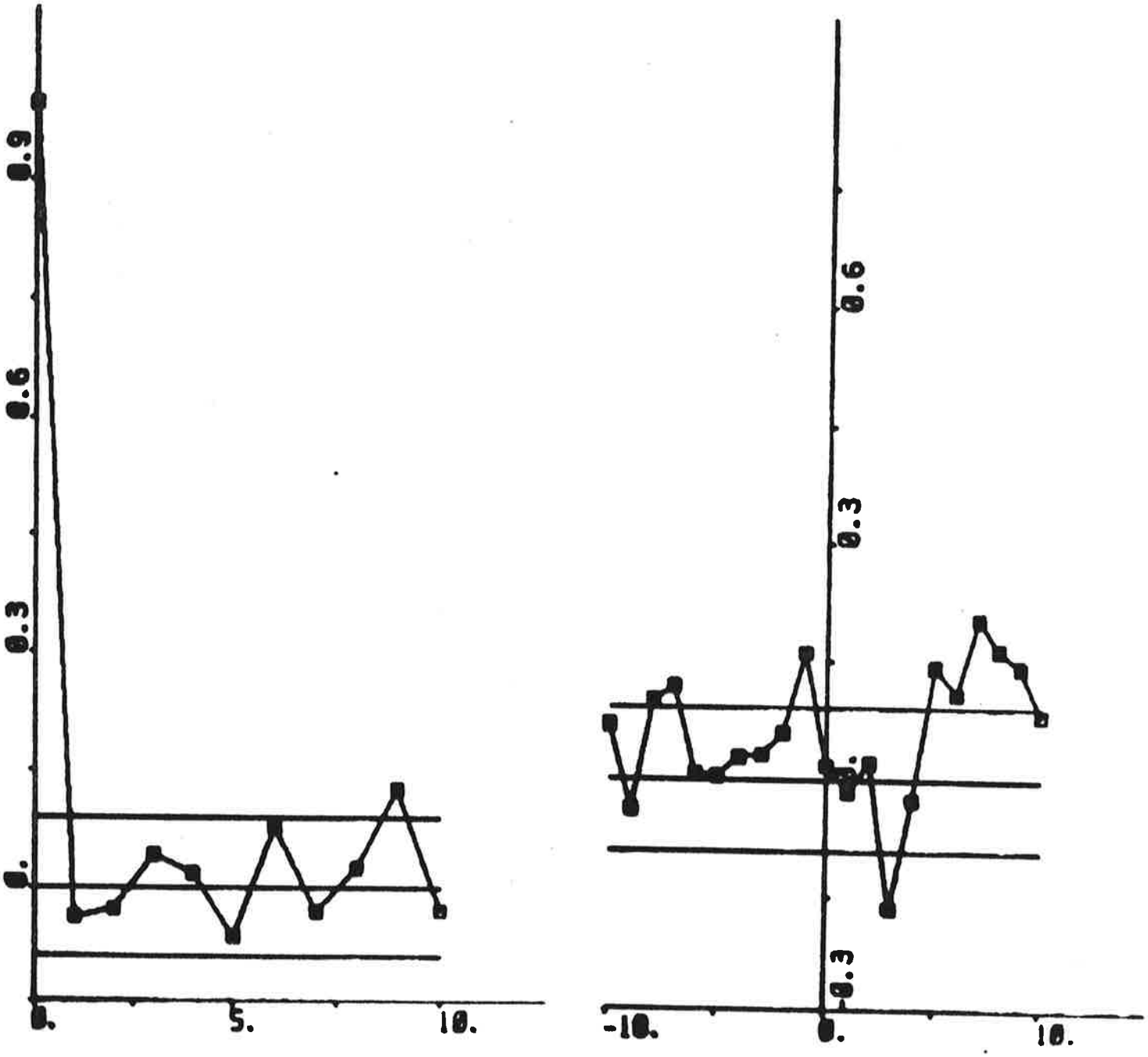

Fig. 6.37 - Autocorrelation function of residuals and cross correlation function between rudder input and residuals, where the residuals are obtained from ML identification using IDPAC to data from experiment E1.

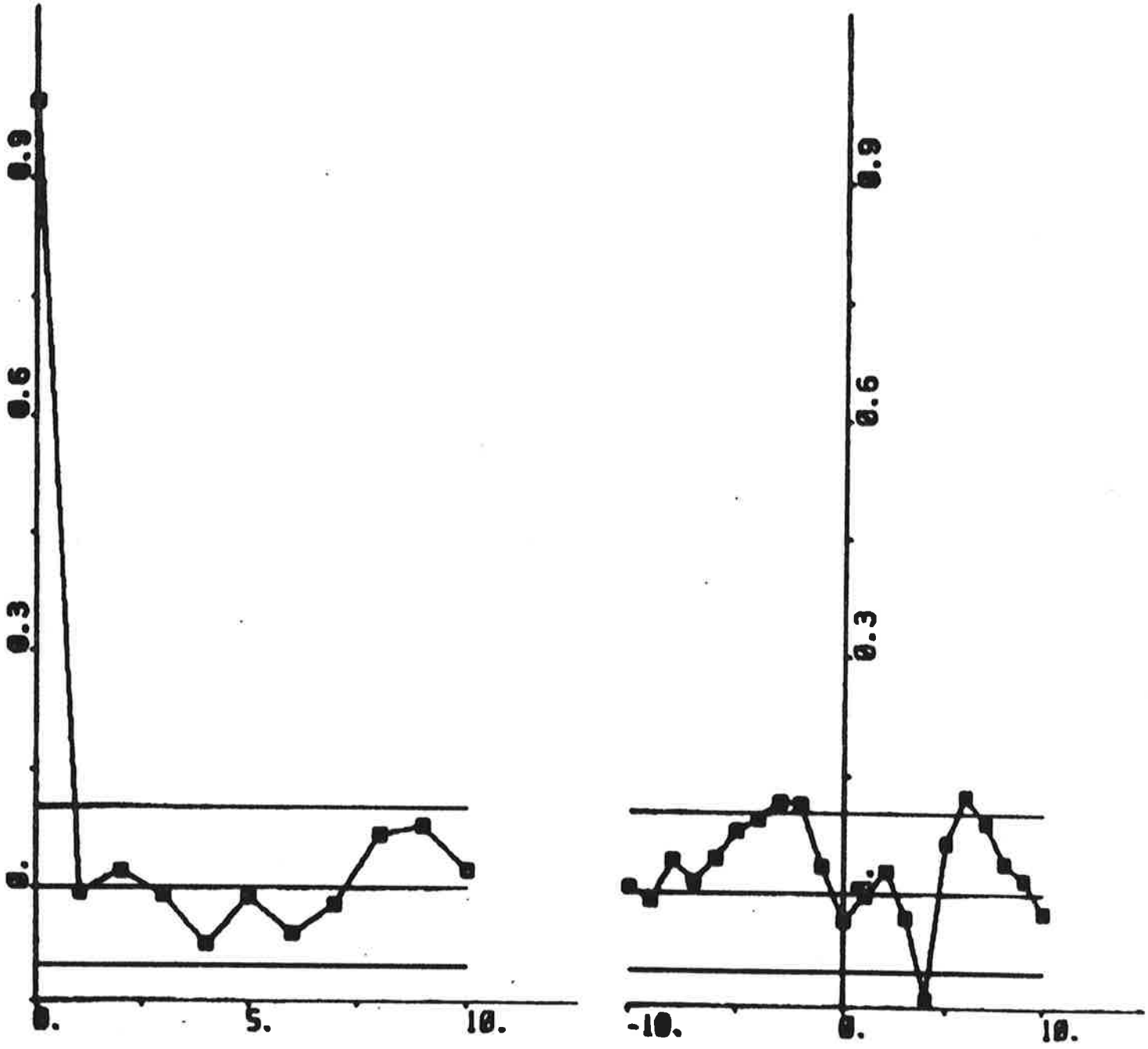

Fig. 6.38 - Autocorrelation function of residuals and cross correlation function between rudder input and residuals, where the residuals are obtained from ML identification using IDPAC to data from experiment E2.

The output error method, the maximum likelihood method and the prediction error method were applied to the data by use of the identification program LISPID. The identifications were based on 3 different models.

The first model is linear and contains hydrodynamic derivatives which are estimated. The outputs of the model are the sway velocities, the yaw rate and the heading angle. Strange parameter values were obtained when the output error method was applied to data from experiments E1 and E2. The estimated hydrodynamic derivatives differed significantly from the values calculated by SSPA from model tests with a tanker similar to the Sea Swift. However, experiments E3 and E4 gave significantly improved results. The estimates of the hydrodynamic derivatives obtained by applying the maximum likelihood method to data from all experiments were bad. However, Akaike´s information criterion indicated distinctly that the process noise should be modelled. Significantly improved results were obtained when the prediction error method was applied to data from the 4 experiments. It was concluded that a prediction interval of about 40 s was appropriate. The estimated hydrodynamic derivatives obtained from the 4 experiments didn´t differ much. The choice of an appropriate prediction interval is thus crucial to obtained good results.

The second model used by LISPID is an extension of the first model, where the nonlinear cross-flow drag is included. The only unknown parameter of the added nonlinearity is the effective cross-flow drag coefficient. Approximately the same results were obtained by using the nonlinear model as were obtained by using the linear model. The estimates of the hydrodynamic derivatives were not changed significantly. However, the effective cross-flow drag coefficient was badly estimated in all cases. The 4 experiments with the Sea Swift were designed to determine the linear ship steering dynamics, so it is not surprising that no improvements are obtained by using the nonlinear model.

Identifications based on a third model were also performed by using LISPID. This linear model contains the parameters of the transfer function relating heading to rudder angle. The only output of this model is the heading angle. The gain and time constant of Nomoto's model were first determined. A rather bad consistency between the estimates from output error identifications to data from the 4 experiments was obtained. The consistency between parameter estimates obtained from maximum likelihood identifications was improved. The results of prediction error identifications were almost equivalent to the results from maximum likelihood identifications. It was thus concluded that a prediction interval of 10 s is sufficiently when the heading angle only is used as output signal. The gain and the 3 time constants of a third-order transfer function were also determined. No significant improvements were obtained when the third-order model was identified instead of Nomoto's model. Akaike's information criterion indicated that Nomoto's model was appropriate to the data when the ML method was used. The additional 2 time constants of the third-order transfer function were estimated badly in all cases.

The rudder input - heading output data from 2 of the experiments were also analysed by the identification program IDPAC. The parameters of a linear difference equation model were estimated by the maximum likelihood method. A model corresponding to Nomoto's model was first identified. The results obtained were equivalent to the corresponding maximum likelihood results from LISPID. A model corresponding to the third-order transfer function was also identified by using IDPAC. A pole on the negative real axis was then obtained. Akaike's information criterion indicated that Nomoto's model was to prefer in front of the third-order model. LISPID and IDPAC thus gave the same model order.

It was thus possible to determine the linear hydrodynamic derivatives by applying the prediction error method to data from the 4 experiments using LISPID. Measurements of sway velocities, yaw rates and headings were then used. It was crucial to use an appropriate prediction interval. It was possible to determine the gain and time constant of Nomoto's model from rudder input - heading output data by using either LISPID or IDPAC. It was,

however, difficult to determine the additional 2 time constants of the third-order transfer function. This was explained by an approximate pole-zero cancellation or by the influence of wave disturbances on the heading measurements.

The analysis showed that there was no difference between the results obtained from open loop and closed loop experiments. It is thus possible to determine the steering dynamics of ships from full-scale experiments performed under autopilot control, provided that the identifiability is secured by adding extra rudder perturbations or by changing the gain of the regulator.

8. ACKNOWLEDGEMENTS

This work has been supported by the Swedish Board for Technical Development under contracts 754053 and 775766.

The author would like to express his gratitude to Kockums Shipyard, Malmö, and to the Salén Shipping Companies, Stockholm, for their positive attitude to this type of research. The author also thanks Mr. N.E. Thorell, Kockums Automation AB, who assisted during the experiments, and Mr. L. Sjöberg, who was captain of the Sea Swift.

The manuscript has been expertely typed by Mrs. L. Andersson.

9. REFERENCES

Akaike, H (1972): Use of an information theoretic quantity for statistical model identification. Proc. 5th Hawaii International Conference on System Sciences, pp. 249-250, Western Periodicals Co, North Hollywood, California, USA.

Åström, K J, and T Bohlin (1965): Numerical identification of linear dynamic systems from normal operating records. Proc. 2nd IFAC Symp on the Theory of Self-Adaptive Control Systems, Teddington, Great Britain.

Åström, K J (1970): Introduction to Stochastic Control Theory. Academic Press, New York.

Åström, K J, and C G Källström (1973): Application of system identification techniques to the determination of ship dynamics. Proc. 3rd IFAC Symp on Identification and System Parameter Estimation, pp. 415-424, the Hague/Delft, The Netherlands.

Åström, K J, N H Norrbin, C Källström, and L Byström (1974): The identification of linear ship steering dynamics using maximum likelihood parameter estimation. TFRT - 3089, Department of Automatic Control, Lund Institute of Technology, Lund, Sweden. Also available as Report 1920-1, Swedish State Shipbuilding Experimental Tank, Gothenburg, Sweden.

Åström, K J, C G Källström, N H Norrbin, and L Byström (1975): The identification of linear ship steering dynamics using maximum likelihood parameter estimation. Publ. No 75, Swedish State Shipbuilding Experimental Tank, Gothenburg, Sweden.

Åström, K J, and C G Källström (1976): Identification of ship steering dynamics. Automatica, 12, 9.

Byström, L, and C G Källström (1978): System identification of linear and non-linear ship steering dynamics. Paper submitted to the 5th Ship Control Systems Symp., Annapolis, Maryland, USA.

Gustavsson, I, L Ljung, and T Söderström (1977): Identification of processes in closed loop - identifiability and accuracy aspects. Automatica, 13, 59.

Källström, C (1975): The Sea Swift experiments, October 1974. TFRT-7078, Department of Automatic Control, Lund Institute of Technology, Lund, Sweden.